ROBOT ASSISTED MATERIAL HANDLING
FOR SHIRT COLLAR MANUFACTURING
-- TURNING AND PRESSING --
DLA 900-87-0017 Task 0004

FINAL REPORT

VOLUME II:

Robot Assisted Material Handler

CENTER FOR ADVANCED MANUFACTURING

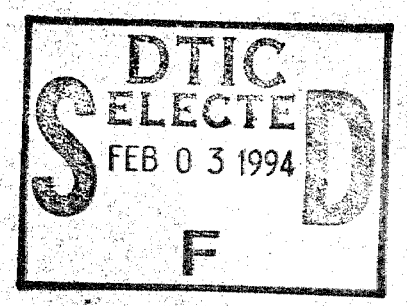

CLEMSON UNIVERSITY
College of Engineering
Clemson, South Carolina 29634

ROBOT ASSISTED MATERIAL HANDLING FOR SHIRT COLLAR MANUFACTURING -- TURNING AND PRESSING --

DLA 900-87-0017 Task 0004

FINAL REPORT

VOLUME II:

Robot Assisted Material Handler

Frank W. Paul
Principal Investigator

and

Ajay Gopalswamy
Research Assistant

Center for Advanced Manufacturing
and
Clemson Apparel Research

Clemson University
Clemson, SC

June 1992

P00011 to DLA900-87-D-0017

SECURITY CLASSIFICATION OF THIS PAGE

REPORT DOCUMENTATION PAGE

1a. REPORT SECURITY CLASSIFICATION Unclassified	1b. RESTRICTIVE MARKINGS
2a. SECURITY CLASSIFICATION AUTHORITY	3. DISTRIBUTION / AVAILABILITY OF REPORT Unclassified Distribution Unlimited
2b. DECLASSIFICATION / DOWNGRADING SCHEDULE	
4. PERFORMING ORGANIZATION REPORT NUMBER(S)	5. MONITORING ORGANIZATION REPORT NUMBER(S)
6a. NAME OF PERFORMING ORGANIZATION Clemson University/ Clemson Apparel Research 6b. OFFICE SYMBOL (If applicable)	7a. NAME OF MONITORING ORGANIZATION Defense Personnel Support Center
6c. ADDRESS (City, State, and ZIP Code) 500 Lebanon Road Pendleton, SC 29670	7b. ADDRESS (City, State, and ZIP Code) 2800 South 20th Street P.O. Box 8419 Philadelphia, PA 19101-8419
8a. NAME OF FUNDING / SPONSORING ORGANIZATION Defense Logistics Agency 8b. OFFICE SYMBOL (If applicable)	9. PROCUREMENT INSTRUMENT IDENTIFICATION NUMBER DLA 900-87-D-0017 Delivery Order 0004
8c. ADDRESS (City, State, and ZIP Code) Room 4B195 Cameron Station Alexandria, VA 22304-6100	10. SOURCE OF FUNDING NUMBERS PROGRAM ELEMENT NO. 78011S; PROJECT NO.; TASK NO.; WORK UNIT ACCESSION NO.

11. TITLE (Include Security Classification)
Robot Assisted Material Handling for Shirt Collar Manufacturing: Turning and Pressing
Vol. II: Robot Assisted Material Handler - unclassified

12. PERSONAL AUTHOR(S)
F. W. Paul, Principal Investigator; Ajay Gopalswamy, Research Assistant

13a. TYPE OF REPORT	13b. TIME COVERED	14. DATE OF REPORT (Year, Month, Day)	15. PAGE COUNT
Final	FROM n/a TO	1992 June 23	160

16. SUPPLEMENTARY NOTATION

17. COSATI CODES			18. SUBJECT TERMS (Continue on reverse if necessary and identify by block number)
FIELD	GROUP	SUB-GROUP	

19. ABSTRACT (Continue on reverse if necessary and identify by block number)

This document presents Volume II of the report of research into the automation of shirt collar manufacturing using robotic methods. Presented are the robot assisted material handler and its evaluation for manipulation of three-dimensional apparel workpieces.

The design concept evolved from studies of manual handling of shirt collars. The concept used gravity and grippers to stretch fabric for control of drape along the workpiece. Orientation of the workpiece can be changed through an end-effector pitching motion. The results of the evaluation show that the robot and end-effector can successfully manipulate shirt collars to accomplish shirt collar manufacturing tasks associated with turning and pressing. System control is accomplished through workstation integration of the robot and end-effector with the turning and pressing devices.

20. DISTRIBUTION / AVAILABILITY OF ABSTRACT ☒ UNCLASSIFIED/UNLIMITED ☐ SAME AS RPT. ☐ DTIC USERS	21. ABSTRACT SECURITY CLASSIFICATION Unclassified
22a. NAME OF RESPONSIBLE INDIVIDUAL Frank W. Paul	22b. TELEPHONE (Include Area Code) 803-656-3291 22c. OFFICE SYMBOL

DD FORM 1473, 84 MAR 83 APR edition may be used until exhausted. All other editions are obsolete.

SECURITY CLASSIFICATION OF THIS PAGE

ACKNOWLEDGMENTS

The authors would like to thank all those who were involved with support of this project. Especially, it is appropriate to thank the Defense Logistics Agency, Department of Defense, for support of this work under contract number DLA 900-87-0017 Task 0004. This work was conducted through Clemson Apparel Research, a facility whose purpose is the advancement of apparel manufacturing technology and by the Center for Advanced Manufacturing, Clemson University.

ABSTRACT

Many apparel manufacturing operations involve the handling of multiple-ply workpieces. Previous efforts at automating apparel handling operations has concentrated on planar fabric handling operations of single-ply workpieces. Specialized end-effectors are needed to handle and manipulate flexible multiple-ply assemblies in three dimensional space. This requirement has been addressed by (1) developing concepts for three dimensional manipulation of multiple-ply apparel workpieces, and (2) designing and evaluating an end-effector for demonstration of these concepts.

The end-effector design concepts have been developed by observing the manual handling of a shirt collar. The end-effector grasps and manipulates a single workpiece using two parallel jaw grippers. The individual plies of the workpiece are separated from one another by gravitational force. The location of the grippers are varied so that the fabric ply can be stretched. Stretching the grasped ply enables the end-effector to control fabric drape at the workpiece edges. The orientation of the grippers can be changed by a pitch motion on the end-effector.

The gripper translation motion has been designed to minimize interferences with the robot workspace. The pitch motion employs a novel design concept to reduce the peak torque required by the motor driver. The design uses the

end-effector motors to counterbalance the weight of the remainder of the end-effector while undergoing the pitch motion.

A step motor actuates the translation motion of the grippers. The velocity and acceleration parameters of the step motor have been determined by an experimental procedure. The end-effector pitch motion is actuated by a DC servo motor. The controller gains for the closed loop pitch motion control system have been analytically determined. Experimental trials conducted with the end-effector show that the analytical predictions of the pitch motion performance are valid in the linear range of the motor drive. Non-linearities present in the system such as actuator saturation and gearbox backlash need to be considered to more accurately predict the analytical dynamic behavior of the system.

The end-effector has been integrated into a workstation that processes shirt collars without human intervention. Collar handling demonstrations show that the end-effector is capable of handling a multiple-ply apparel component in three dimensional space. Future research should include improvements in mechanical design and refinements in analysis techniques.

TABLE OF CONTENTS

Table of Contents (Continued)

LIST OF FIGURES

List of Figures (Continued)

List of Figures (Continued)

CHAPTER I

INTRODUCTION

Robotic handling of apparel components is being investigated to improve the productivity of apparel manufacturing operations and hence make the domestic apparel industry more competitive. Past research efforts have mainly concentrated on developing robot systems for handling single ply fabric panels. However, there exist numerous operations involving the three dimensional manipulation of multiple-ply apparel components. Such operations are currently performed manually requiring a high degree of operator dexterity. Few attempts have been made at automating three dimensional manipulation operations. The topic of the current research is to develop an end-effector for the three dimensional manipulation of multiple-ply apparel components. An example of a multiple-ply apparel component that assumes a three dimensional shape while undergoing processing is the shirt collar. The design concepts developed in this research will be demonstrated for the robotic manipulation of shirt collars.

This chapter provides a background to the apparel manipulation problem and identifies the objectives of the research. A survey of previous work documenting the development of end-effectors is presented, with special reference to apparel handling manipulators. The chapter concludes with a brief summary of the thesis format.

Background

Automation of Apparel Manufacturing Operations

Due principally to high labor costs, the apparel industry in the United States is finding it difficult to compete with foreign manufacturers. Continual fashion changes from season to season have increased the pressure on apparel manufacturers to respond more rapidly to market demands. Research efforts have been initiated in the United States, Japan, and Western Europe to automate many of the operations in apparel manufacturing to reduce production costs and turn-around times.

Apparel manufacturing operations can be classified into two broad categories , namely joining and handling. Joining operations include sewing, and adhesive and ultrasonic bonding. Handling operations consist of ply separation, pick-and-place, folding, guiding fabric panels during joining operations, and inversion of assembled workpieces (such as collars and cuffs). Most of the joining operations are currently implemented using "hard automation". Gaetan [1] believes that fabric handling is the major labor and time consuming part of apparel manufacture. The productivity of apparel manufacturing operations can be significantly improved by automating fabric handling operations. High capital costs and technological limitations has hindered the application of advanced automation in the apparel industry. With recent advances in technology such as development in

CAD/CAM and robotics, automation of apparel manufacturing operations has become more feasible.

As robotics researchers have realized, fabric handling operations are the most difficult of the apparel manufacturing operations to automate due to the inherent flexible and unpredictable behavior of fabric. For robotics to be effectively applied to apparel manufacture, various issues such as the design of suitable end-effectors and the development of sensing and control strategies must be addressed.

Even with recent developments in robot technology, fabric handling poses a special challenge due to the unusual behavior of the fabric material. Various research projects have been initiated that involve the application of robots to fabric handling. The problem of separating a single ply from a fabric stack has been extensively investigated. Parker, Dubey, Paul, and Becker [2] explored the use of pins, adhesives and vacuum suction to separate individual fabric workpieces from a stack. Kemp, Taylor, Taylor, and Pugh [3] developed a gripper for separating fabric plies by the use of an air jet attached to the upper jaw of the gripper. Taylor, Monkman, and Taylor [4] experimented with a device that makes use of the electrostatic attractive force that develops between the gripper material and fabric to separate fabric plies from a stack.

Robot-assisted sewing of fabric pieces represents the next level of sophistication in the automation of apparel manufacturing. Torgerson and Paul [5] developed a robot

workcell for vision-assisted manipulation of single-ply fabric workpieces with arbitrary contours under a simulated sewing needle. Gershon and Porat [6] describe a flexible robotic sewing system called FIGARO. The system manipulates fabric panels through a sewing machine to attain a seam parallel to the panel's edge. The Japanese Ministry of International Trade and Industry (MITI) [7] has sponsored a research program that "will center around the creation of machinery that can handle soft, porous and stretchable fabrics with the same dexterity and precision as industrial robots now handle metals." As part of the program, a robot system for three dimensional sewing of fabrics was developed by Nakamura et al. [8]. Two instances of three dimensional manipulation tasks that have been successfully automated using robots have been described in the literature. Taylor and Koudis [9] describe a technique for the robot assembly of the front, back and gusset panels for the manufacture of men's briefs. The Charles Stark Draper Laboratory has developed a robot workstation for the assembly of sleeves for men's tailored suits [10].

A project to automate certain shirt collar manufacturing operations is being undertaken at Clemson University. The shirt collars before being processed consist of two plies sewn together on three sides as shown in Figure 1.1. One of the plies has a fused lining to impart stiffness to the collar. Stitching the collar on three sides forms two corners or "collar points". The two plies enclose a "collar

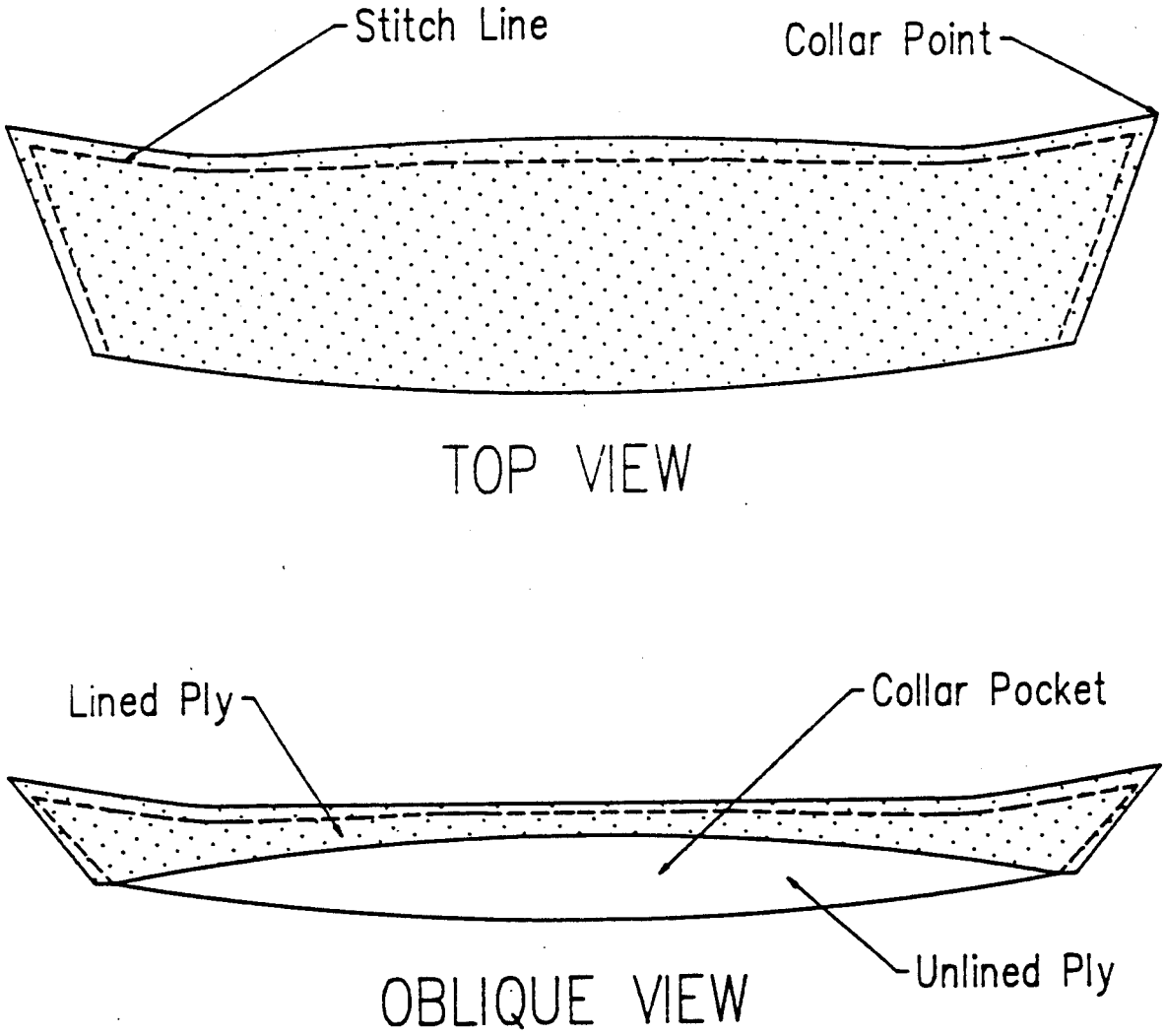

Figure 1.1. Shirt Collar Construction

pocket". Before being processed, the stitch line is visible on the outer surface of the collar. In order to conceal the seam edge, the collar must be inverted. The process of inversion is called "turning". After the turning process is complete, the collar points must be "pressed" to obtain sharp collar points. The purpose of the Defense Logistics Agency (DLA) sponsored project is to design, develop and demonstrate a robotic system which will turn and press shirt collars without operator assistance. The project involves the development of a Robotic Fabric Handling System (RFHS), comprising a robot and an end-effector, which are to be integrated with other dedicated collar turning and pressing devices. The topic of this research is to develop an end-effector that can manipulate shirt collars and hence demonstrate concepts for the larger problem of manipulation of multiple-ply three dimensional apparel components.

Need for a Specialized End-Effector

A robot interacts with its environment through an end-effector usually mounted at its wrist. The end-effector can be a gripper for grasping objects or a tool for performing tasks such as welding, spray painting etc. An end-effector can also incorporate mechanisms for enhancing the motion capabilities of the robot.

Robots can easily manipulate rigid objects once their shape and geometry are known or determined. However, apparel workpieces such as shirt collars behave in an unpredictable

manner due to the flexible or limp nature of the fabric material. In order to manipulate apparel workpieces, it is necessary that the transformation of a geometric characteristic of the workpiece be determined with respect to the robot. Another important task that the end-effector has to perform while manipulating multiple-ply apparel components is to keep the individual plies of the workpiece apart. Separation of the workpiece plies is required during processing operations carried out on the workpiece.

Robot wrist motions are required to orient the end-effector (and hence the grasped object). End-effector orientation can be described in terms of three parameters: pitch, roll and yaw angles. Additional degrees of freedom may be provided by the end-effector orientation to correctly orient the apparel workpiece on external devices that carry out processing operations.

An end-effector which satisfies these design specifications is often required for apparel manipulation. Custom designed end-effectors for manipulation of multiple-ply, three dimensional apparel components are often necessary for apparel automation.

Literature Survey

Research into end-effectors has been directed at two levels: (1) general purpose end-effectors which can handle a wide variety of objects and (2) specialized end-effectors which are limited to handling objects having specific properties. A survey of general purpose end-effectors and end-

effectors developed to handle limp material will be presented to obtain an overview of the state-of-the-art in the field.

General Purpose End-Effectors

General purpose end-effectors are designed to handle a wide class of objects typically by emulating human actions. One approach towards designing an end-effector for handling flexible objects is to design an anthropomorphic end-effector. Such an approach might be effective considering the manual dexterity needed to handle fabric material. Two general purpose end-effectors described in the literature are discussed.

The most ambitious research project regarding the development of a general purpose end-effector is the Utah/M.I.T. dexterous hand [11]. The hand illustrated in Figure 1.2 consists of three fingers, each incorporating four degrees of freedom and a thumb, also possessing four degrees-of-freedom, placed opposite to the fingers. The hand was designed to emulate human capabilities. The sixteen joints of the hand are driven by antagonistic tendons which are independently actuated by pneumatic air cylinders. The actuators are located remotely to reduce the weight and size of the hand. Feedback information to the controller is provided by tendon and joint position sensors. The Utah/M.I.T. hand can be controlled by teaching it various motions using a "data glove" that records motion trajectory points. Due to its kinematic complexity and high cost, the Utah/M.I.T. dexterous hand has been used only as a research tool in laboratories.

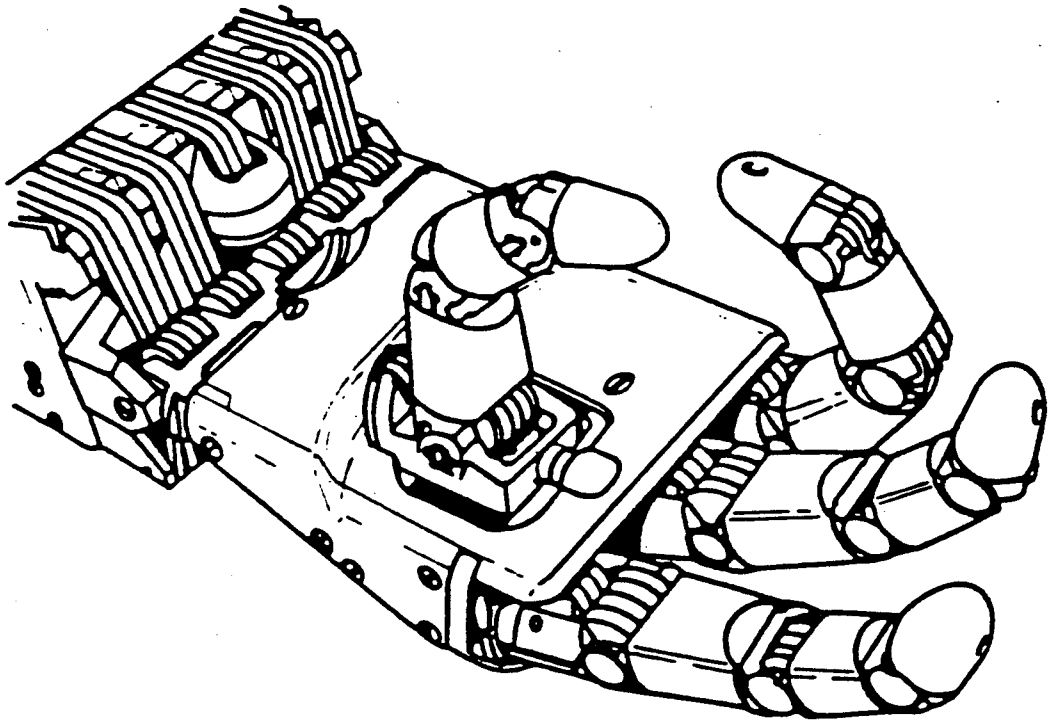

Figure 1.2. Utah/M.I.T. Dexterous Hand
(Source: Jacobsen et al. [11], International Journal of Robotics Research)

Another important general purpose end-effector is the Stanford/JPL hand [12]. The Stanford/JPL hand illustrated in Figure 1.3 consists of three fingers; each finger is provided with three degrees-of-freedom. The individual joints are actuated by DC motors which drive antagonistic tendons. Control of the fingers' contact forces is achieved through a hemispherical force sensor mounted on each finger tip. No industrial applications of the Stanford/JPL hand have been reported for the same reasons as for the Utah/M.I.T. dexterous hand.

Designing an end-effector which incorporates general anthropomorphic features for handling fabric is difficult because the level of technology is complex and the cost is difficult to justify. A more realistic approach is to develop a dedicated end-effector designed specifically for the task of handling particular fabric components. Future technological developments that reduce the complexity and lower costs of anthropomorphic end-effectors may make their use in industrial applications more feasible.

Apparel Handling End-Effectors

The sophistication of apparel handling end-effectors has grown over the years. The first generation of apparel handling end-effectors were used for pick-and-place operations. Pick-and-place end-effectors are designed to separate a single fabric workpiece from a stack and transport it to another location. Destacking a single workpiece is a challenging problem due to the tendency of adjacent fabric plies

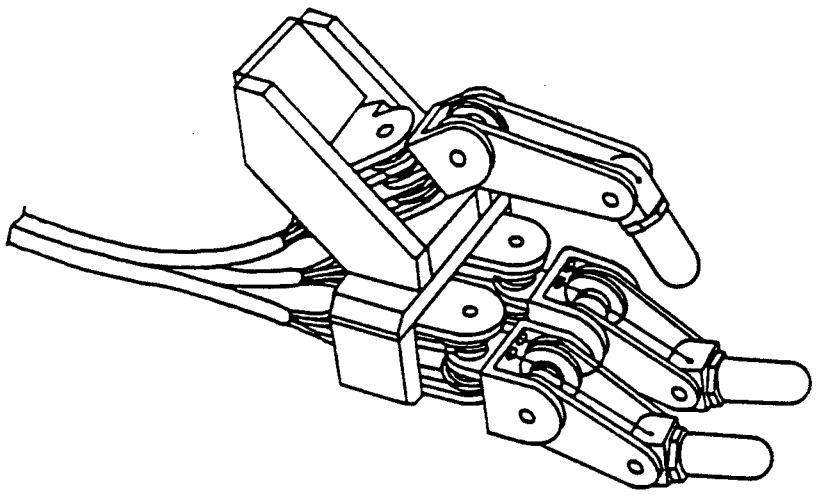

Figure 1.3. Stanford/JPL Hand
(Source: Grupen et al. [13], International Journal of Robotics Research)

to adhere to each other at the cut edges. Designs of pick-and-place end-effectors differ in the mechanism they employ to separate individual workpieces from a stack. The various ply-separation methods that have been reported in the literature use pins, adhesives and vacuum [2], the air-jet principle [3] and electrostatic forces [4].

The next generation of apparel handling end-effectors were used to guide fabric panels over a flat surface during sewing operations. Torgerson [14] developed a robot end-effector that can guide a fabric workpiece under a simulated sewing needle. The end-effector uses adhesive tape to acquire a single workpiece from a stack. The unique feature of this end-effector is that the grasp locations can be varied automatically to accomodate workpieces of different sizes. The adhesive pads are mounted on compliant springs so that the end-effector can guide the workpiece smoothly along a flat surface. The drawbacks associated with this end-effector is that large workpieces tend to sag in the middle since they are supported only at the edges and that an external mechanism is needed to separate the workpiece from the end-effector due to the use of adhesives as the grasping mechanism. Gershon [15] developed an end-effector for guiding the workpiece across a sewing needle. The end-effector consists of two fingers whose relative distance is variable. The fingers are equipped with rubber pads whose friction coefficient with respect to the fabric is greater than the friction coefficient between the fabric and the worktable surface.

This was done to prevent slip between the fingers and the workpiece. The difficulty reported with this end-effector is its inability to prevent buckling of the fabric when rotating the workpiece about the sewing needle. Gershon recommended the use of additional fingers whose relative positions can be automatically reconfigured under program control.

The highest level of sophistication among apparel handling end-effectors are those that can manipulate apparel workpieces in three dimensional space. The Charles Stark Draper laboratories developed an end-effector that was able to fold sleeves for men's suits [10]. The end-effector is comprised of numerous "cloth pickers" that are mounted along a flexible mechanical spline. The spline consists of three segments - a central stationary segment and right and left segments that can be moved with respect to the central piece. The shape of the spline can be adjusted to C and S shapes that conform to most sleeve edges. The configuration of the spline is controlled by visual feedback of the location of the sleeve edge. No performance measures of the end-effector were reported; however, the cloth folding workstation comprising the robot, end-effector, vision system and the cell controller performed reliably. Another end-effector capable of three dimensional manipulation was developed by Taylor and Koudis [9]. The end-effector assists in the assembly of the front, back and gusset panels of men's briefs. The end-effector consists of two rollers that are used to roll the front and back panels of the briefs and lay it on the gusset

panel. A sewing machine joins the panels together to complete the assembly. The rollers on the end-effector rotate by 180 degrees to turn the assembly inside out thus concealing the seam.

The end-effectors described above make use of different design strategies to solve specific fabric handling problems. Concepts must be developed that enable the design of robot end-effectors for the manipulation of multiple-ply three dimensional apparel components.

Problem Statement and Research Objectives

This research problem can formally be stated as:

> Development of an end-effector for the three dimensional manipulation of multiple-ply apparel workpieces and demonstration of its operational capability by integrating it into a workstation for processing shirt collars.

The first objective towards achieving this goal is to evaluate and analyze the requirements for manipulating three dimensional apparel workpieces. Identifying the requirements of the end-effector will enable the conceptualization of the mechanical design of the end-effector. Apart from satisfying the apparel manipulation requirements, the mechanical design must consider physical constraints that influence the design such as robot payload and workspace. Control schemes developed for the end-effector axes of motions must be compatible with the overall control structure for the collar processing workstation. The second objective of the thesis is to physically realize an end-effector design incorporating the developed concepts. Realization of the design will involve

mechanical component design, integration of control electronics with the mechanical hardware and development of software routines to command end-effector motions from a digital computer. The final objective of this research will be to evaluate the performance of the developed end-effector.

Thesis Organization

Manipulation primitives for multiple-ply apparel components are developed in Chapter II. These primitives are obtained after studying human operators performing a similar task. The concepts that are evolved in Chapter II are translated into an implementable design in Chapter III. The design includes the mechanical and control design of the end-effector. The performance of the end-effector will be evaluated in Chapter IV. Finally, the conclusions and recommendations of this research will be presented in Chapter V. Appendices A through E contain material that detail the thesis work.

CHAPTER II

END-EFFECTOR DESIGN CONCEPTUALIZATION

The design of the end-effector must be based upon certain general concepts for three dimensional manipulation of multiple-ply apparel components. These manipulation primitives are developed after studying the manual manipulation of a particular multiple-ply apparel component, the shirt collar. A strategy for machine manipulation of apparel components can evolve from this study. A conceptual design is developed that specifies the motion requirements for the end-effector.

Definitions

Definition of the terms used in the present and subsequent chapters are given below:

Manipulation : Operation or handling of an object after it has been grasped. Examples of manipulation operations on an apparel workpiece are changing its position and orientation, folding etc.

Grasping : The physical operation of holding an object. Grasping can be achieved by any of a number of methods such as gripping, vacuum suction, temporary bonding with the workpiece etc.

Gripper : A mechanism that grasps an object by trapping it between two or more "jaws".

Ply-Separation : In a multiple-ply apparel component, the action of keeping the individual plies apart.

Analysis of Manual Apparel Manipulation

In order to devise a reliable grasping strategy, it would be desirable to analyze and predict the behavior of the collar. Unfortunately, very little research has been directed towards the study of fabric behavior under the action of various loads and boundary conditions. A few studies have been initiated to understand fabric behavior; however, no published results exist that predict analytically the behavior of multiple-ply apparel components. The end-effector design must thus be based on visual observation of the behavior of a multiple-ply, three dimensional apparel component under manual operation. The manual manipulation of a shirt collar, which is an example of a multiple-ply apparel component is studied to develop a set of manipulation requirements for the end-effector.

The shirt collar must be turned and pressed before it can be assembled with the rest of the shirt. State-of-the-art collar turning and pressing is performed manually on a single machine. One version of the machine, the Lunapress, is illustrated in Figure 2.1. This machine is designed so that a human operator can perform both turning and pressing operations while seated. The turning components of the machine consist of a "clipper" and a "turner". The clipper is a stationary flat triangular blade which points towards the operator. The turner is a conical component attached to the end of a pneumatic cylinder's rod. The cylinder when actuated forces the turner's tip against that of the clipper.

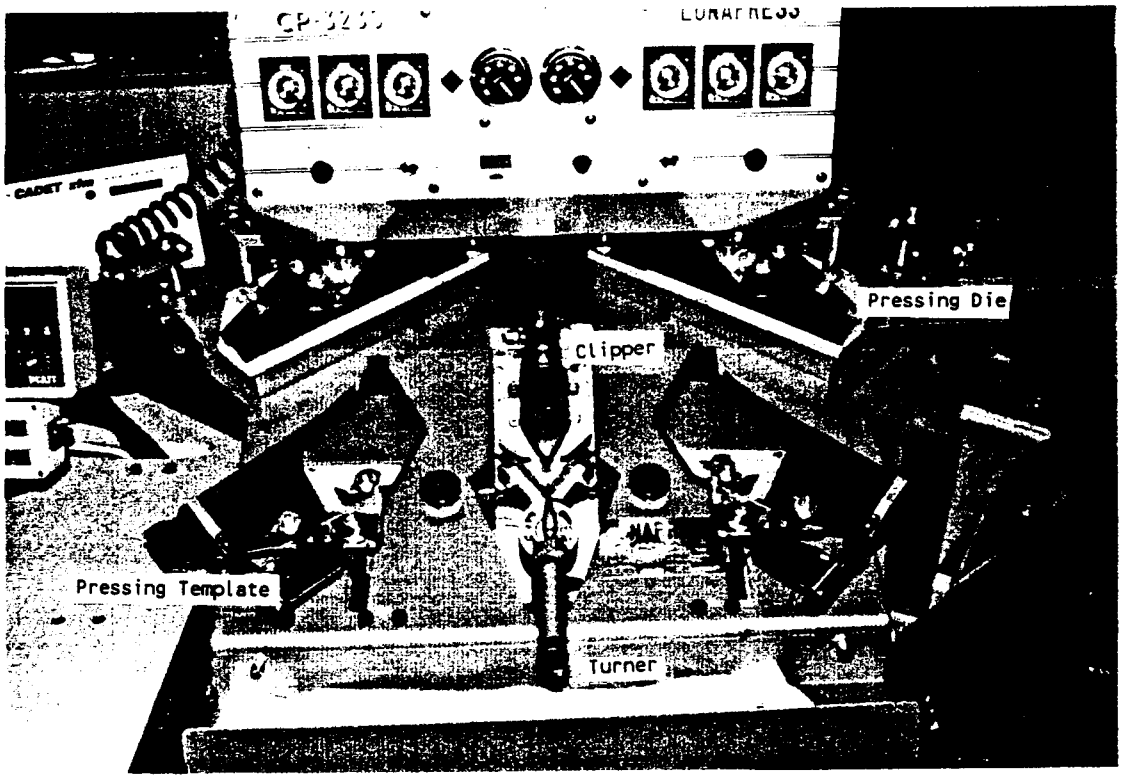

Figure 2.1. Layout and Components of the Lunapress

The pressing components consist of templates which are actuated into pressing dies by means of pneumatic cylinders.

Manual shirt collar turning is done by turning each collar point sequentially. The operator begins the process by acquiring a single workpiece after visual location of the workpiece stack. He/she then uses both hands to separate the two collar plies. After completing this step, the operator slides his/her hands into the collar pocket so that the right hand grips the collar at the stitch line while the left hand grips the collar ply at a location 3-5 inches away from the location of the right hand. The bottom ply and the left half of the collar are allowed to sag while the top right side is held taut in this configuration. The collar is loaded onto the clipper as shown in Figure 2.2(a), with the quality of the finished collar depending upon the collar point resting precisely against the tip of the clipper. The turner is actuated forward to trap the collar tip against the clipper while the operator pulls the collar to invert the collar point as depicted in Figure 2.2(b). This motion of turning the collar point involves a pitching motion of about 180 degrees at the wrist of the operator. The procedure is repeated for the second collar point resulting in an inverted collar.

The collar is transported from the turning section to the pressing section and is inserted over the right template such that the collar seam aligns perfectly with the template edge as shown in Figure 2.3(a). Seam alignment is critical

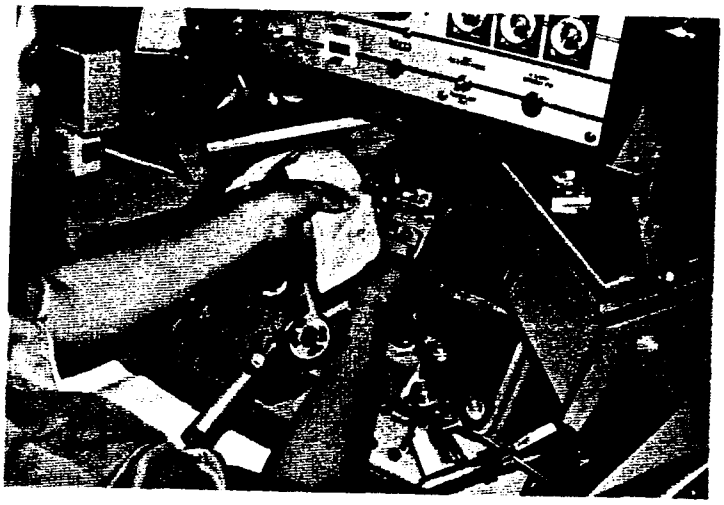

(a)

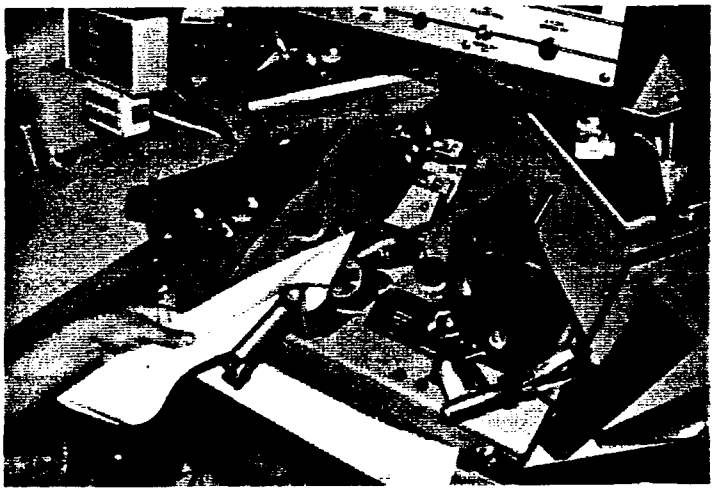

(b)

Figure 2.2. Manual Shirt Collar Turning

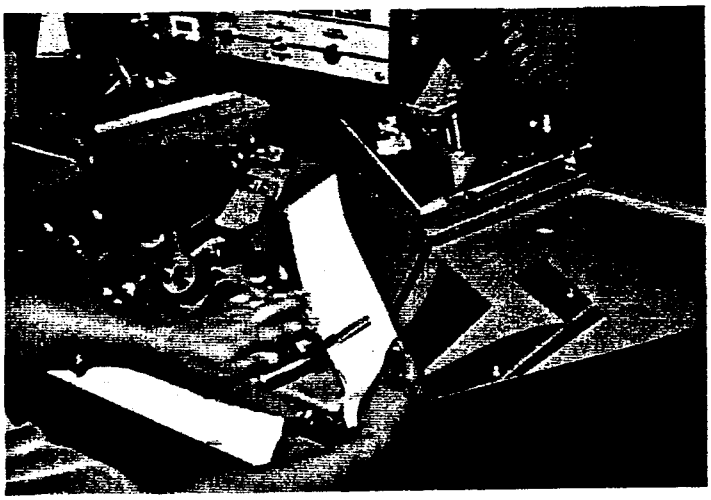

(a)

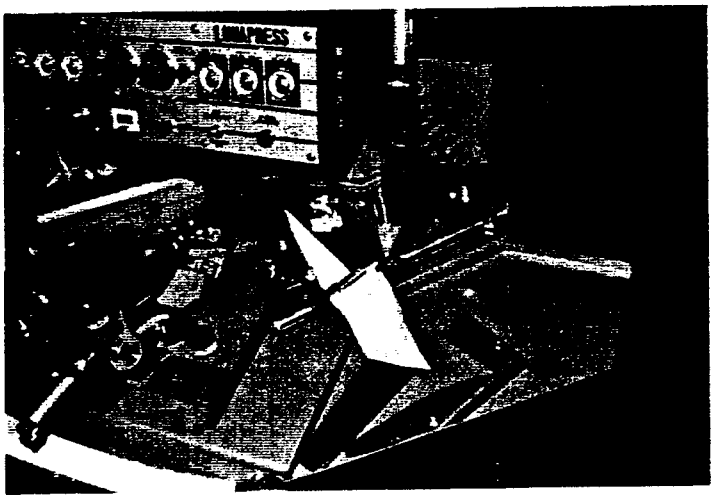

(b)

Figure 2.3. Manual Shirt Collar Pressing

to attaining a good quality on the finished collar. Improper seam alignment causes "puckering" of the collar seam once it is pressed. The operator ensures proper seam alignment by rolling the seam over the template edge. The template is actuated into the pressing dies as shown in Figure 2.3(b), where the collar undergoes pressing. The procedure is repeated for the right half of the collar.

Manual turning and pressing operations on this type machine are labor intensive requiring a high degree of dexterity and hand-eye coordination on the part of the operator. Implementing a robot assisted workstation with such a machine is difficult for two reasons. First, the machine requires frequent releasing and regrasping of each workpiece during the turning and pressing procedures. Grasping the collar at a desired location is not difficult for a human operator who makes use of elaborate tactile and visual sensory capabilities. The same task, however, is difficult for a robot with its limited decision making and sensory capabilities. Second, a robot will encounter problems in maneuvering within the constrained space of the machine to carry out the various manipulation tasks.

In view of these limitations, the apparel assembly workstation for turning and pressing shirt collars requires turning and pressing devices capable of processing both collar points simultaneously. This change from the manually operated machine will reduce the occurrences of releasing and regrasping the workpiece by the robot assisted process.

Implementing the turning and pressing operations on autonomous machines requires the robot to transport the collar from one device to the other as shown in Figure 2.4. Manipulating the collar between the autonomous turning and pressing machines is easier for the robot than attempting to maneuver the collar within the constrained space of the manually operated machine.

Conceptual Design

Workpiece Acquisition

Workpieces are stacked in a bundle to be processed in the apparel industry. Multiple-ply apparel workpieces, such as shirt collars are stacked one on top of the other after the individual plies are sewn together. Acquisition of a single workpiece from a stack by a robot can be accomplished with a destacking mechanism implemented in one of two possible ways:

1. The destacking mechanism is incorporated into the end-effector design itself.
2. The destacking operation is accomplished using an independent destacking device that presents a single workpiece to the robot end-effector.

Destacking mechanisms incorporated into the end-effector design also act as mechanisms to hold and manipulate the workpiece [2, 3, 4]. The advantage of including the destacking mechanism in the design of the end-effector is that the need for a separate device is eliminated, thus reducing system cost. However, mechanisms that perform the destacking

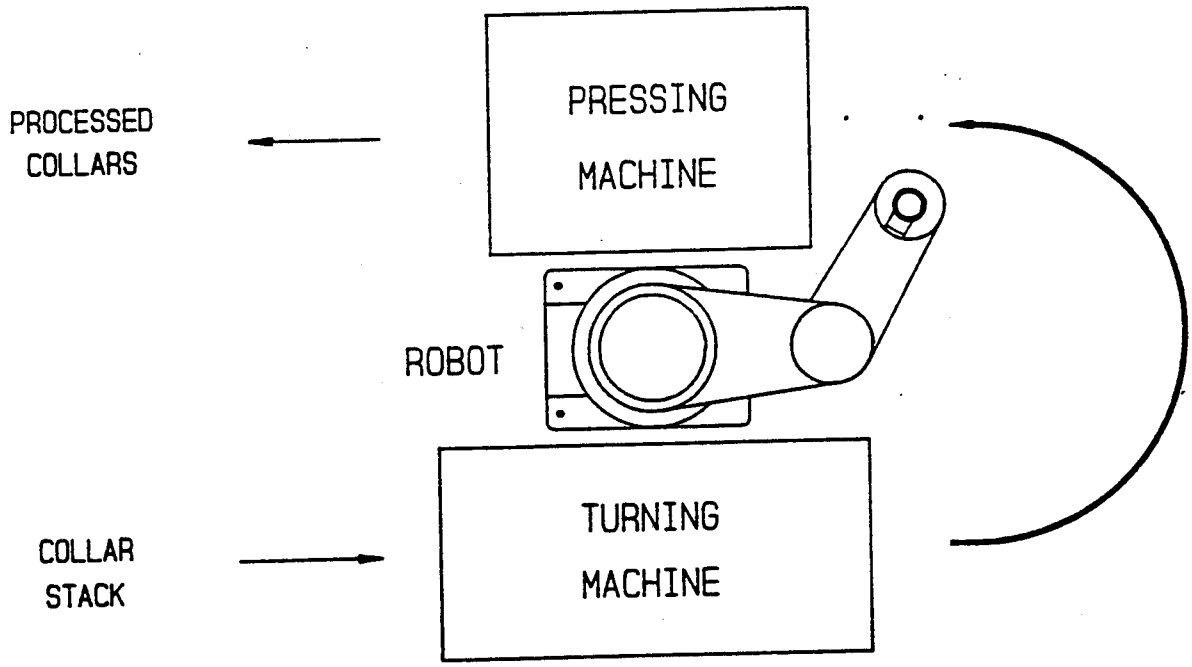

Figure 2.4. Layout of Apparel Assembly Workstation Incorporating Autonomous Double Point Turning and Pressing Devices

operation are not very suitable for grasping and manipulating a multiple-ply apparel component.

Various devices are commercially available that can reliably pick and separate a single workpiece from a stack. These devices, examples of which are the Walton picker and Jetsew's Clupicker, are being widely used in the apparel industry. Such devices could be used to separate a single workpiece and present it to the robot end-effector for grasping. The design of the end-effector can, therefore, focus on the manipulation of three dimensional apparel components. The external destacking device should present the workpiece with its individual plies separated to the end-effector grasping mechanism.

Grasping Mechanism

The grasping mechanism provides the end-effector with a physical means of holding and manipulating the workpiece. Grasping mechanisms that have been used previously with limp materials are pins, adhesives, vacuum suction devices, electrostatic grasping devices and pinch grippers.

The use of pins as a grasping device involves protruding the pins at an angle into the fabric. The tension imposed on the fabric by the angled pins provides the holding force. Fabric is released by simply retracting the pins. The disadvantage of this grasping method is that delicate fabric may be damaged due to the intrusion of pins into the fabric. Experiments were conducted to explore the possibility of using vacuum suction for grasping fabric. Studies conducted

with vacuum gripping showed that although vacuum suction provides a strong grasping force, the porous nature of fabric allows the vacuum force to act on more than one fabric ply.

Another method to grasp an apparel workpiece could be to use adhesives. However, the adhesive surface needs to be replenished because of deterioration. Workpiece release with an adhesive grasping device can only be accomplished by the use of an external device to physically separate the workpiece from the end-effector. Electrostatic methods depend on different electric characteristics of the workpiece and the grasping device to develop an attractive force. The disadvantage of this method is that turning off the voltage on the grasping device does not ensure release of the workpiece. Either an external mechanism or a reverse voltage needs to be applied to separate the workpiece from the end-effector. The final grasping mechanism that will be reviewed is the pinch gripper. The gripper jaws apply forces on either side of the grasped object to keep it in equilibrium.

The selection of a particular grasping method was based on the application of two criteria which are important for three dimensional apparel manipulation:

1. the ability of the grasping mechanism to retain its hold when forces are applied on the workpiece by external processing machines and

2. the ability of the grasping mechanism to acquire the workpiece off an external device when the workpiece is in a three dimensional configuration.

Apparel workpieces are subjected to different forces applied by external devices as they undergo processing. The

application of forces by external devices are considered for the shirt collar. Metal blades called clippers that assist in the turning process apply forces at the collar points as shown in Figure 2.5. Forces applied at the collar points are transmitted back to the grasp locations. During the pressing operation also, forces are applied along the collar seam which are perceived at the grasp locations. Due to the non-positive grasping action of pins, adhesives, vacuum suction and electrostatic grasping mechanisms, there is a possibility that the forces transmitted back to the grasp locations will cause the workpiece to slip relative to the end-effector. In the case of pinch grippers, it is always possible to design a mechanism that can apply sufficient normal force on the workpiece to ensure that no slip occurs between the gripper jaws and the workpiece.

During turning and pressing operations, the shirt collar assumes a three dimensional configuration at two instances:

1. after the collar has been destacked by the external destacking mechanism and is presented to the end-effector for acquisition and
2. after it has been turned and is ready to be unloaded from the turning machine.

At these instances the collar is supported at only two points and suspended in space with its two plies separated. As shown in Figure 2.6, a grasp technique that acts on only one surface of the fabric ply would be unsuccessful because any unidirectional force will simply deform the fabric without obtaining a grasp of the fabric. Grasping devices such

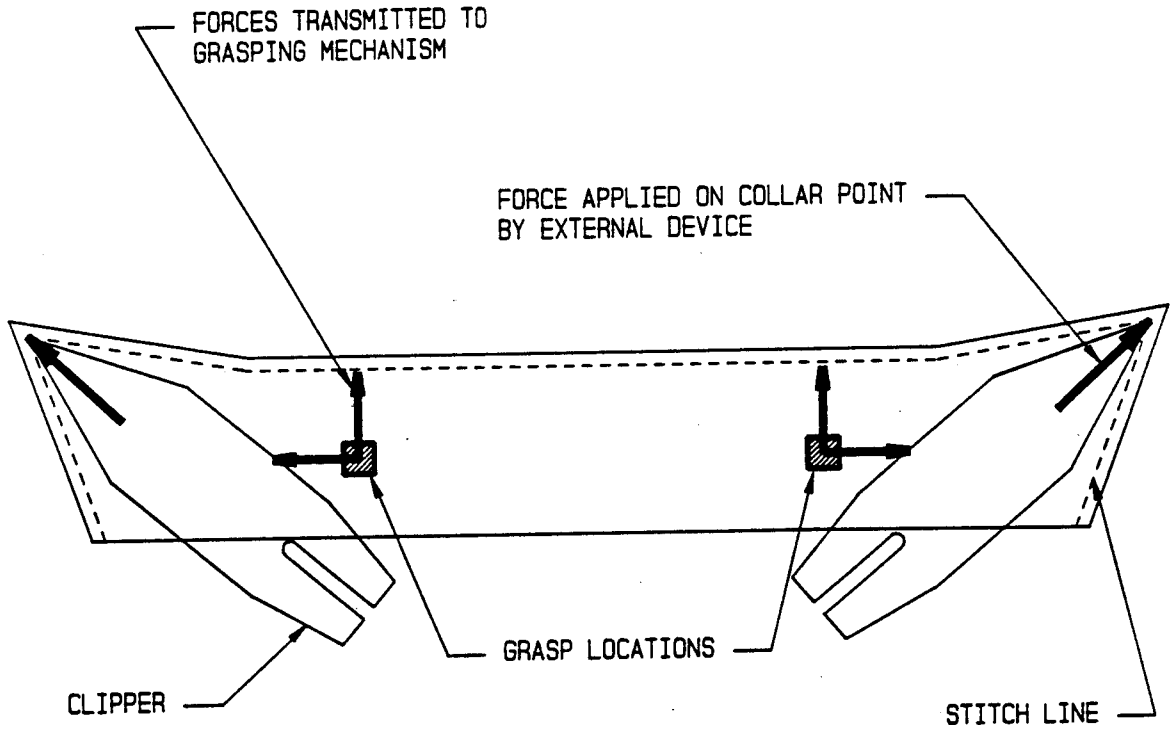

Figure 2.5. Application of Forces at the Collar Tips during the Turning Process

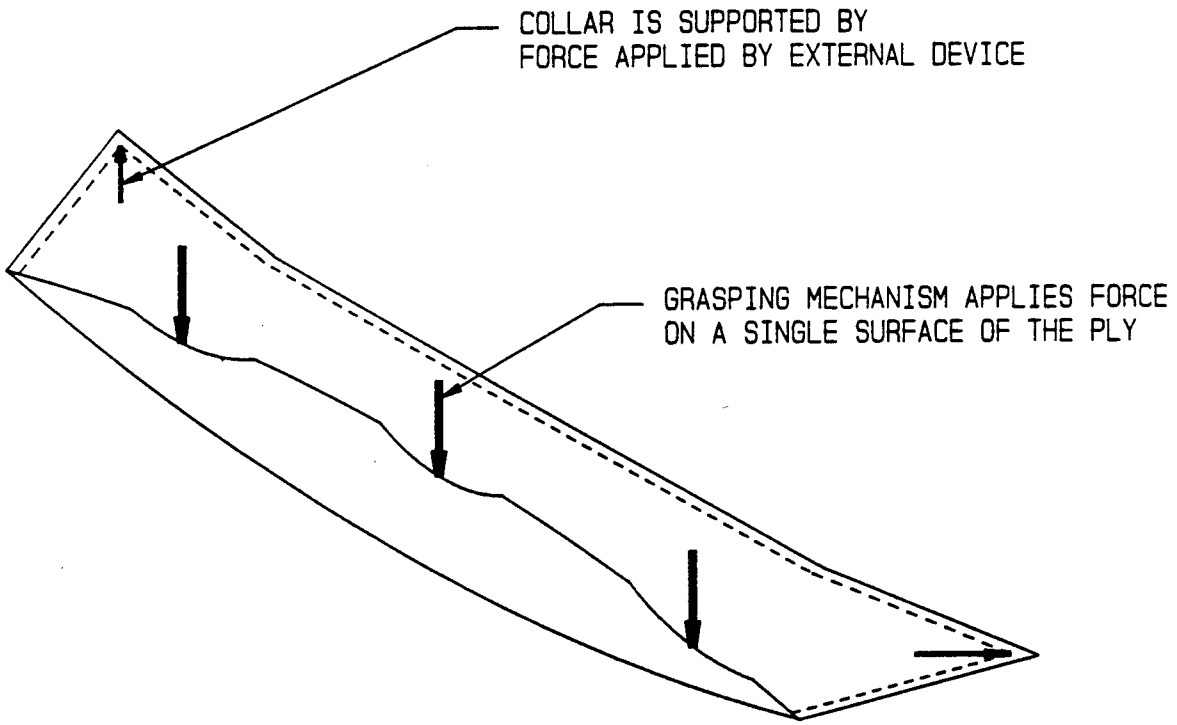

Figure 2.6. Effect of a Grasping Force Acting on a Single Surface of the Workpiece Ply

as pins, adhesives, vacuum suction and electrostatic grasping methods can grasp a fabric workpiece only when it is supported against a flat surface; these methods are not reliable when trying to acquire a freely suspended apparel component due to the lack of a rigid support. A two-jaw pinch gripper applies a normal force on both sides of the collar as depicted in Figure 2.7. This ensures that the workpiece is grasped without distorting its shape.

Grasp Locations

While handling apparel components, the workpiece needs to be temporarily transformed from a limp object into an object whose attributes can be predicted and/or controlled. This can be accomplished by stiffening the fabric by chemical means or by stretching the fabric between the grasp locations. Stiffening the fabric can be accomplished by chemically treating it; however, the time and cost of the additional process is difficult to justify. The fabric can also be rendered stiff by grasping the workpiece at suitable locations at the edges so that fabric droop is minimized. Determination of the number and placement of the grasp locations is the next step in the conceptual design of the end-effector.

A robot can position and orient a rigid object by grasping it at a single stable location. Once it has been grasped, the transformation between the object and the robot base is deterministic throughout the motion sequence. Hence, transporting the grasped object from one location to another

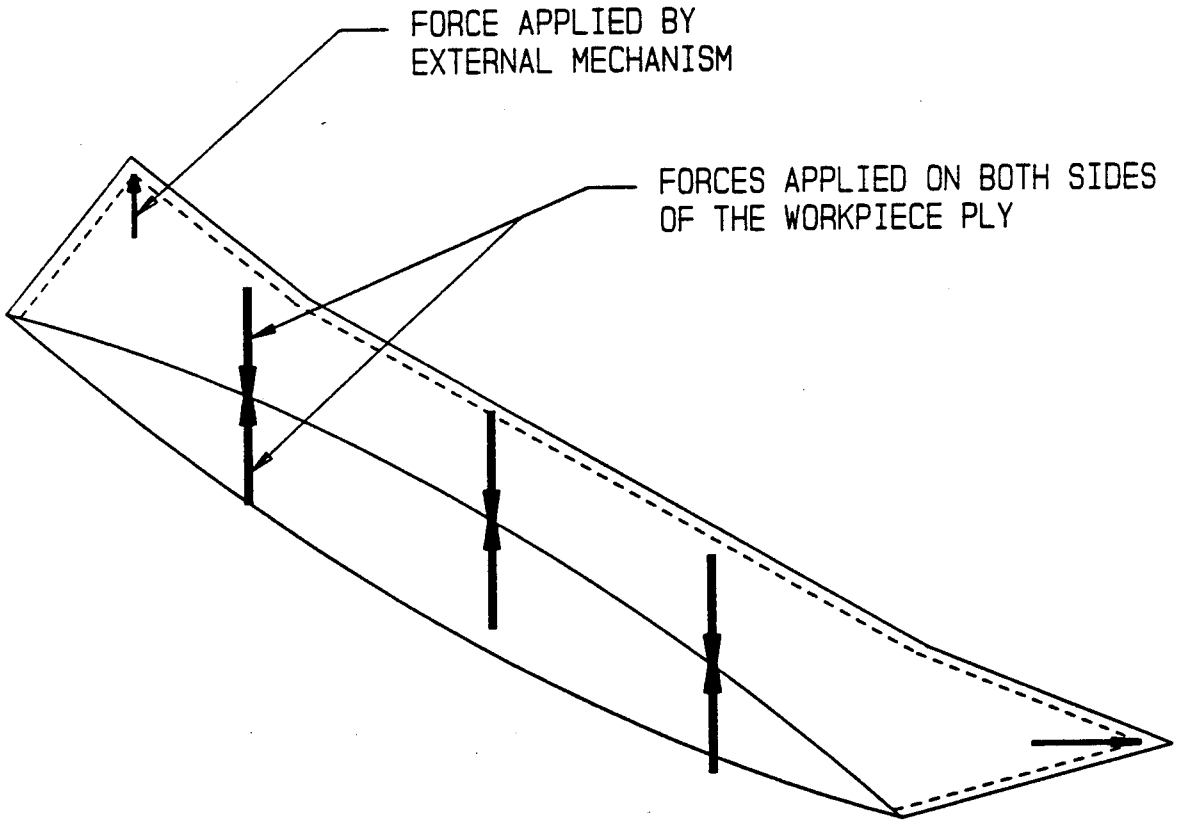

Figure 2.7. Application of Forces on Both Sides of a Fabric Ply by a Pinch Gripper

simply involves the solution of the inverse kinematics of the robot manipulator. The process of manipulating an apparel component is different from that for a rigid body because of the limp behavior of the workpiece. Figure 2.8 shows the assignment of frames for the robot, end-effector, workpiece, and the turning machine for loading the collar on the turning machine. The operation of loading the collar on the turning machine has been represented as a two dimensional occurrence for convenience. However, the following analysis can be extended to take into account the three dimensional nature of the collar manipulation process.

The equation determining ${}^{C}T_{B}$, the transformation between the collar tip and the base of the robot, is given by

$$ {}^{C}T_{B} = {}^{C}T_{E}\ {}^{E}T_{B} \ . \qquad (2.1) $$

${}^{C}T_{E}$ is the transformation between the collar tip and the end-effector base and ${}^{E}T_{B}$ is the transformation relating the position and orientation of the end-effector base with the base of the robot. In order to determine ${}^{C}T_{E}$, the collar must be controllable to minimize fabric droop at the edges. Grasping a limp apparel component at only one location will cause the fabric to droop excessively so that the transformation between the fabric edges and the end-effector base cannot be determined. Grasping the workpiece at two locations spaced sufficiently apart ensures that fabric droop at the edges is minimized. Sagging of the fabric between the two grasp locations can be minimized by moving the grasp locations laterally apart till the workpiece is taut. These

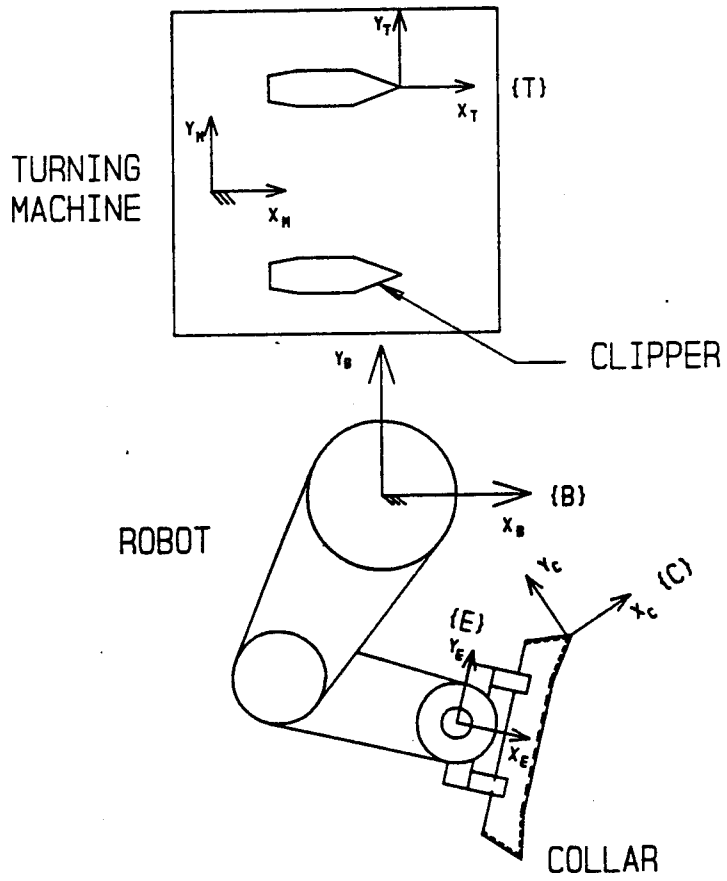

Figure 2.8. Frame Assignment for the Shirt Collar Processing System

grasp locations must be on one of the component plies to keep the workpiece in a horizontal configuration.

The location of the clipper tip with respect to the robot base ${}^{T}T_{B}$ can be determined from

$$ {}^{T}T_{B} = {}^{T}T_{M}\ {}^{M}T_{B} \ . \qquad (2.2) $$

When the collar point coincides with the clipper tip, ${}^{C}T_{B}$ and ${}^{T}T_{B}$ are identical i.e.,

$$ {}^{C}T_{B} = {}^{T}T_{B} \ . \qquad (2.3) $$

Substituting for ${}^{T}T_{B}$ from Equation 2.1, we get

$$ {}^{T}T_{B} = {}^{C}T_{E}\ {}^{E}T_{B} \ , \qquad (2.4) $$

and, hence, ${}^{E}T_{B}$, the required end-effector position and orientation to correctly load the collar points on the turning machine clippers is determined by

$$ {}^{E}T_{B} = {}^{C}T_{E}^{-1}\ {}^{T}T_{B} \ . \qquad (2.5) $$

Ply-Separation

Individual plies of multiple-ply apparel components need to be separated while being manipulated so that device elements that assist in processing operations can be introduced between the workpiece plies. During shirt collar turning and pressing operations, flat metal blades called clippers and pressing templates are inserted between the collar plies.

Different possibilities exist for ensuring separation of component plies. One possibility is to make use of an external mechanism to separate the individual plies. Another possibility is to make use of gravity force to ensure ply-separation. Figure 2.9 conceptualizes the design of a device

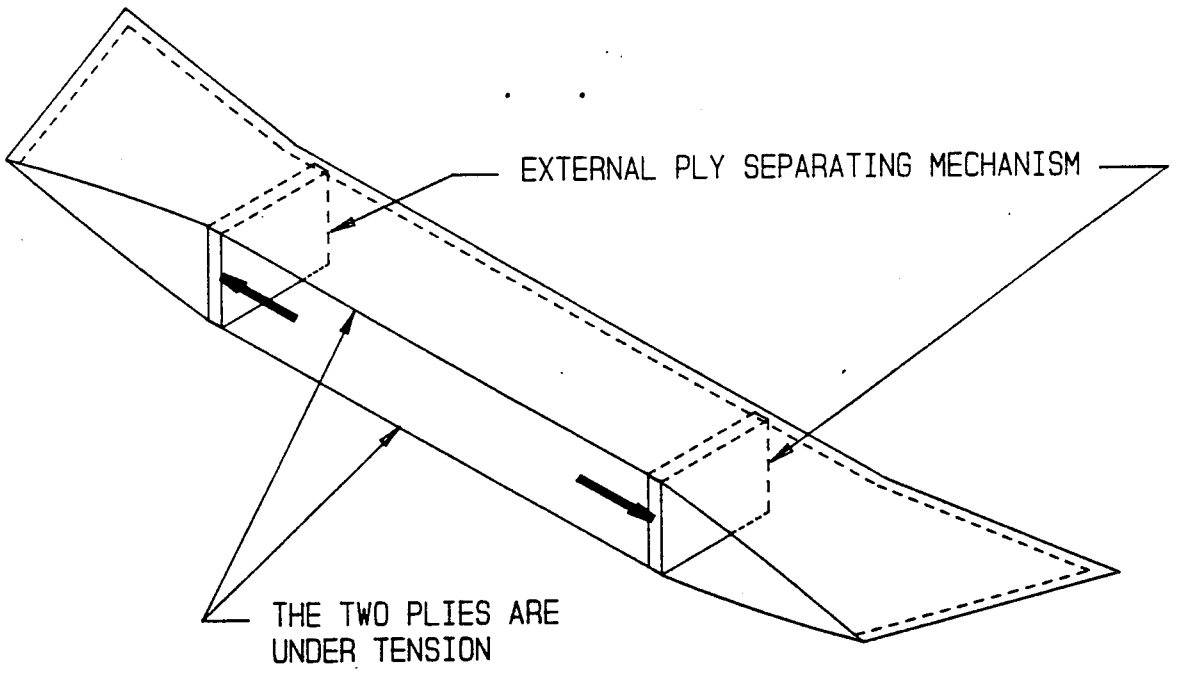

Figure 2.9. External Ply-Separating Mechanism

that when introduced between the plies stretches the workpiece between opposite seams. Due to the physical presence of the device between the workpiece plies and the stretching action of the device, the plies remain separated. The disadvantage of this method is that the presence of a ply-separating device between the workpiece plies interferes with other elements or components that are introduced into the apparel workpiece.

A multiple-ply apparel component held in a horizontal configuration and grasped on its upper ply, results in the lower ply sagging due to gravity. Since the upper ply is in tension due to the lateral force applied between the two grippers, and the lower ply is sagging, a pocket opening is created between the two plies as shown in Figure 2.10. Observation showed that workpieces of the same size when grasped at the same two locations consistently develop equal openings between the two plies. Also this method has an advantage over positive action ply-separation devices in that no devices are introduced into the apparel workpiece, minimizing interferences with external mechanisms. The disadvantage associated with this method is that gravity separation of component plies works only when the workpiece is being manipulated parallel to the horizontal ground surface.

End-Effector Orientation Motions

Many apparel manufacturing and assembly operations are carried out in horizontal planes. SCARA (Selective Compliance Assembly Robot Arm) robots use two degrees-of-freedom to

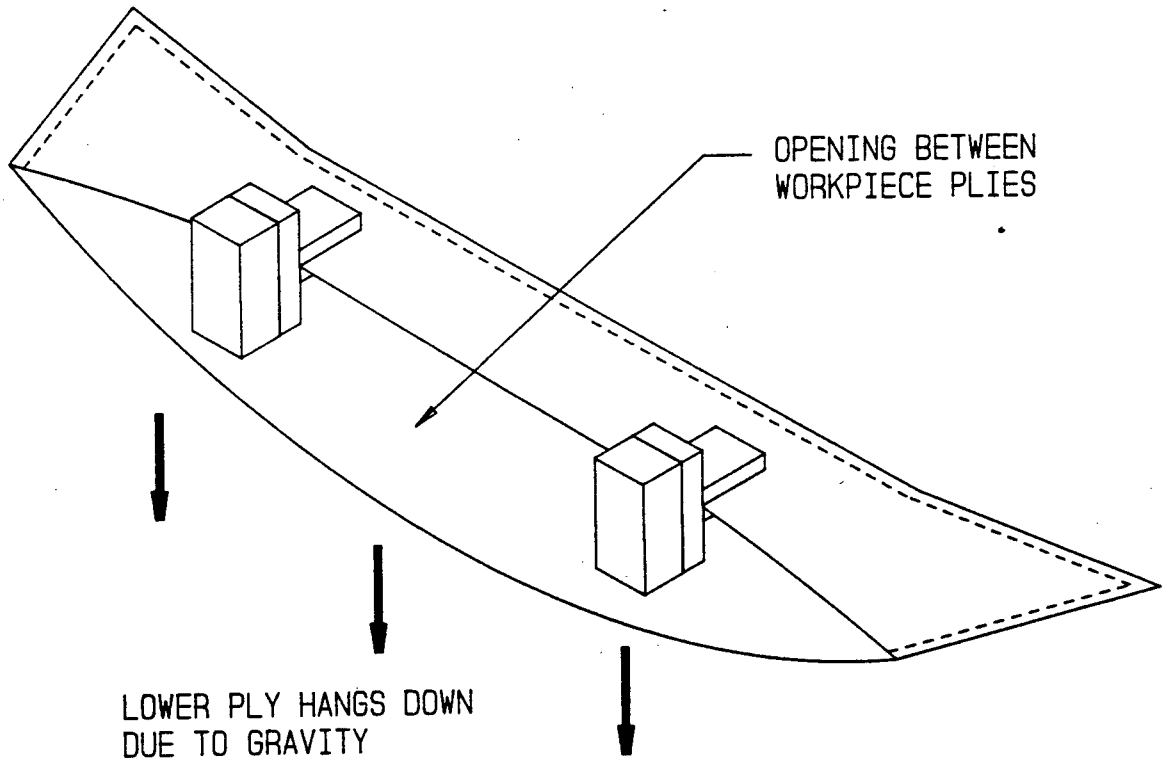

Figure 2.10. Gravity Separation of Workpiece Plies

position a workpiece in a plane and a third degree-of-freedom to move the workpiece between planes and hence would be suitable for apparel processing operations. An AdeptOne robot, depicted in Figure 2.11, which is a SCARA robot is to be used in the research. The robot incorporates three degrees-of-freedom to position the payload within its workspace. In general, three end-effector orientation angles - roll, pitch and yaw are required to orient a grasped object. One possible combination of the orientation angles for a SCARA robot is depicted in Figure 2.12.

The roll motion is required while orienting the collar on the turning and pressing machines. The AdeptOne robot is equipped with the roll motion and thus need not be incorporated in the design of the end-effector. Yaw is a rotation of the end-effector about an axis perpendicular to the roll axis. Since all operations are carried out in horizontal planes that are parallel to one another, the yaw motion is not required for the manipulation of workpieces in horizontal planes. The third orientation angle is the pitch and is the motion that changes the elevation of the end-effector with respect to the robot wrist. Pitching the end-effector causes the grasped ply to change its orientation whereas the freely suspended ply remains relatively unaffected by the pitch motion. Hence, the end-effector pitch motion increases/-decreases the opening between the plies as shown in Figure 2.13. Also, the pitch motion ensures that the end-effector

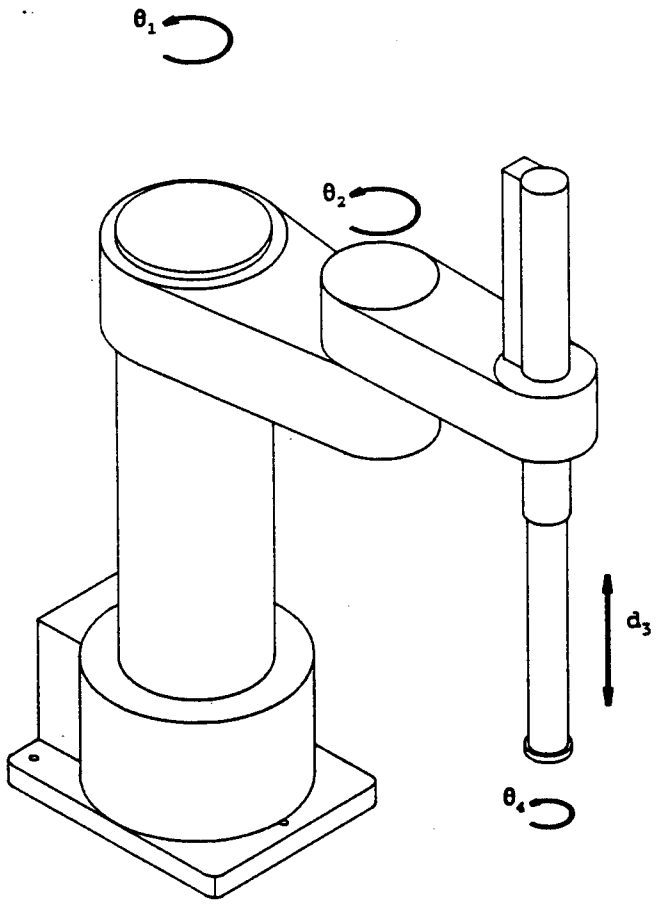

Figure 2.11. AdeptOne SCARA Robot Joint Configuration

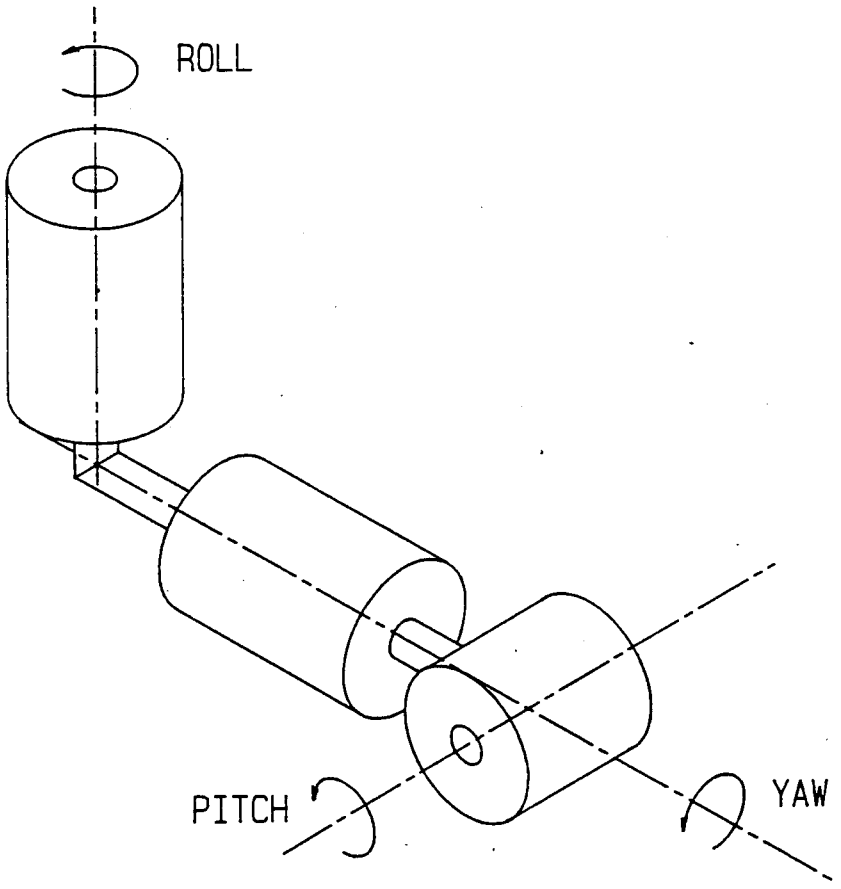

Figure 2.12. End-Effector Orientation Angles on a SCARA Robot

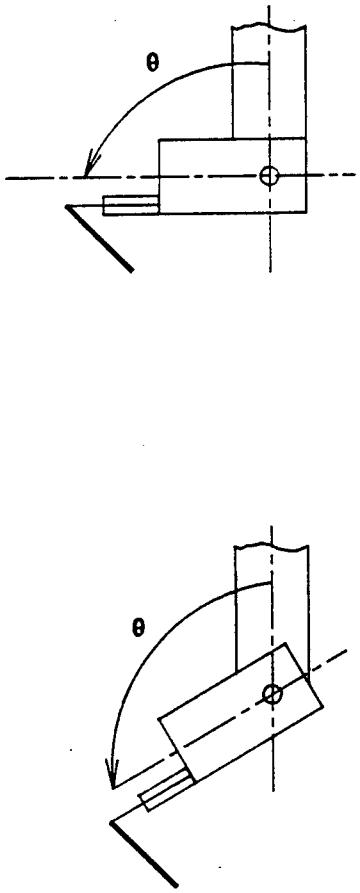

Figure 2.13. Increasing Ply-Separation Using End-Effector Pitch Motion

is oriented to avoid collisions with the turning and pressing machines while loading and unloading the collar.

Conceptual Design Summary

The conceptual design has identified the following manipulation primitives and motion requirements of the end-effector for the three dimensional manipulation of multiple-ply apparel workpieces.

1. Two pinch grippers are required to hold the top ply. The bottom ply is allowed to sag freely, providing ply-separation. The grippers are to accept the workpiece from an external destacking mechanism.

2. The distance between the grippers should be adjustable to stretch the grasped ply. The motion allows control of fabric drape at the collar tips. Variability in the grasp locations enables the end-effector to handle a range of workpiece sizes.

3. A pitch orientation motion is required on the end-effector to orient the grippers for collar acquisition from the destacking and turning machines and to load the grasped collar on the turning and pressing machines. The pitch motion also enables control of the separation between the individual plies of the workpiece.

Figure 2.14 shows a schematic of the conceptual design.

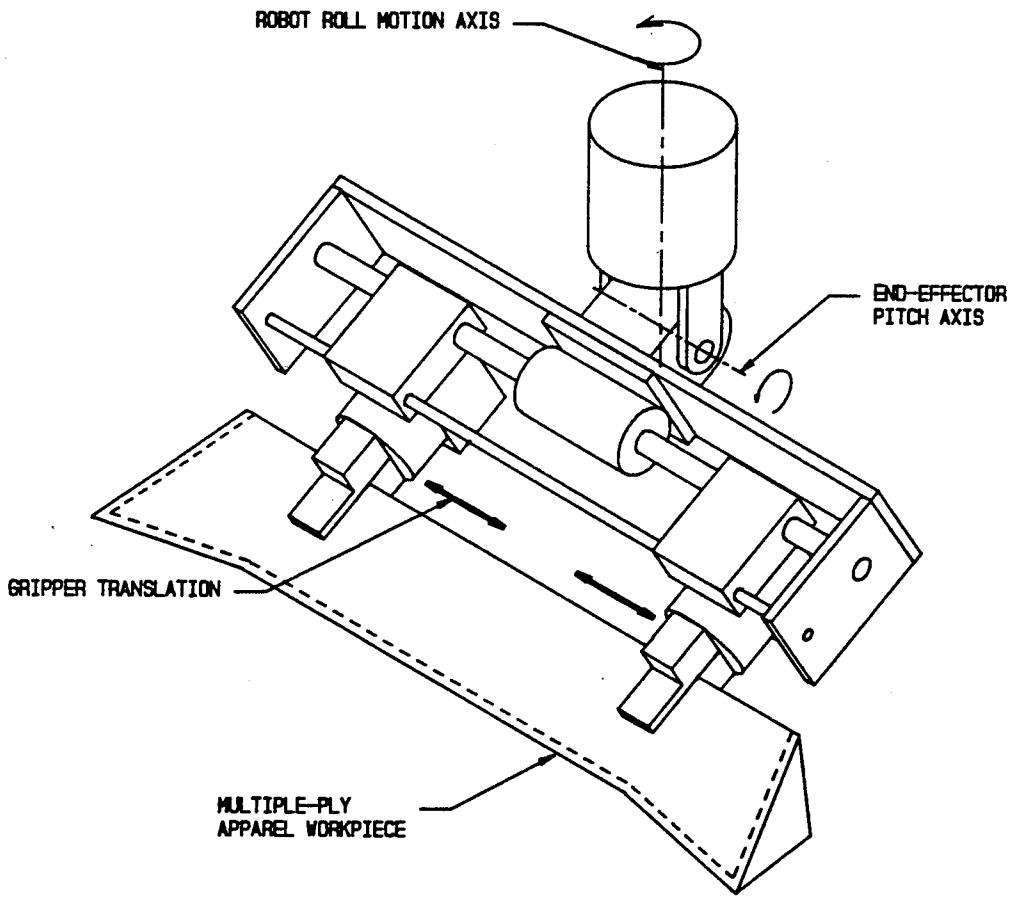

Figure 2.14. Conceptual End-Effector Design

CHAPTER III

MECHANICAL AND CONTROL SYSTEM DESIGN

Introduction

Mechanical and control hardware must be developed to implement the end-effector motions required for the three dimensional manipulation of multiple-ply apparel workpieces. The following factors must be addressed in sequence to effect each of the motions on the end-effector:

1. selection of mechanisms that can physically realize the conceptualized motions,
2. selection of actuators to drive the mechanisms and
3. design of controllers for each actuator.

The design concepts developed in the previous chapter will be demonstrated for robot assisted processing of shirt collars. The required attributes of the end-effector were quantified before developing the detailed design. The end-effector is to be integrated with the robot that assists shirt collar manufacturing operations. The end-effector design considers constraints imposed by the robot workspace and payload. The control system for the end-effector is compatible with the hierarchical control scheme that supervises and controls all operations of the collar processing workstation.

End-Effector Specifications

Specifications were defined that quantified the desired characteristics of each end-effector motion. The specifications satisfy the requirements for shirt collar manipulation since the end-effector is to be integrated with a workstation for processing shirt collars.

The gripper jaw opening should be wide enough so that the collar is reliably grasped by both grippers. The jaws of the two grippers are always at the same horizontal elevation due to the SCARA robot configuration. However, fabric drape is not predictable and maybe greater at one part of the collar than the other. When the workpiece is not horizontal, the end-effector cannot grasp the collar at both locations if the gripper jaws are not wide enough as shown in Figure 3.1. Any errors in the transmission systems of the robot and/or the end-effector joints will manifest itself as an error in the position of the gripper jaw opening. The opening between the two gripper jaws must be wide enough to compensate for these errors. A gripper jaw opening of 0.5 inch appears sufficient to grasp the collar during the processing operations.

Observations indicate that the minimum distance between the grippers while handling the smallest size of collars is about 6 inches and the maximum distance between the grippers while handling the largest size of collars is about 15 inches. Hence, a range of motion that will position the grippers from 6 inches to 15 inches apart relative to one another is

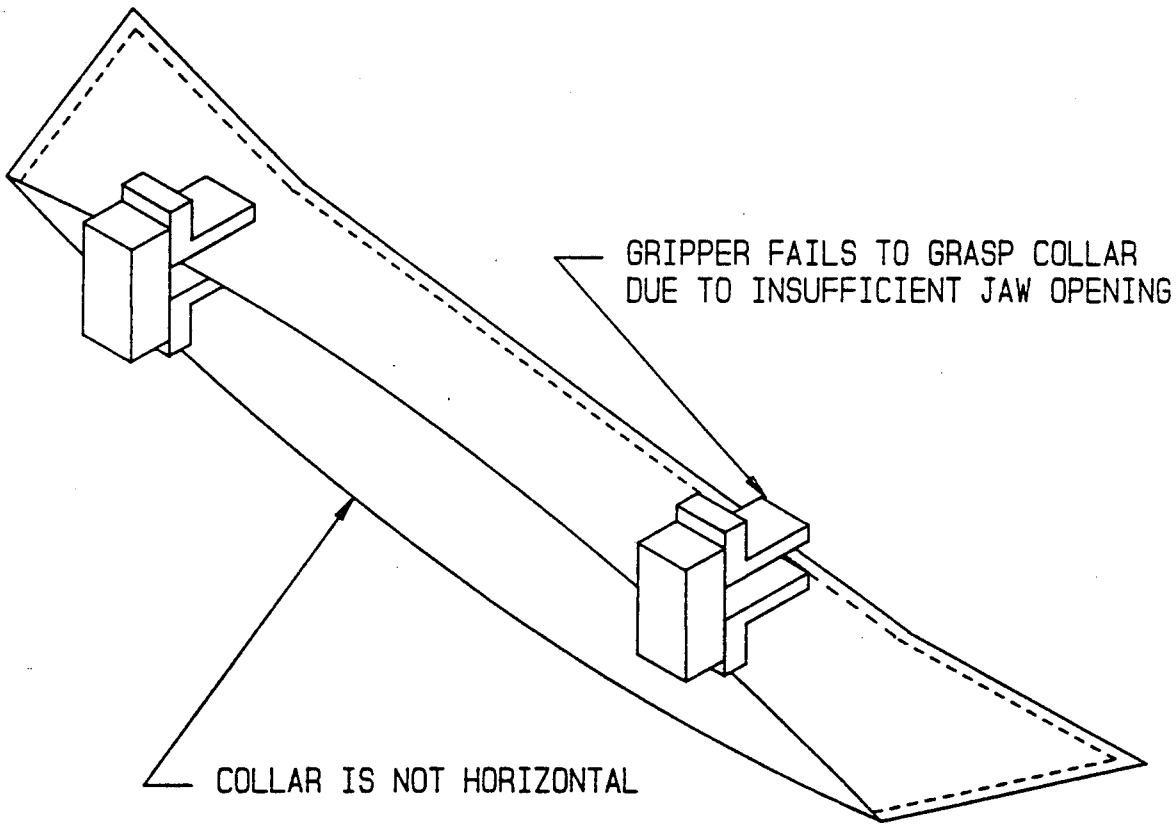

Figure 3.1. Inability of End-Effector to Grasp Collar Due to Insufficient Jaw Opening

adequate. A relative velocity of 2 inches/second between the grippers will ensure quick process execution. The pitch motion is to be designed for a range of +90 to -90 degrees with a maximum speed of +/- 45 degrees/second.

Robot Workspace and Payload

The workspace of the AdeptOne robot is depicted in Figure 3.2. The outer boundary of the robot workspace extends to 31.5 inches from the robot base while the inner boundary is 9 inches from the center of the robot base. The end-effector must be compact so that it does not collide with the robot column when the arm is fully retracted. The payload of the AdeptOne robot is limited to 20 pounds. Since the weight of the apparel workpiece is almost negligible, the weight of the end-effector should be within the robot payload.

Hierarchical Control for the Collar Processing Workstation

A hierarchical semi-autonomous control scheme is proposed for accomplishing the collar processing operations [16]. The hierarchy consists of the strategic planner, system coordinator, and devices that alter the state of the collar. The workstation hardware consists of the robot, end-effector, turning and pressing devices, vision sensors, robot controller, vision controller and system supervisor. Figure 3.3 shows the layout and components of the apparel assembly workstation for processing shirt collars. The strategic planner and system coordinator is implemented on a PC/AT

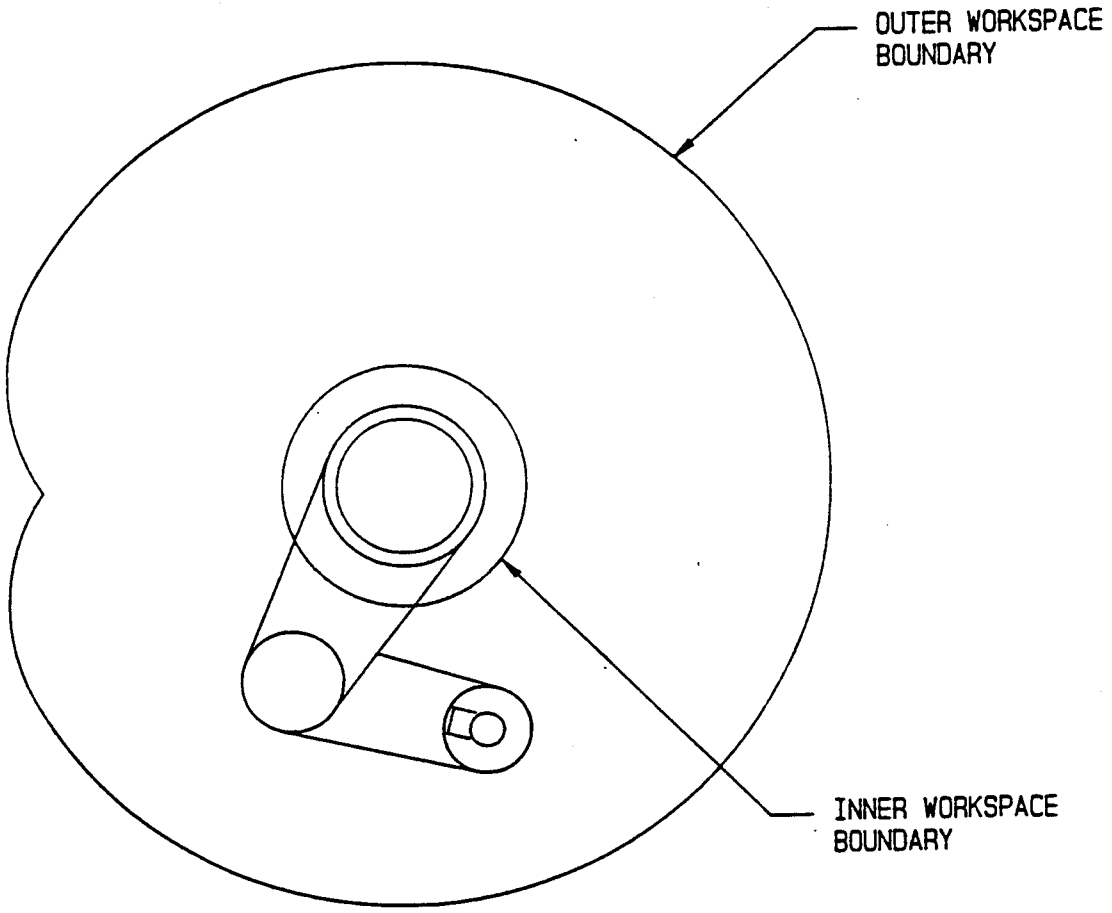

Figure 3.2. Workspace of AdeptOne Robot

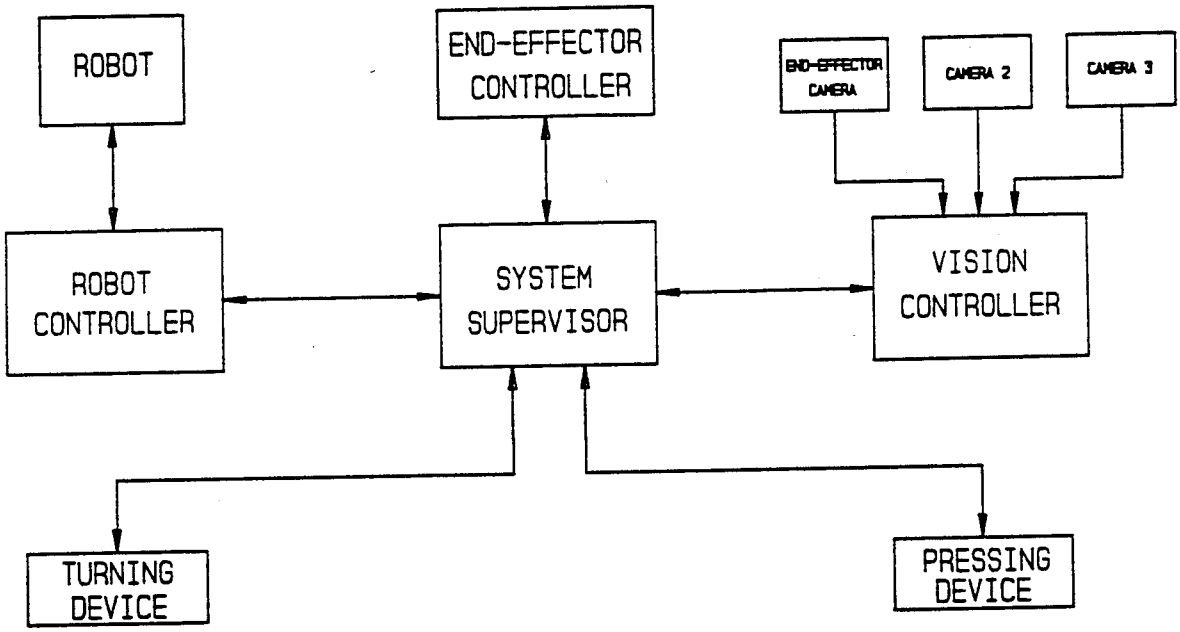

Figure 3.3. Control Hierarchy for the Collar Processing Workstation

compatible computer designated as the system supervisor. The system supervisor communicates with the robot and vision controllers through RS-232 lines. The end-effector and the turning and pressing devices receive commands and report their status through the backplane interface of the PC bus. The operator leads the system through the various steps for collar turning and pressing. The strategic planner determines off-line the plan for all activities which when executed in the correct sequence accomplish the required task. The system coordinator generates commands for each individual activity such as motion, sensing, communication between computers etc.

The end-effector must be capable of interpreting and executing the high level commands issued by the system coordinator. The end-effector controller is implemented on a motion controller board that can control up to eight axes of motion. Figure 3.4 shows the block diagram of the end-effector controller. The motion controller board consists of a 'mother' board that can accommodate up to eight different modules and mounts onto a slot on the backplane of a PC/AT compatible computer. Each module on the mother board is capable of controlling a single actuator. The board also includes 16 lines of digital I/O lines for controlling and recording the status of binary devices and four 8-bit analog to digital converters for data acquisition.

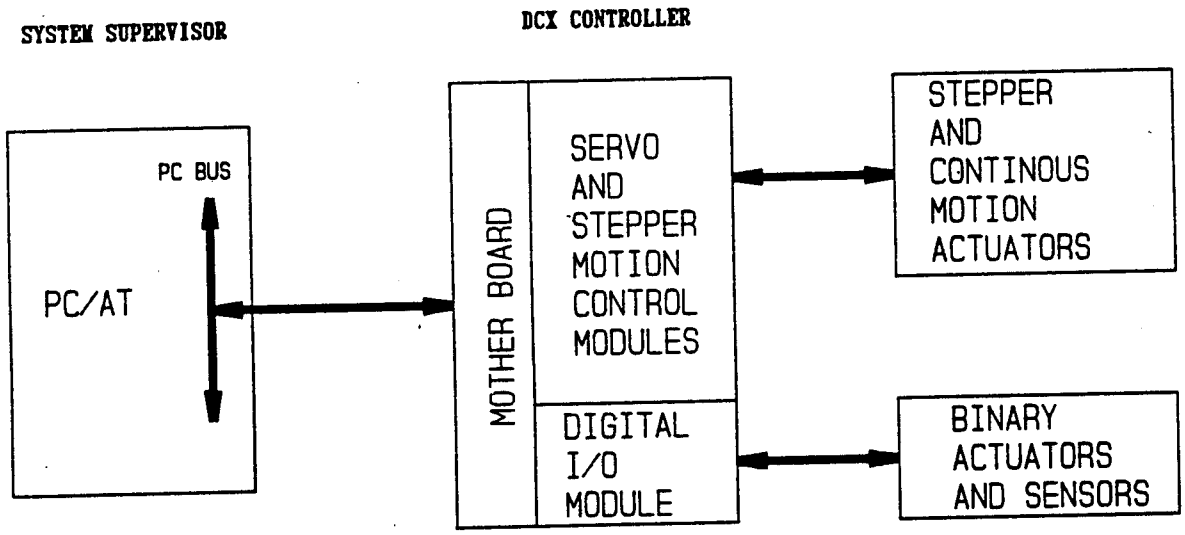

Figure 3.4. End-Effector Controller Block Diagram

Gripping Motion

The end-effector employs pinch grippers to grasp the apparel workpiece. Various mechanisms exist that can accomplish the two jaw gripping action [17]. The gripping action can be implemented either by custom designing the mechanism or by selecting the mechanism from a commercial vendor. Commercial grippers that address the requirements of the application are available in two configurations - parallel and angular motion grippers. Gripping action for angular motions is accomplished by swivelling the gripper jaws about a pivot point. The parallel motion gripper which employs a translatory jaw motion, is chosen for handling collars for the following reasons:

1. Parallel motion type grippers apply a uniform force across the surface area of the gripper jaw.
2. Parallel motion of the jaws provides the opportunity to introduce break beam sensors for future additions to the end-effector design.

Avoidance of collisions of the end-effector with external devices while loading or unloading the collar must be considered in the design of the gripper jaws. An L-shaped jaw design depicted in Figure 3.5 decreases the possibility of the end-effector colliding with the turning and pressing devices. The gripping surface consists of a rubber pad bonded onto an aluminum backing. The rubber pads consist of tiny circular elevated areas that help in trapping the fabric material firmly between the gripper jaws.

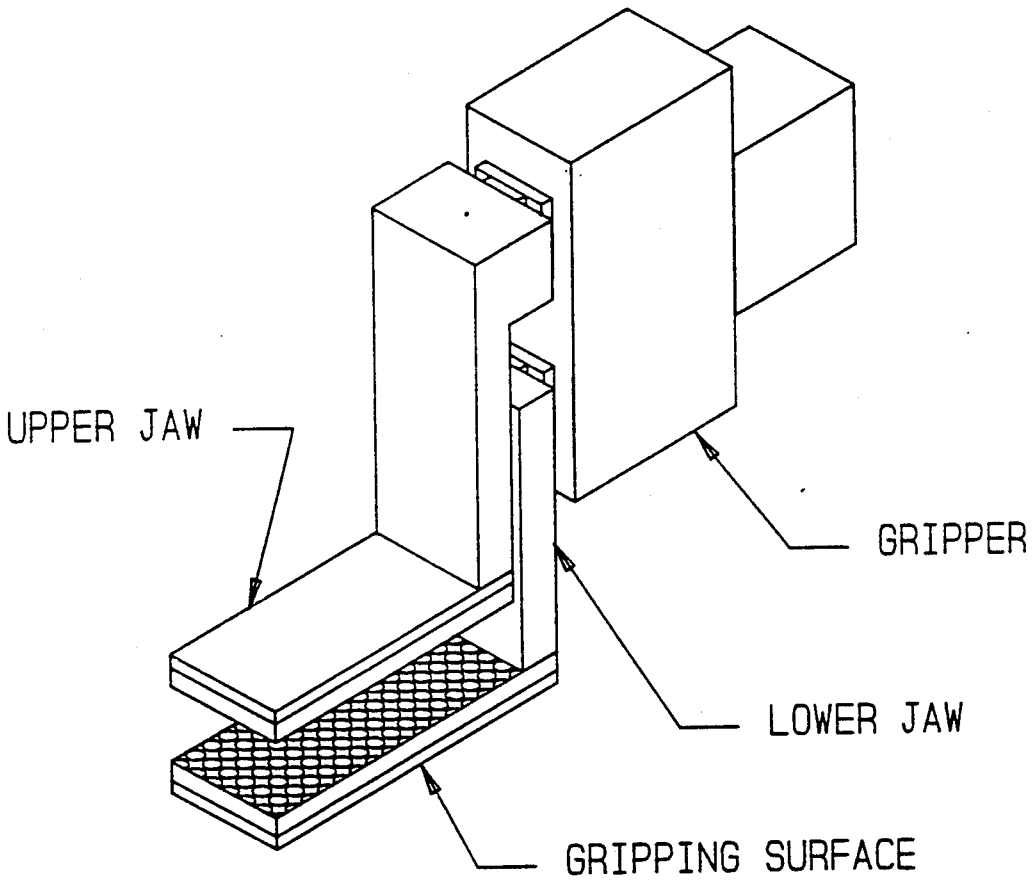

Figure 3.5. L-Shaped Gripper Jaw Design

Control of the grippers could be achieved in a number of ways: electrical, hydraulic or pneumatic. Pneumatic actuators are ideally suited to control the type of two state motion represented by the open and close motion of the grippers. The gripper that was procured has a built-in air cylinder to actuate the gripper jaws. The state of the air cylinder is controlled by pneumatic solenoid valves, directly commanded from the digital I/O lines of the end-effector controller.

The open and close motion of each gripper is controlled independently to correct for possible offset of the grasp locations from the center of the collar as shown in Figure 3.6(a). Since the turning and pressing machines process both collar points simultaneously, it must be ensured that both collar points are loaded correctly on the external processing devices. When the collar is unsymmetrically grasped, transformations of each collar point with respect to the robot wrist have to be determined in turn. This increases the computational burden on the robot controller and will involve additional motions by the end-effector.

The entire process is rendered slower and more complicated due to the unsymmetrical grasping of the collar. This situation can be corrected by actuating the gripper that is closer to the center line of the collar and allowing the other to remain open (see Figure 3.6(b)). Moving the two grippers apart will cause the collar to move with respect to the open gripper as illustrated in Figure 3.6(c). After

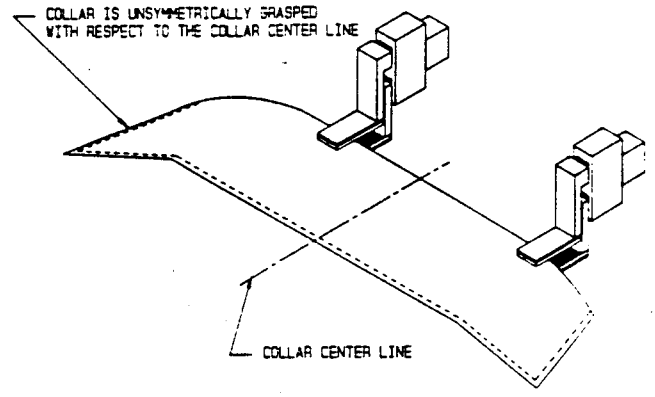

(a)

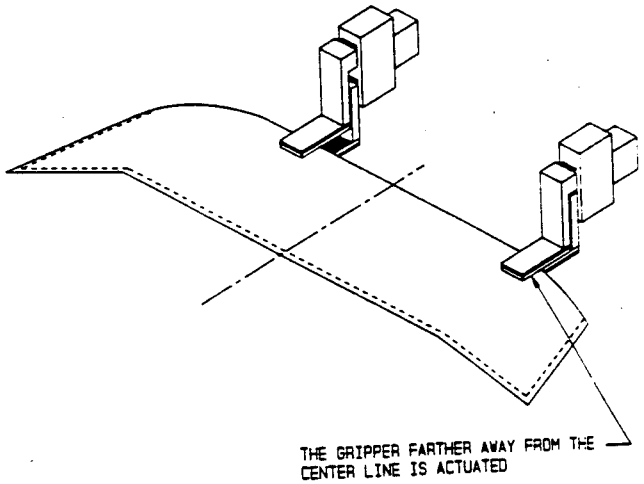

(b)

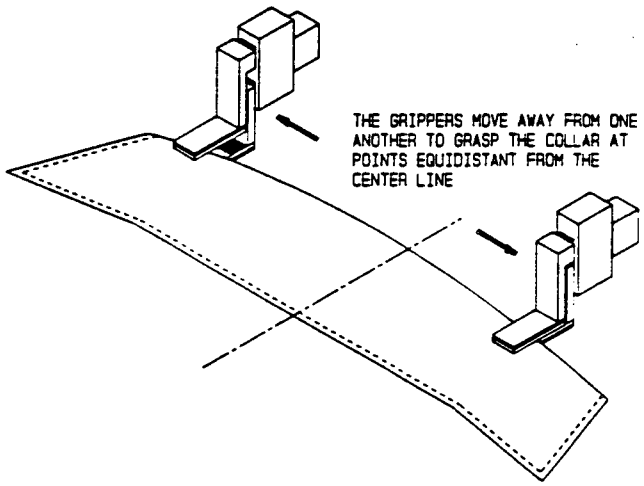

(c)

Figure 3.6. Independent Actuation of End-Effector Grippers to Correct for Unsymmetric Grasping of the Workpiece

moving the grippers so that the center line of the collar is in between the two grasp locations, the open gripper is actuated to grasp the collar.

Lateral Gripper Motion

The motion of the grippers that moves them relative to one another is implemented for the following reasons:

1. to tension the fabric,
2. to be able to handle different collar sizes,
3. to be able to vary the grasp locations during a cycle of operation and
4. to be able to adjust for any unsymmetric grasping of the apparel workpiece.

The lateral motion of the two grippers can be such that (a) each gripper translates independently of the other or (b) the grippers translate simultaneously with respect to one another. Translating the grippers independently of one another will disturb the symmetric location of the grippers with respect to the collar center. The undesirable effects of this situation has been explained in the previous section. Hence the implementation of the lateral gripper motion on the end-effector will be such that the grippers translate simultaneously relative to one another.

Three different mechanisms were considered for implementing the lateral motion of the grippers. Figure 3.7 illustrates a mechanism employing pneumatic actuation of the motion. The pneumatic cylinder transmits motion to the grippers through a cable drive. The return motion of the grippers is actuated by springs. A servo valve continuously

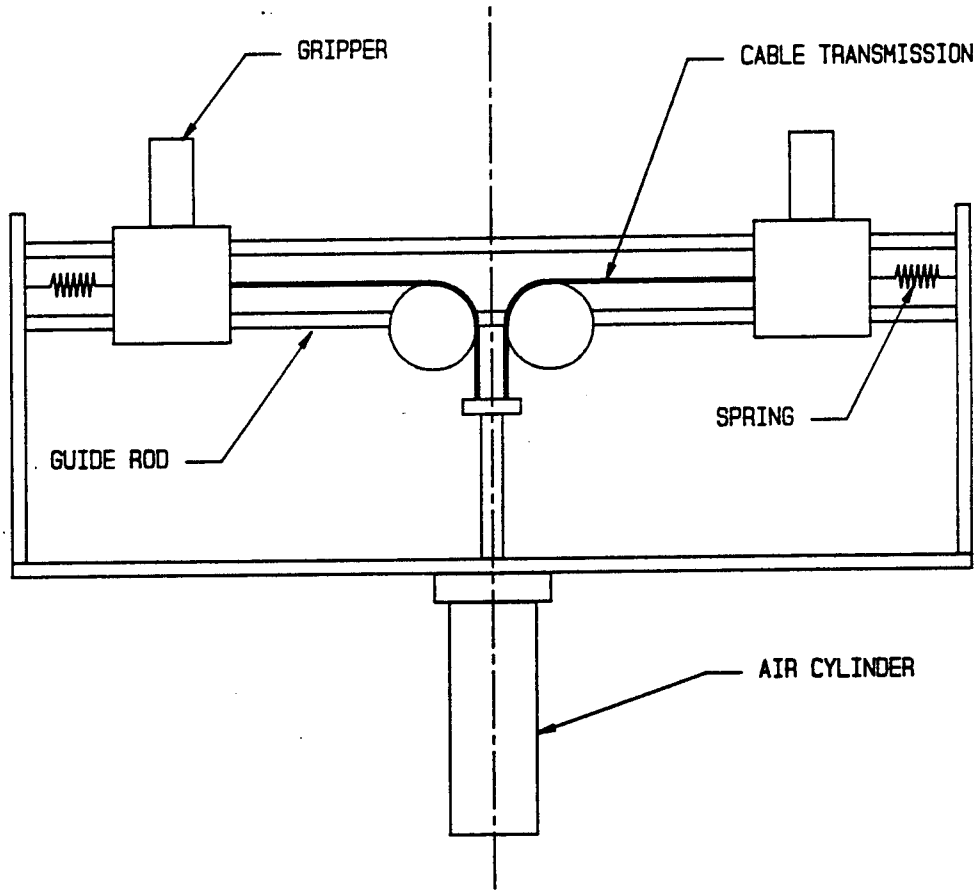

Figure 3.7. Pneumatically Actuated Lateral Gripper Motion

controls the position of the pneumatic cylinder. Feedback is achieved through a linear potentiometer that directly monitors the position of the air cylinder. Pneumatic cylinders are low cost and light weight, and can be easily incorporated in the apparel industry, where typically "shop" air supply is widely available. However, the large dimension of the air cylinder makes the end-effector design bulky and could cause interferences with the robot workspace. Various other problems have been reported with pneumatic servo control of robot mechanisms such as air compressibility and transport delay [18].

The second alternative depicted in Figure 3.8 moves the grippers through a belt drive. The carriages that transport the gripper are attached to segments of the belt that move in opposite directions. The disadvantage of this method is that the unequal pulling forces on the tight and slack sides of the belt may cause different dynamic behavior of the grippers.

The mechanism represented in Figure 3.9 involves the use of an electric motor. The motor actuates left and right hand ball screws so that depending on the direction of motor rotation, the ball nuts move towards or away from each other. The ball screw mechanism was chosen for its low friction, tight tolerances and high efficiency.

The arrangement of the lateral gripper motion as shown in Figure 3.9 occupies considerable space. Since the distance between the grippers is to range from 6" to 15", the

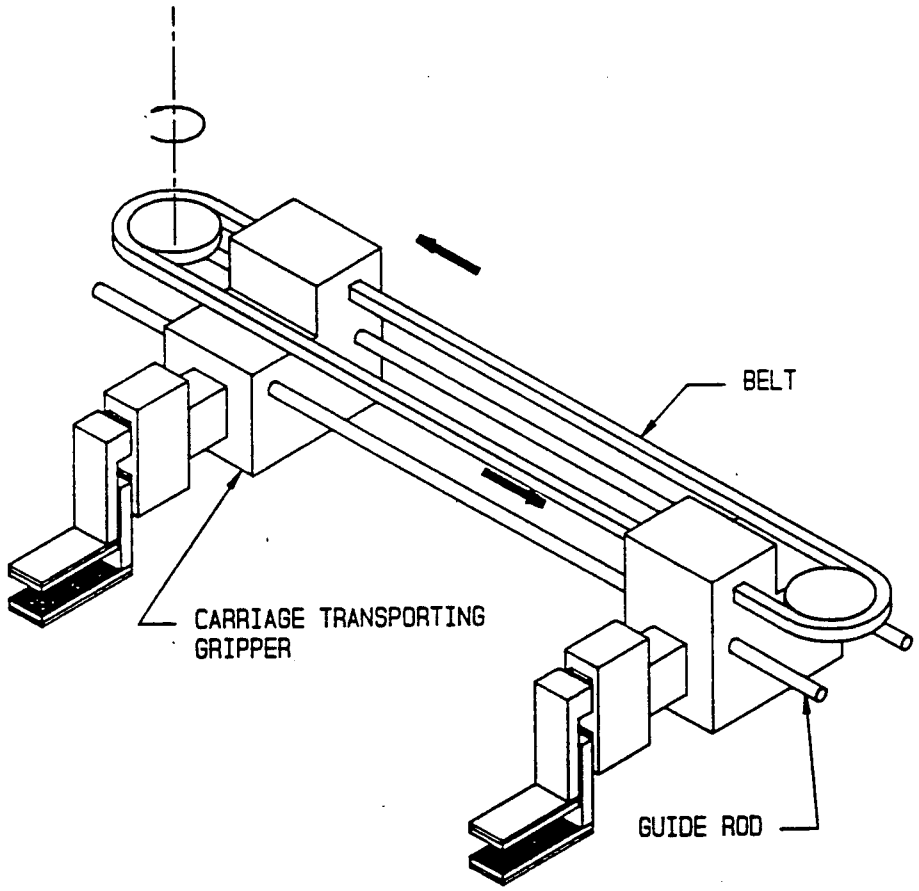

Figure 3.8. Belt Drive for Lateral Gripper Motion Actuation

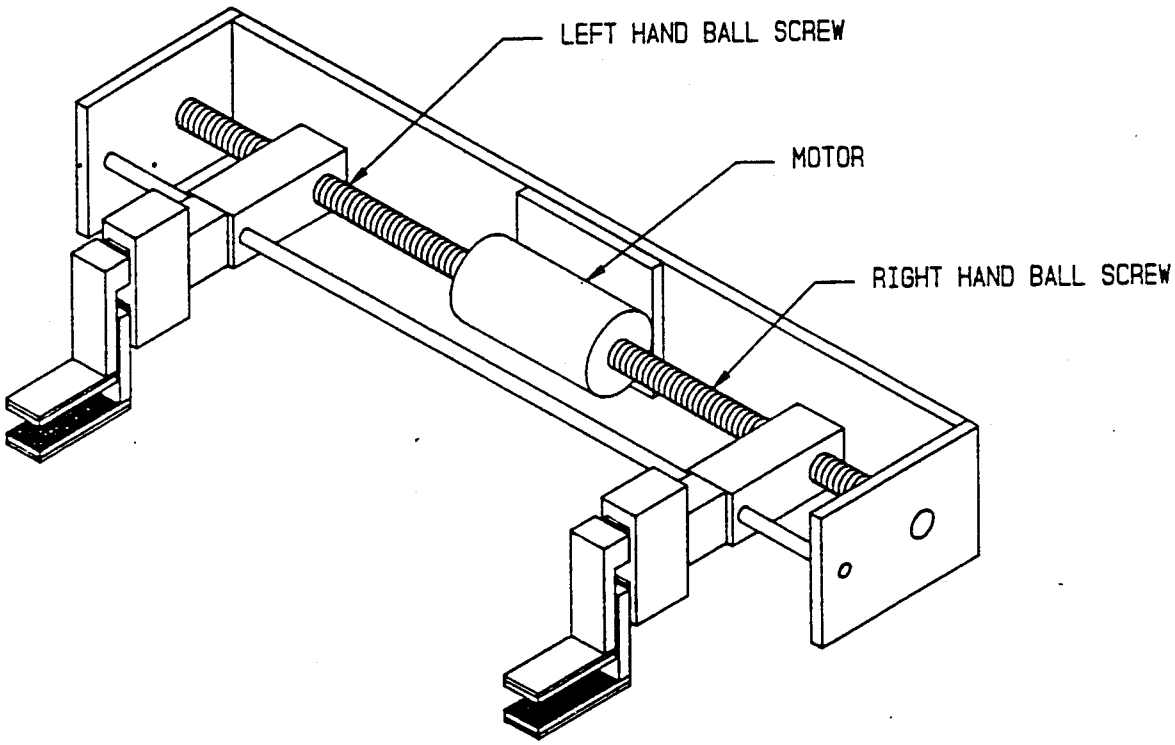

Figure 3.9. Ball Screw Mechanism for Lateral Gripper Motion Actuation

dimension of the end-effector along the direction of motion of the grippers will be at least 15". The clearance between the robot base post and the center of the robot tool post is less than 6" when the robot is fully retracted. As shown in Figure 3.10, execution of a roll motion in this robot position is likely to result in the end-effector colliding with the robot base. To avoid collision with the robot, 'soft stops' nee to be programmed into the robot workspace. Soft stops prevent the robot from accessing certain regions in its workspace. The ball screw mechanism is modified to avoid reducing the operating space of the robot. The grippers can be drawn close together as shown in Figure 3.11(a) when the end-effector needs to perform a roll motion near the inner boundary of the robot workspace, so that the end-effector clears the robot post. Figures 3.11(a) and (b) show the overlapping motion of the ball nuts that enables the end-effector design to be compact.

The selection of the actuator was narrowed to a choice between a stepper motor and d.c. servo motor. Since a more or less uniform torque is required to actuate the lateral gripper motion, it is unlikely that an open loop stepper motor would loose steps. Even a few steps that might be missed would not significantly affect the accuracy of the motion due to the small lead (0.125") of the ball screw mechanism.

The selection of the stepper motor was based on a selection procedure which involves ensuring that the inertia of

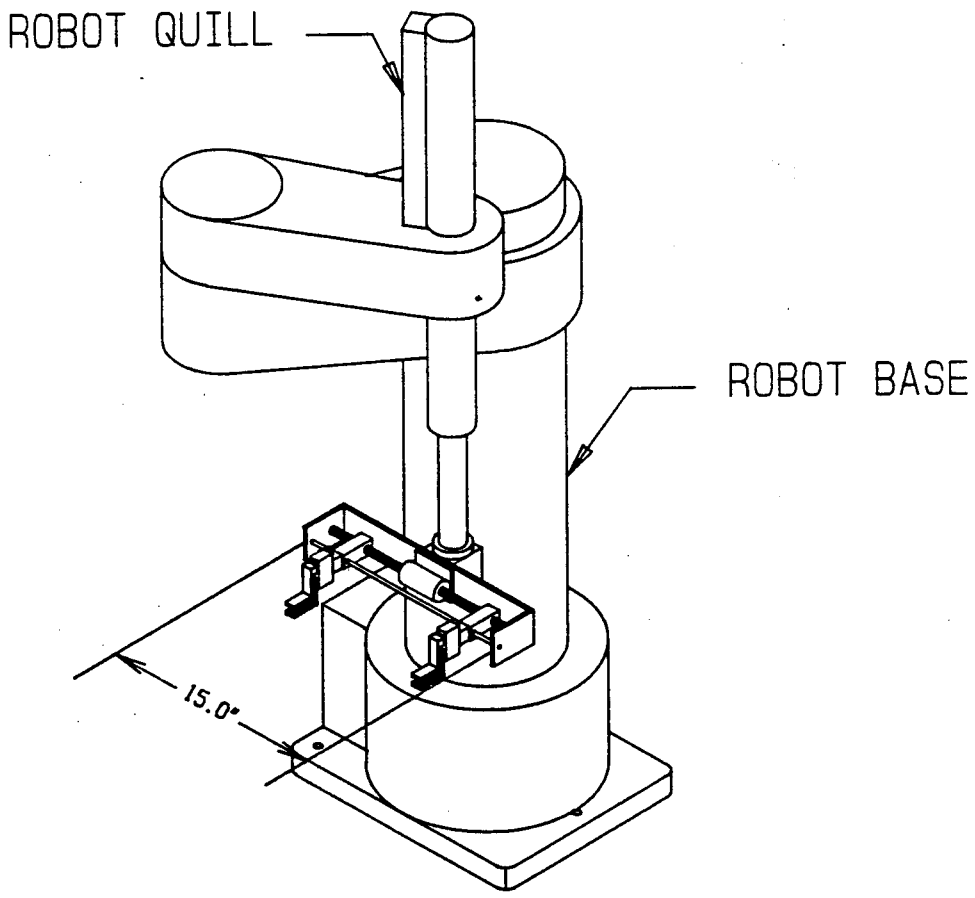

Figure 3.10. Arm Fully Retracted towards Robot Post

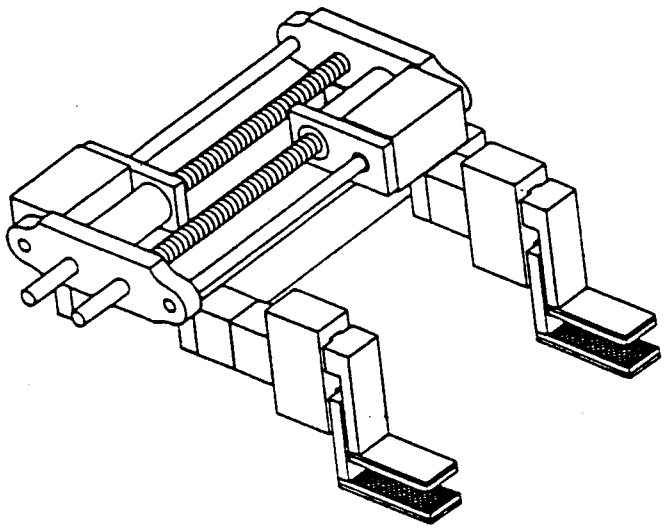

(a)

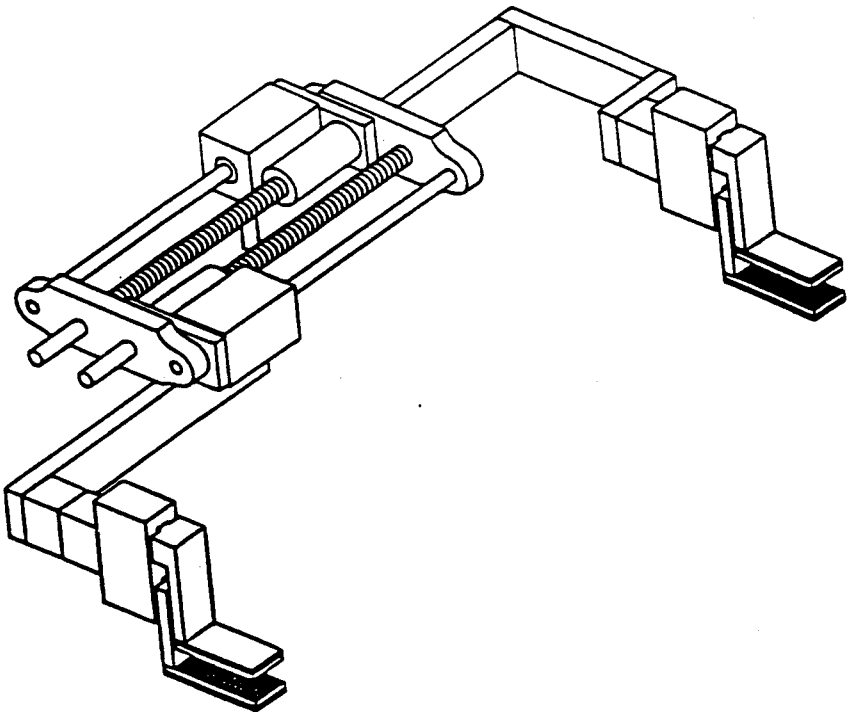

(b)

Figure 3.11. Lateral Gripper Motion Design to Reduce Interference with Robot Workspace

the load and the motor rotor are matched so that resonant conditions do not occur. The selection procedure also ensures that the desired speed and acceleration can be achieved by the candidate motor. A motor-driver package was chosen that satisfied the torque and speed requirements of the application. A two to one speed reduction ratio achieved through a timing belt drive is required to match the load inertia with the inertia of the motor rotor.

The block diagram of the step motor system is shown in Figure 3.12. The system supervisor sends out high level commands to the end-effector controller to actuate the lateral gripper motion. The mother board of the end-effector controller commands the step motor controller module to output the step and direction signals to the motor driver. The driver translates the step and direction signals into the correct motor winding on and off sequences to rotate the motor by the desired number of steps in the required direction. The driver also performs the function of amplifying the signals into voltage levels that can drive the motor. The motor converts the electrical input from the driver into rotational movement. The load represented by the ball screw mechanism driving the grippers is driven by the timing belt.

Pitching Motion

The pitching motion of the end-effector was implemented for the following reasons:

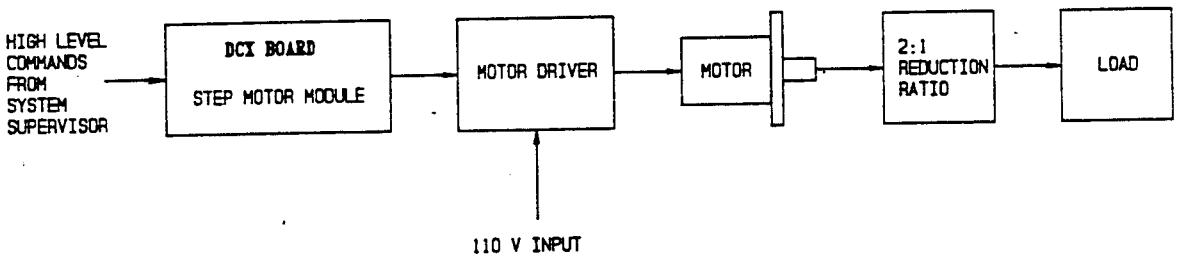

Figure 3.12. Block Diagram of Lateral Gripper Motion

1. to correctly orient the grippers prior to acquiring the collar from the destacking device and the turning machine,

2. to align the grasped collar on external processing devices and

3. to increase or decrease the opening between the workpiece plies.

The initial design concept considered for the pitch motion is shown in Figure 3.13. This design requires the motor actuating the pitch motion to support the large static imbalance torque developed because of the mass of the grippers and the mechanism that moves the two grippers laterally with respect to each other. The maximum torque required by the actuator can be reduced by bringing the center of gravity of the end-effector as close as possible to the pitch axis. The center of gravity of the end-effector can be shifted closer to the pitch axis by using a counterbalancing mass.

The strategy adopted to counterbalance the gripper mass is illustrated in Figure 3.14. Motion is transmitted from the motor to the pitch axis by a positive belt drive. The driven pulley is fixed relative to a non-rotating shaft. A torque applied at the axis of the rotating pulley develops a reaction moment about the shaft axis causing the end-effector to swivel about the axis. Since the motor is mounted on the opposite side of the gripper mass, it acts as a counterbalance to the rest of the end-effector mass.

Two types of motors, d.c. servo and stepper motors, were considered to actuate the pitch motion. Step motors do not perform well when required to handle large inertial loads.

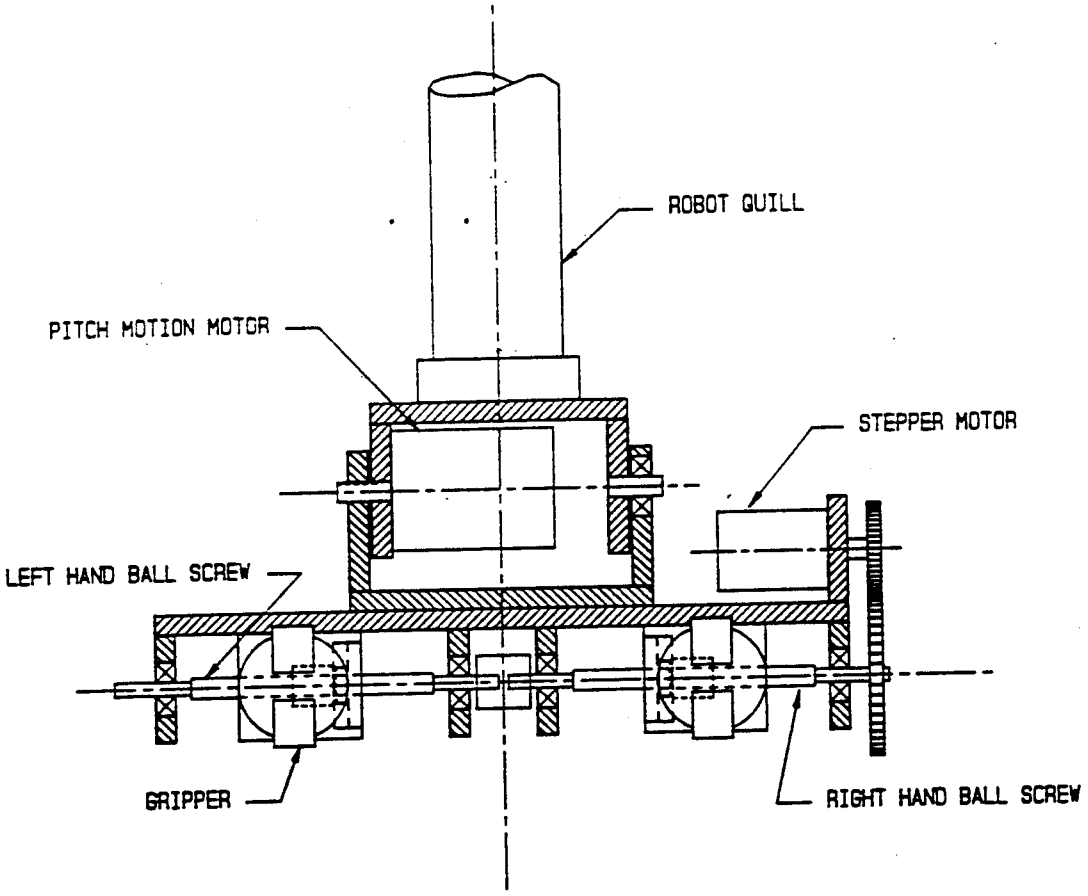

Figure 3.13. Preliminary End-Effector Design

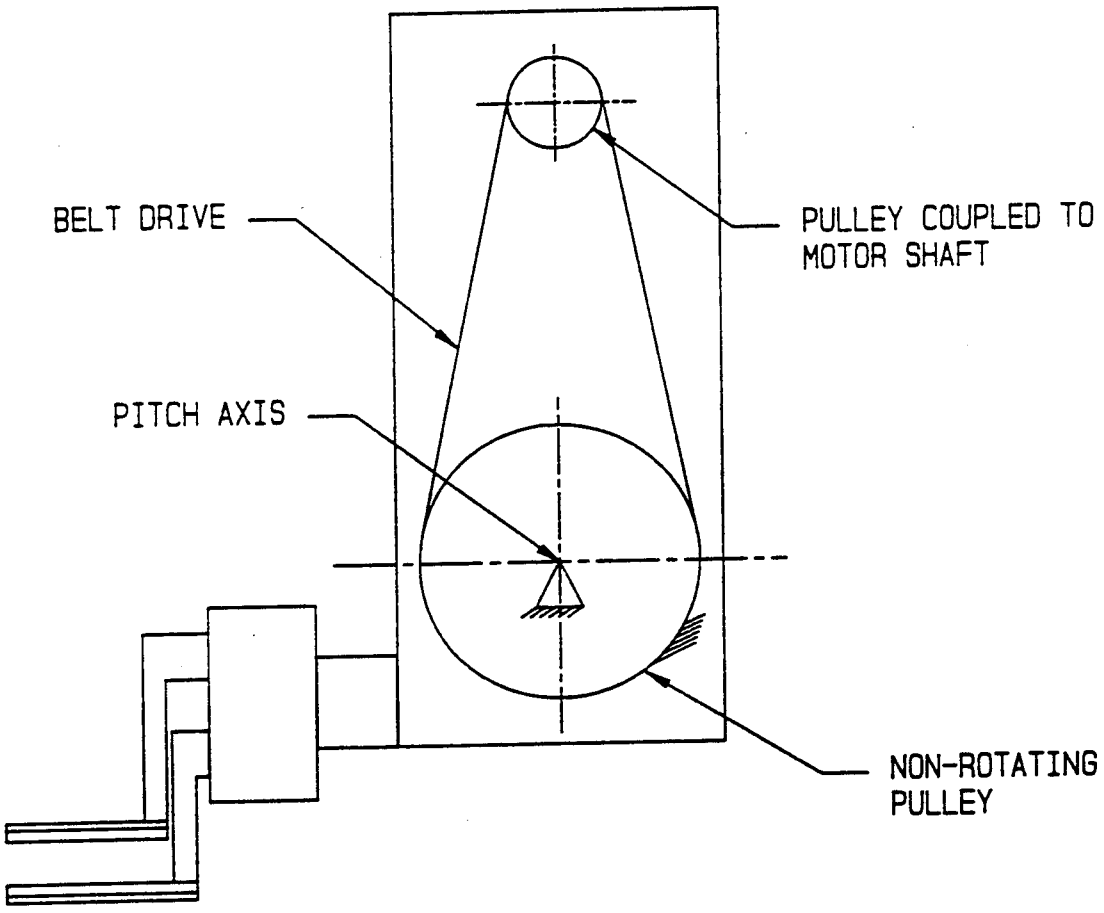

Figure 3.14. End-Effector Pitch Motion Incorporating Counterbalancing Concept

Steps missed by a step motor due to temporary overloads would cause loss of positional information of the pitch axis. This uncertainty about the status of the pitch motion is likely to lead to poor end-effector performance. Hence, a d.c. servo motor with a position feedback sensor was chosen as the actuator for the pitch motion.

A gear ratio was chosen to ensure that the inertia of the motor matched the reflected inertia at the pitch axis. Two possible candidates were considered for implementing the gear ratio: planetary gearhead and harmonic drive. The planetary gearhead was chosen for its low backlash, high efficiency, low cost, compact size and its integration with the servo motor. A gear ratio of 105:1 was determined to be required; the ratio is divided between the planetary gearhead (35:1) and the positive drive belt (3:1). The division of the gear ratio causes the reflected backlash (of the gearhead) to be reduced in the 3:1 ratio at the pitch axis.

A linear servo amplifier operating in a torque control mode drives the d.c. motor. An optical incremental encoder with quadrature output performs the function of the position feedback device. Angular positional information can be obtained either at the motor axis or at the axis of the pitch motion. Locating the encoder at the motor shaft provides more encoder counts per degree of rotation of the pitch axis due to the large gear ratio. The resulting increased resolution of the position measurement improves the accuracy of the pitch motion. However, backlash and compliance present in

the transmission system cannot be sensed by an encoder mounted at the motor axis.

Mounting the encoder at the axis of rotation can compensate for backlash and compliance present in the load system; however, the decreased resolution and the tendency of the mechanism to hunt for the desired position requires the location of the encoder at the axis of the motor shaft. Encoder signals are read by a position counter, detecting each logic transition occurring at the quadrature inputs. This increases the resolution of the encoder by a factor of four.

The control system block diagram for the pitch motion is shown in Figure 3.15. The servo module on the end-effector controller board contains a trapezoidal velocity profile generator. A digital Proportional-Derivative-Integral control algorithm is implemented in the module according to the following equation:

$$u(kT) = K_p e(kT) + K_i \sum_{k=0}^{k} e(kT) + K_d[e(kT')-e(k-1)T'] \quad (3.1)$$

where

K_p = proportional gain,

K_d = derivative gain,

K_i = integral gain,

e(kT)= error signal at instant kT,

T = sampling time, and

T' = sampling time for the derivative part.

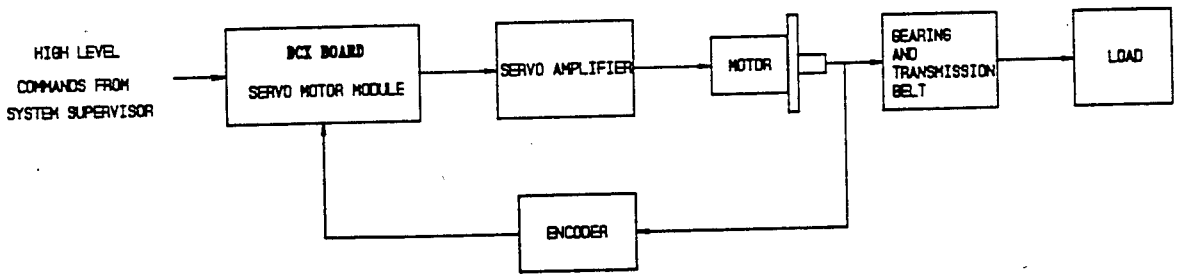

Figure 3.15. Block Diagram of Pitch Motion System

The proportional term provides a signal that is proportional to the position error. The derivative term provides rate feedback information by increasing the apparent system damping. The integration term ideally drives the error to zero. (However, presence of coulomb friction and dead zones in real systems causes a small steady state error to be present.)

Analysis of Pitch Motion

An analysis of the pitch motion was conducted to understand the kinematic and dynamic characteristics of the counterbalancing concept. The kinematic relationship between the angular rotation of the motor shaft and the pitch displacement is shown in Figure 3.16. The kinematic equation of the pitch motion is given by

$$\frac{\dot{\phi}}{\dot{\theta}} = \frac{R}{r} = 1 \quad . \tag{3.2}$$

The absolute angular velocities of the motor shaft and the pitch rotation are $\dot{\phi}$ and $\dot{\theta}$ respectively. The radii of the non-rotating and rotating pulleys are R and r respectively.

The following assumptions were made in the derivation of the end-effector pitch dynamic equations of motion:

1. The dynamics of the robot and the end-effector are decoupled. This is true during most motion trajectories involving simultaneous end-effector and robot motion. The end-effector executes the pitch motion during collar loading or unloading operations on external processing devices, during which times the robot links are either stationary or moving at very low velocities.

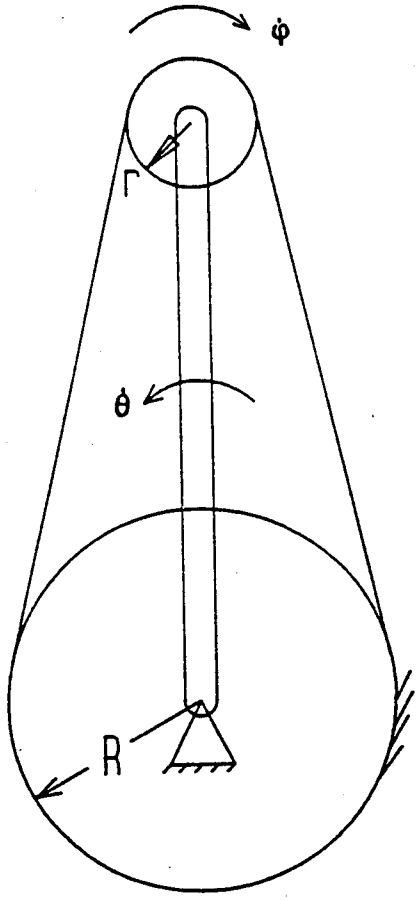

Figure 3.16. Kinematic Relationship between Pitch and Motor Shaft Angular Velocities

2. Belt compliance and torsional deflections of the transmission, backlash in the motor gearbox, friction at the motor shaft and damping at the pitch load shaft are assumed negligible.

3. The end-effector mass is assumed to be concentrated at a single point.

The conceptual model of the end-effector depicting the angular displacements, system parameters and external forces acting on the system is shown in Figure 3.17. The equation of motion of the end-effector pitch rotation, derived in Appendix A, is given by

$$J\ddot{\theta} + D\dot{\theta} + W_T a\sin\theta - W_T b\cos\theta = \tau \quad , \tag{3.3}$$

where J is the equivalent moment of inertia of the end-effector reflected at the pitch axis given by

$$J = J_m n_p^2 \left(\frac{R}{r}-1\right)^2 + m_T(a^2+b^2) \quad . \tag{3.4}$$

The total weight W_T of the end-effector acts through the center of gravity whose coordinates are a and b respectively.

The equivalent damping, D, at the pitch axis is given by

$$D = D_m n_p^2 \left(\frac{R}{r}\right)^2 \quad . \tag{3.5}$$

The reflected torque, τ, at the axis of rotation is given by

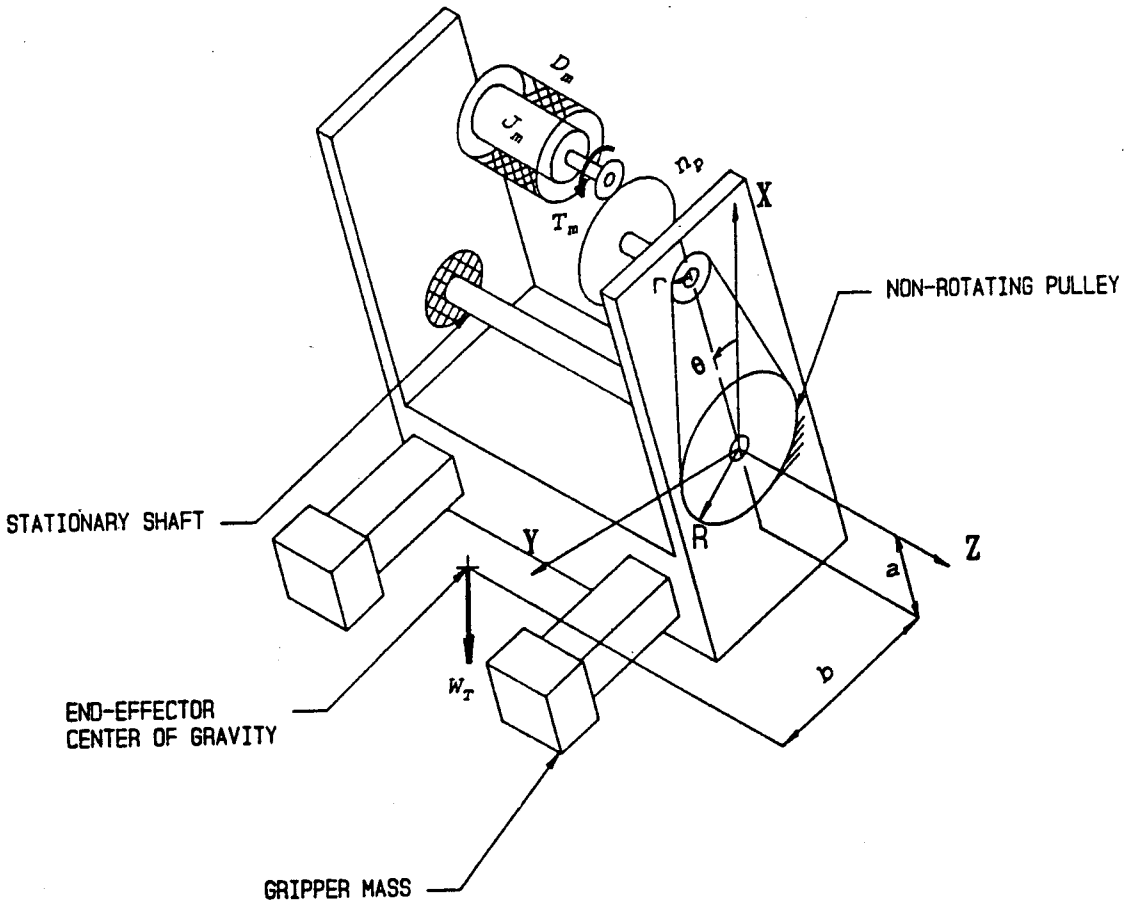

Figure 3.17. Conceptualization of End-Effector Pitch Motion

$$\tau = T_m n_p \frac{R}{r} \tag{3.6}$$

where T_m is the torque generated by the motor and n_p is the transmission ratio of the planetary gearhead.

The end-effector parameter values are listed in Table I, and their computation given in Appendix B. Figure 3.18 shows the simulation block diagram of Equation (3.3), which is non-linear due to the presence of the sine and cosine terms. Linearization of Equation (3.3) about the equilibrium position of the end-effector, θ_o gives

$$J\ddot{\hat{\theta}} + D\dot{\hat{\theta}} + (W_T a\cos\theta_o + W_T b\sin\theta_o)\hat{\theta} = \hat{\tau} \quad . \tag{3.7}$$

The displacement of the end-effector in the equilibrium position is shown in Figure 3.19. The transfer function of the linearized end-effector dynamics is given by

$$\frac{\hat{\theta}(s)}{\hat{T}_m(s)} = \frac{158.1}{s^2+70.5s+18.1} \quad . \tag{3.8}$$

The input to the open loop model of the end-effector is the torque applied by the pitch motor and the output is the pitch displacement of the end-effector. The roots of the characteristic equation of Equation (3.8) are

$$s_1 = 70.25$$

$$s_2 = 0.25 \quad .$$

Table I. End-Effector Parameters

Quantity	Value	Units
R	2.674	inches
r	0.891	inches
n_p	35.0	-
J	0.664	lb-in-sec^2
D	46.86	lb-in-sec
W_I	8.0	lbs
a	0.75	inches
b	1.30	inches

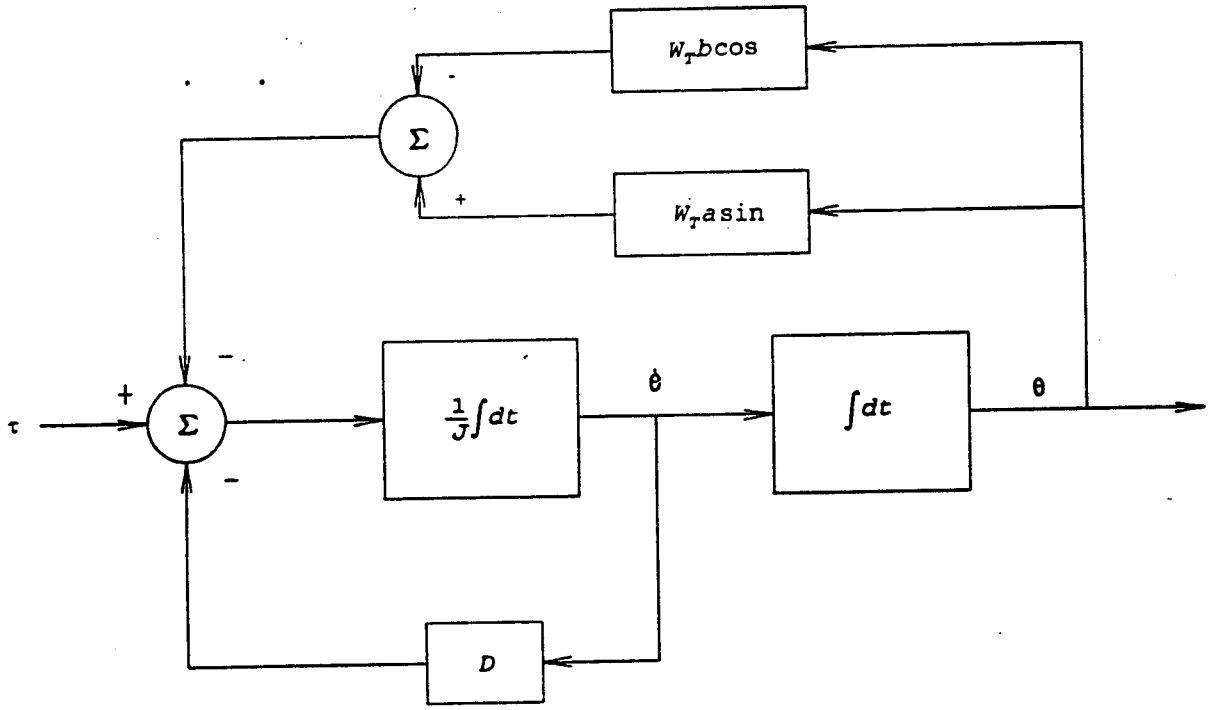

Figure 3.18. Simulation Block Diagram of Non-Linear End-Effector Dynamics

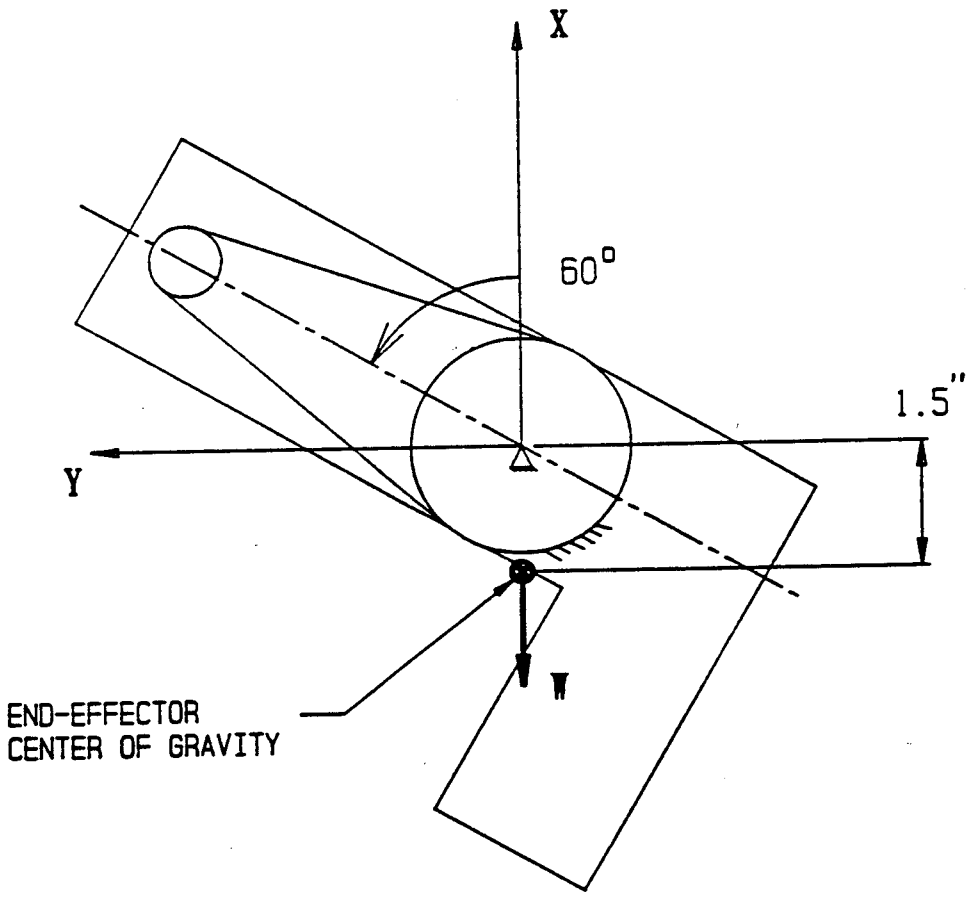

Figure 3.19. End-Effector Equilibrium Position

Since one of the roots (s_1) lies far to the left of the imaginary axis in the s-plane, the end-effector dynamics is dominated by the slower root (s_2). The system can then be analyzed as a first order system whose transfer function can be approximated by

$$\frac{\hat{\theta}(s)}{\hat{T}_m(s)} = \frac{8.75}{(4.0s+1)} \quad .$$

The time constant of this first order approximate system is 4.0 seconds.

The linearized simulation block diagram of the end-effector system is shown in Figure 3.20. A pulse torque input is applied to the system. The width of the input pulse is kept constant at 0.1 seconds while the amplitude of the pulse is varied for different simulation runs. Simulations are carried out with the end-effector initially at its equilibrium position. The response of the non-linear and linearized end-effector dynamic equations to a pulse torque input with an amplitude of 0.4 in-lb is shown in Figure 3.21(a). The system requires approximately 20 seconds to come to rest because of the long time constant.

For torque inputs with pulse amplitude less than 0.4 in-lbs, resulting in approximately 45 degrees angular displacement from its equilibrium position, the two response curves are similar, confirming that the non-linear model of the end-effector can be approximated by the linearized model. At greater torque input levels (>1.0 in-lb), the response of the

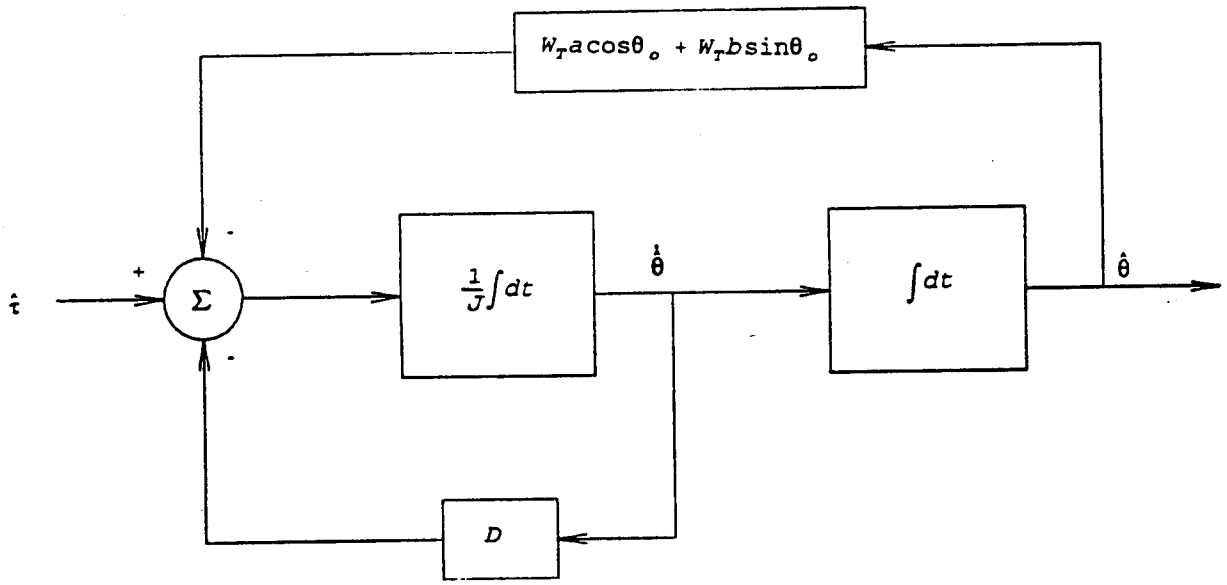

Figure 3.20. Simulation Block Diagram of Linearized Pitch Motion Dynamic Equation

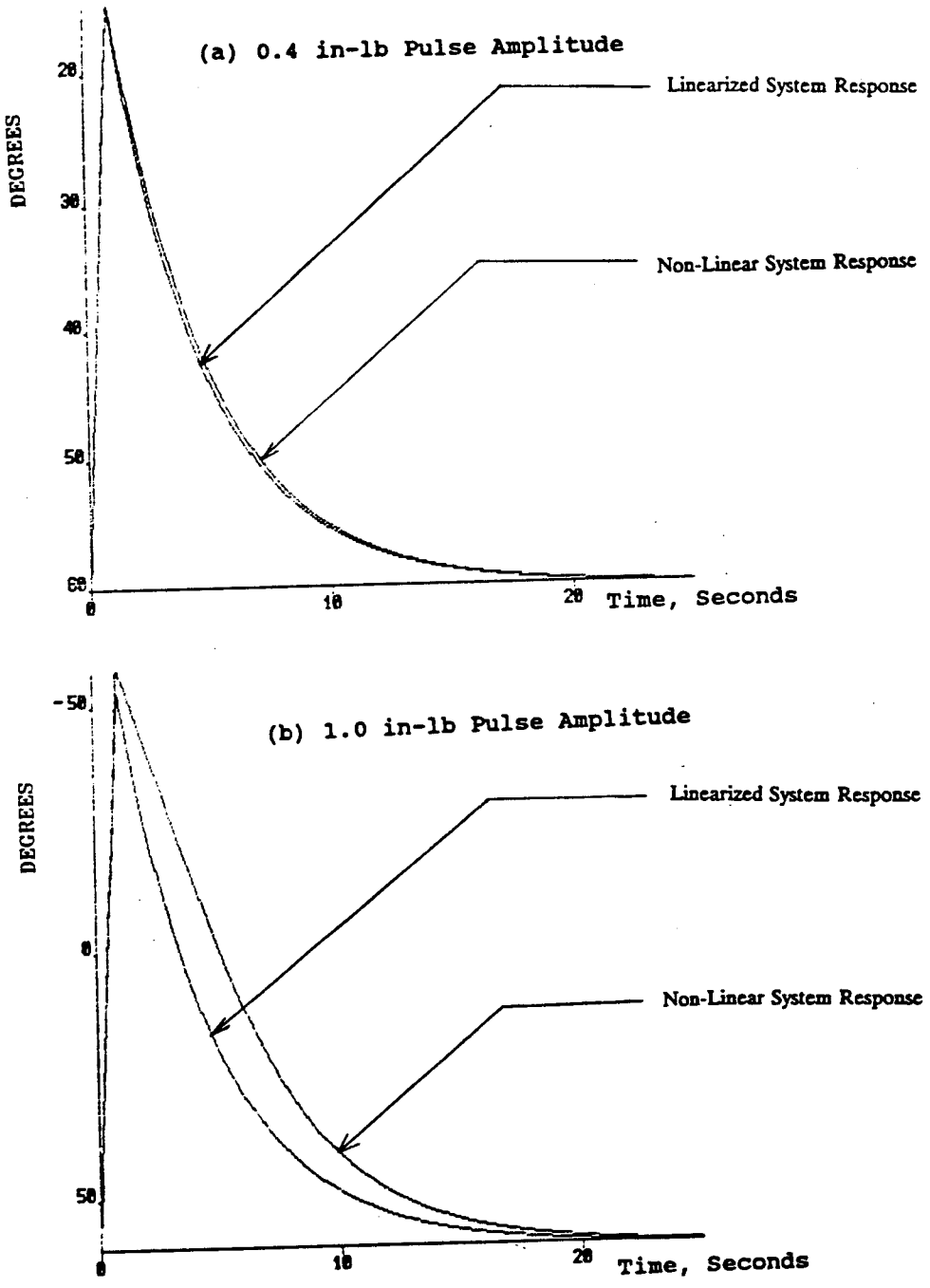

Figure 3.21. Simulated Response of End-Effector to Pulse Torque Input

linearized system differs significantly from the non-linear model of the end-effector as seen from Figure 3.21(b).

Design Summary

The mechanical component design of the end-effector was accomplished using CADKEY, a three dimensional computer aided design and drafting package. Figure 3.22 shows the design of the end-effector in three dimensional form. The end-effector was fabricated using 6061T aluminum to minimize its weight. The design weight of the end-effector was estimated to be less than 10 pounds. A camera was mounted on the end-effector to provide visual feedback of the turning and pressing processes. Figure 3.23 shows the end-effector mounted on the AdeptOne robot.

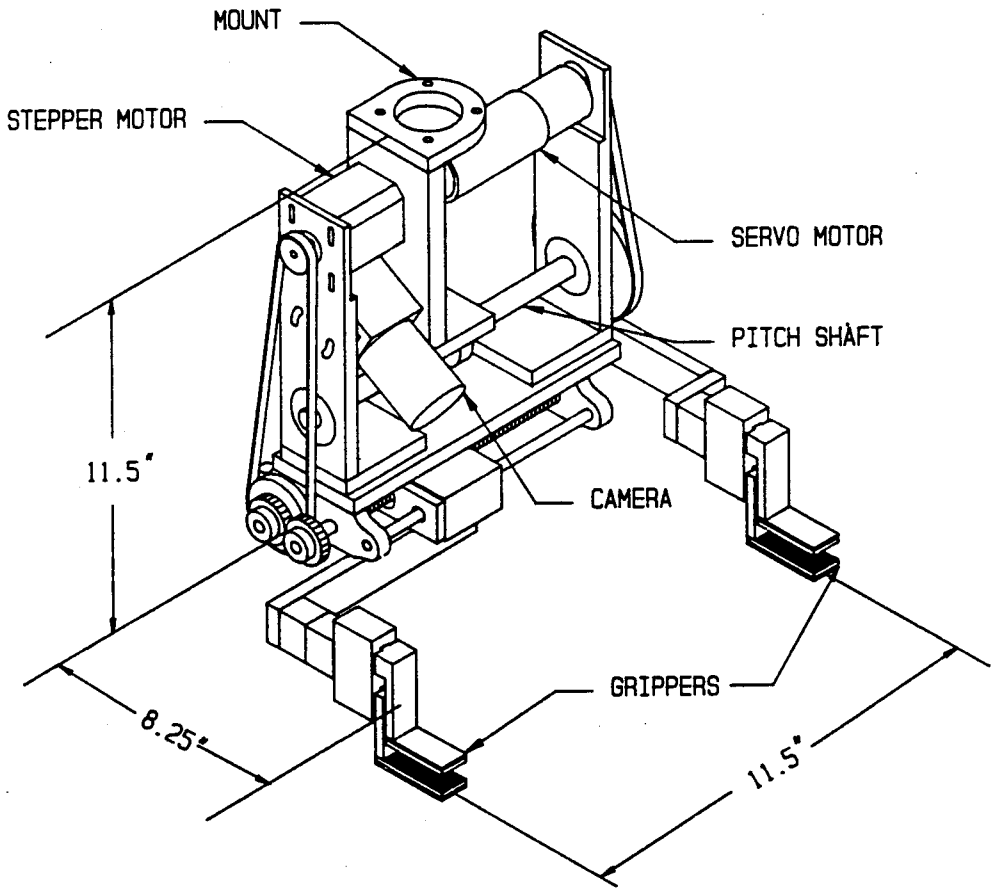

Figure 3.22. End-Effector Design Configuration

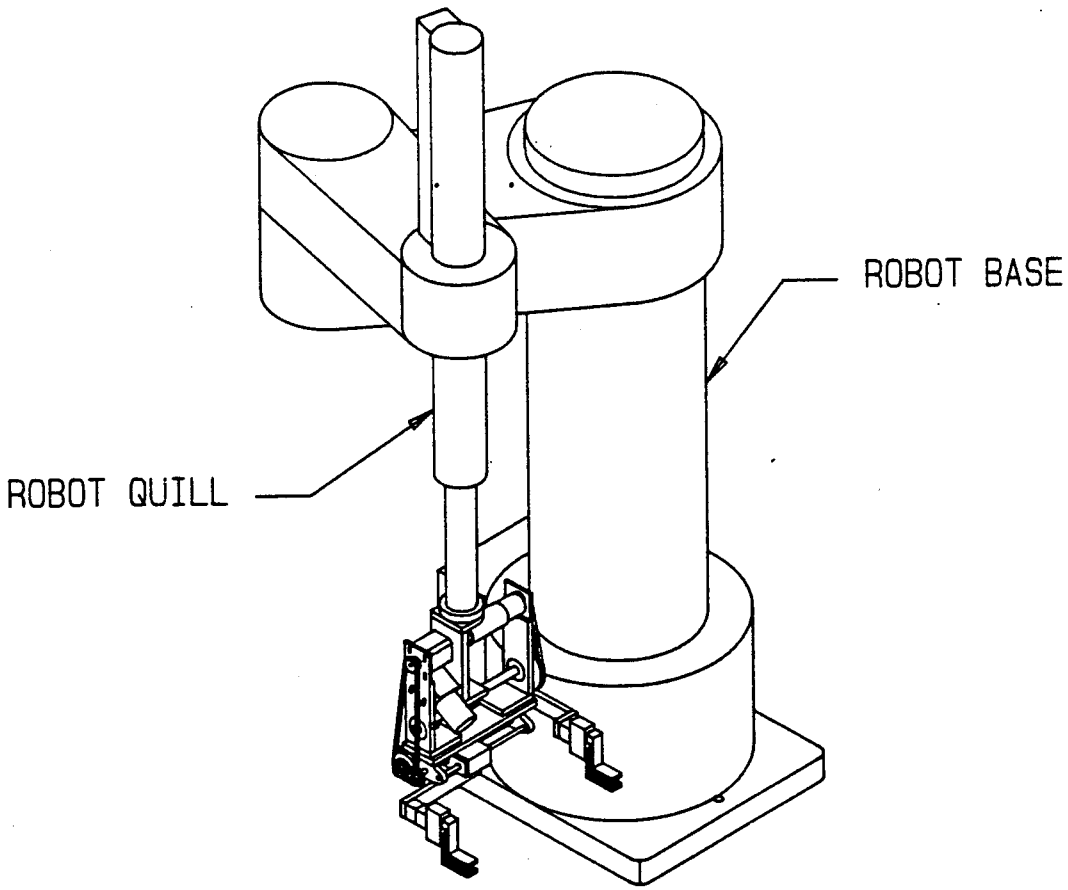

Figure 3.23. End-Effector Mounted on AdeptOne Robot

CHAPTER IV

PERFORMANCE EVALUATION

The pitch motion of the end-effector is controlled through a closed loop control system. The controller gains were determined analytically after modelling individual system components. Non-linearities present in the system were not investigated. The analysis results were verified by digital computer simulation of the modelled control system, and by observing the experimental response of the actual system.

The lateral gripper motion is actuated by a step motor operating in an open loop mode. The command velocity and acceleration values that provide the fastest gripper translation without causing the step motor to loose steps must be determined. This requirement is accomplished using an experimental procedure.

Experimental runs were conducted involving the manipulation of a shirt collar using the developed end-effector. The success of the demonstrations confirm the validity of the end-effector design concepts.

Pitch Motion Control System Analysis and Testing

Analysis

The end-effector pitch motion is implemented through a closed loop control system. The open-loop dynamics of the

pitch motion was developed in the previous chapter. The dynamic equation of pitch motion was linearized and its response to a pulse torque input studied. The response of the linearized model was shown to closely resemble the non-linear model response for the same input provided the pitch displacement was less than 45 degrees.

The following control system criteria were specified to obtain satisfactory end-effector pitch motion performance during manipulation operations:

1. The transient response of the system must be critically damped.
2. Steady state position error is to be less than 0.1%.

The block diagram of the pitch motion control system is shown in Figure 4.1. The following assumptions and approximations were made in the analysis of the control system:

1. Saturation effects in the system are neglected.
2. The DCX servo controller is modelled in the continuous time domain since the sampling time of the controller is extremely small (340 microseconds).
3. The dc servo motor and servo amplifier are modelled as static elements i.e., the electrical power amplifier dynamics are fast compared to the mechanical system dynamics.

Initially, a proportional controller with a gain K_p is used in the control system. The closed-loop transfer function of the system is given by

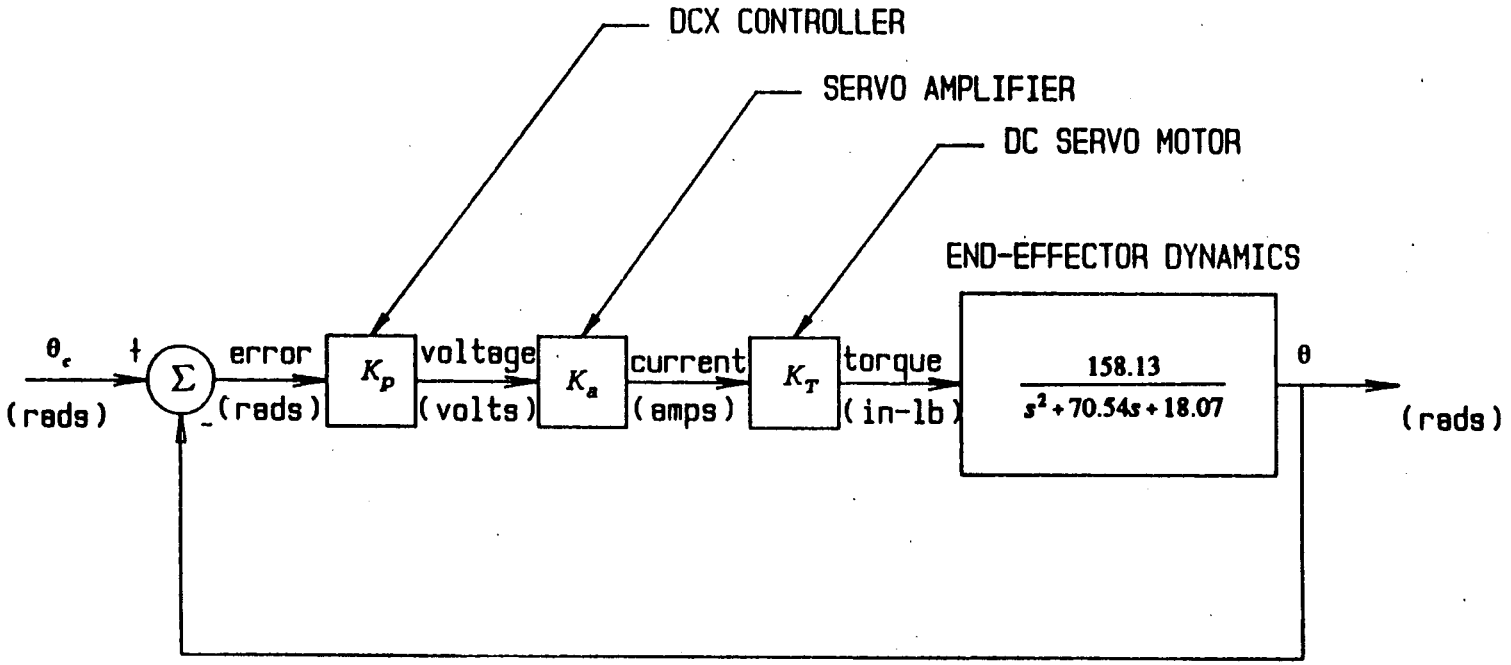

Figure 4.1. Pitch Motion Control System Block Diagram

$$\frac{\hat{\theta}(s)}{\hat{\theta}_c(s)} = \frac{7.35K_p}{s^2+70.54s+(18.07+7.35K_p)} \qquad (4.1)$$

where $\hat{\theta}$ and $\hat{\theta}_c$ are the actual and desired end-effector displacements respectively. The characteristic equation is given by

$$s^2+70.54s+(18.07+7.35K_p) = 0 \ , \qquad (4.2)$$

and is of the form

$$s^2+2\zeta\omega_n s+\omega_n^2 = 0 \ , \qquad (4.3)$$

where ζ and ω_n are the damping ratio and natural frequency of the system respectively. The value of the system natural frequency for the system to be critically damped ($\zeta = 1.0$) is determined as

$$\omega_n = 35.27 \ \ (radians/second) \qquad (4.4)$$

$$\text{or} \ \ \Omega_n = 5.6 \ \ (Hertz) \ .$$

The value of K_p for critical damping was determined to be

$$K_p = 166.7 \ \ (volts/radian) \ . \qquad (4.5)$$

The loop gain, defined as the product of the steady state gains of the transfer functions of the individual loop elements, was determined for the system shown in Figure 4.1 to be

$$(Loop\ Gain)_{analog} = 67.84\,(radians/radian) \quad . \qquad (4.6)$$

The input to the system shown in Figure 4.1 is the desired pitch displacement $\hat{\theta}_c$. However, in the actual system, the input to the DCX controller commands the angular rotation of the servo motor, $\hat{\theta}_m$. The command to the motor is given in terms of the pulses of the encoder mounted at the motor shaft. The controller then computes the error between the desired and actual encoder count. This error is converted to an analog voltage by a digital-to-analog (D/A) converter which then outputs the voltage to the servo amplifier. The block diagram of the control system, modified to include the encoder and D/A converter gains is shown in Figure 4.2. The values of the parameters are listed in Table II.

The loop gain of the actual system was determined to be

$$(Loop\ Gain)_{digital} = 66.3K_{p(digital)}\ (counts/count) \qquad (4.7)$$

Since the loop gains given by Equations (4.6) and (4.7) are non-dimensional and for the same physical system, they can be equated to solve for the equivalent computer control gain $K_{p(digital)}$. This gain value is used in the DCX servo controller. The value of $K_{p(digital)}$ for critical damping was determined to be

$$\begin{aligned} K_{p(digital)} &= 1.023 \\ &\approx 1.0 \quad (counts/count) \quad . \end{aligned} \qquad (4.8)$$

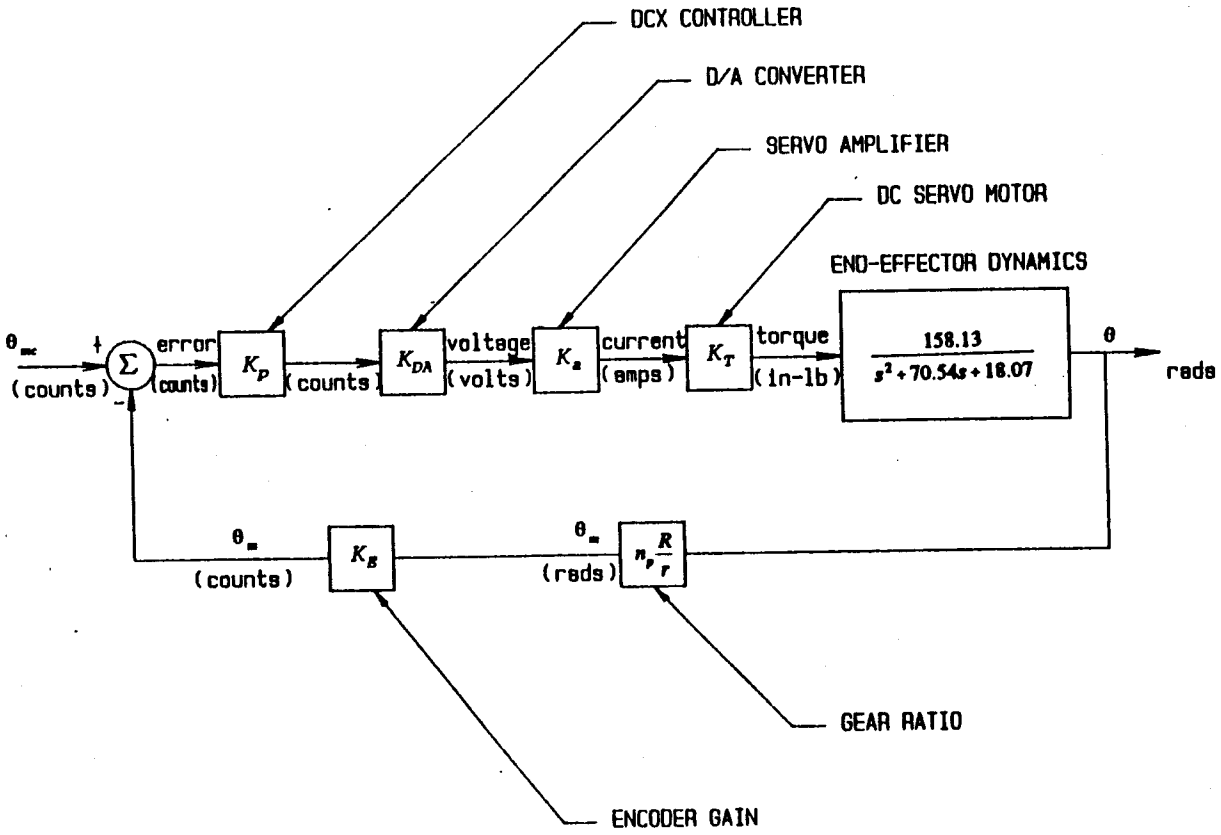

Figure 4.2. Actual System Block Diagram

Table II. Actual Control System Parameters

Symbol	Quantity	Value	Units
K_a	Amplifier Gain	0.1	amperes/ volt
K_T	Motor Torque Constant	0.465	in-lb/ ampere
K_{DA}	D/A Converter Gain	0.00488	volts/count
$n_p R/r$	Gear Ratio	105.0	-
K_E	Encoder Gain	318.0	counts/ radian

Experimental Evaluation

The analysis developed in the previous section was verified by studying the response of the modelled control system to step position commands. The simulations used PC-MATLAB, a mathematical and control systems analysis software package. The actual system response was obtained by reading the encoder counts and writing this data to a file. The file was post-processed using MATLAB and the data points plotted as a function of time. The simulated and actual system responses were plotted on the same graph for comparison. The tests are carried out for small pitch displacements about the equilibrium position of the end-effector to minimize the effects of non-linearities.

The response of the system to a small step command of 1.25 degrees is shown in Figure 4.3. The differences between the simulated and experimental responses are possibly due to differences between the estimated and actual end-effector parameters. The negligible overshoot and small steady state error (between 1 and 2 encoder counts) shown by the experimental response indicates that a proportional controller is adequate to control the position of the end-effector axis. Different gains and step commands were applied to the system to study the validity of the linear pitch control system model.

As the step size is increased for the same value of proportional gain, the experimental response lags the simulated response as shown in Figure 4.4. The dynamic behavior

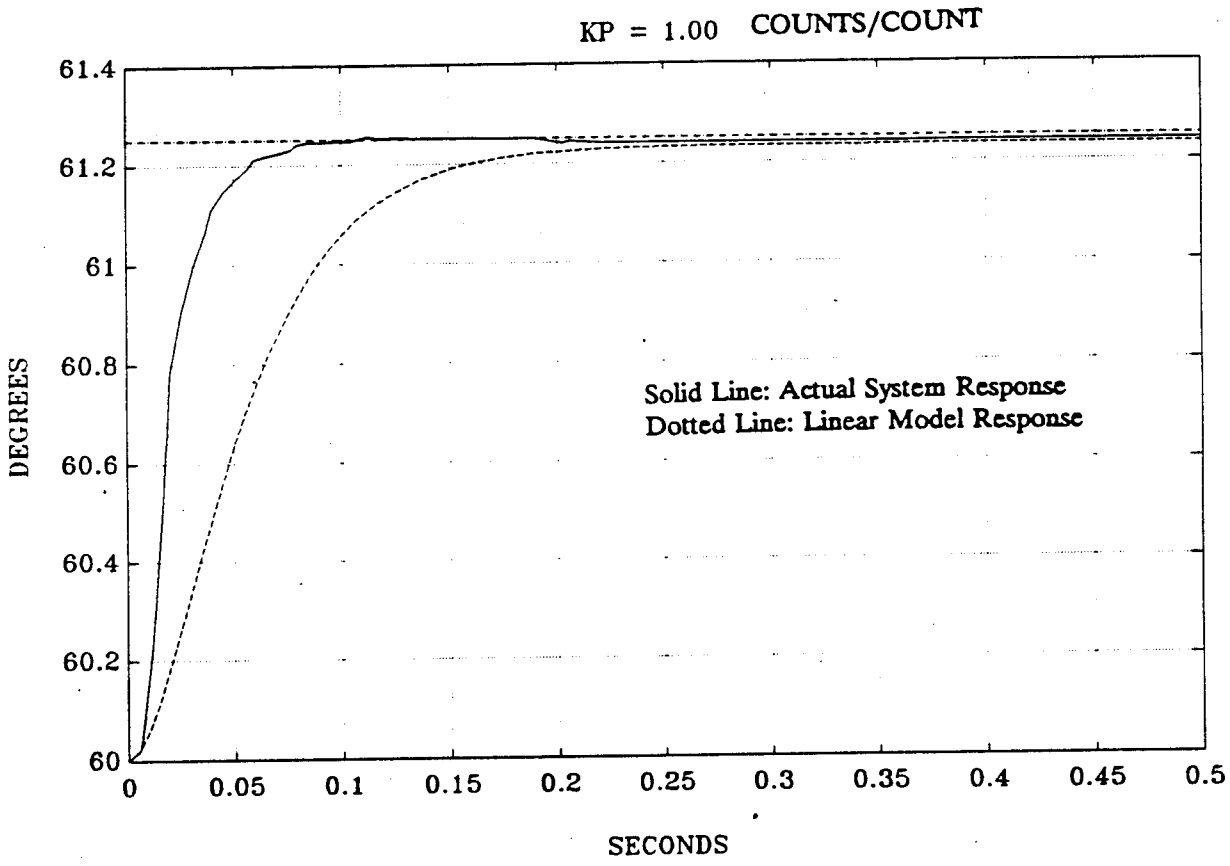

1.25 Degrees Step Angle

Figure 4.3. Simulation and Experimental Responses for Critically Damped System

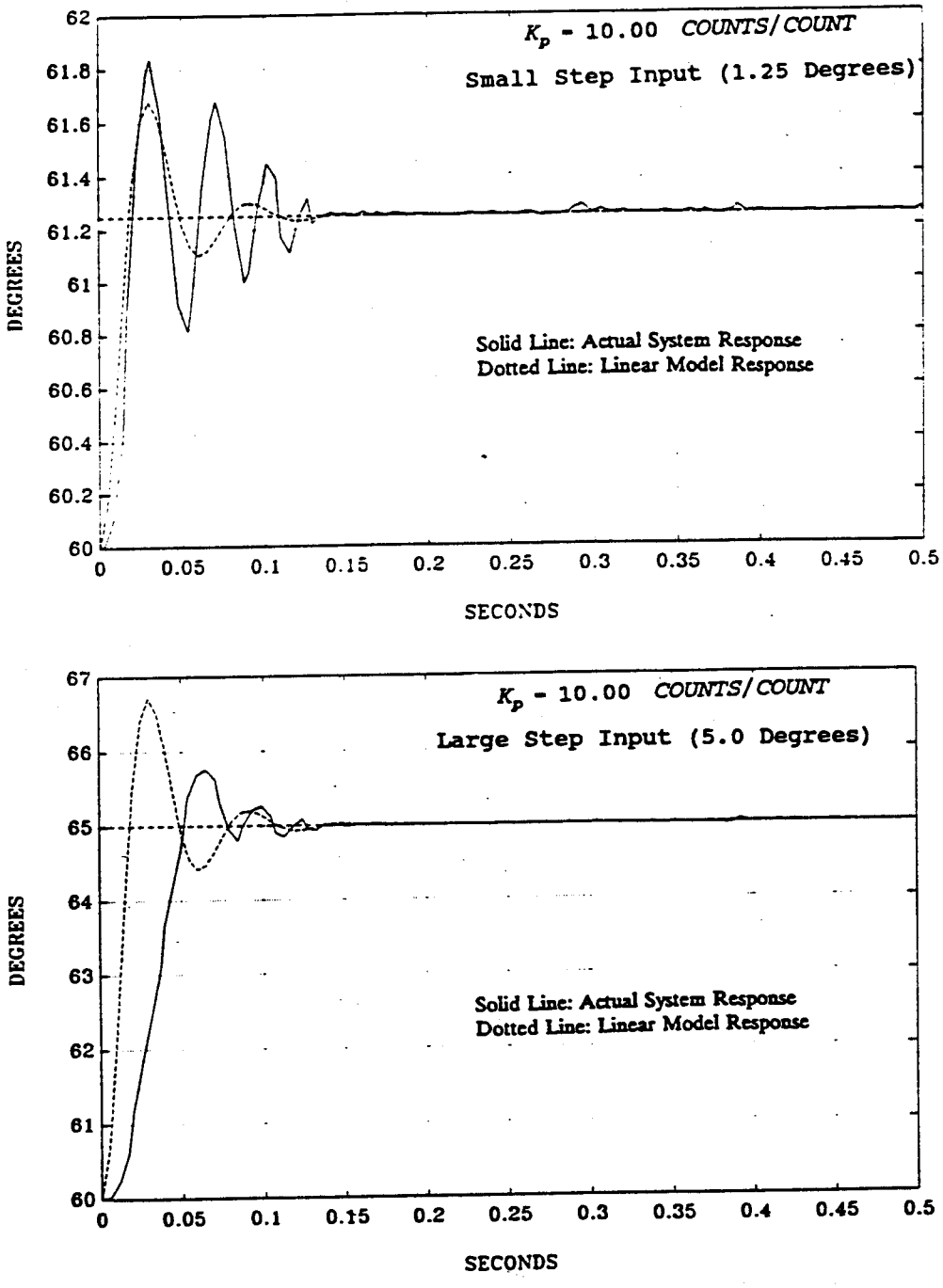

Figure 4.4. Variation between Simulation and Experimental Responses for Large Step Position Commands

indicates that the actual system may be 'saturated'.The phenomenon of saturation, represented in the system shown in Figure 4.5, occurs in physical systems primarily due to the limited dynamic range of actuators and amplifiers. Saturation in the end-effector system could also have occurred due to the limited word length (12 bits) of the D/A converter in the DCX board.

A large reference input to the system will cause the actuator to saturate at u_{max}. Even though the error, e, keeps increasing, the input to the plant $u = u_{max}$, remains constant. Due to the reduced control effort, the output of the plant increases more slowly than if actuator saturation were not present. Hence, the output of the actual system shown in Figure 4.4 is slower than the response of the linear system in which the effects of saturation are not modeled.

As shown in Figure 4.6, when the proportional gain is increased to 20.0, the effect of backlash present in the system becomes evident. A limit cycle is a phenomenon of self-sustained oscillations that occurs in a control system in the presence of non-linearitities. A limit cycle could occur in a servomechanism under the following conditions:

1. The magnitude of the command input is comparable to the backlash present in the system. In Figure 4.6, the peak-to-peak amplitude of the oscillations represents the magnitude of backlash present in the planetary gearhead. The comparable magnitudes of the backlash (0.5 degrees) and the command input (1.25 degrees) could have caused the limit-cycle to be excited.

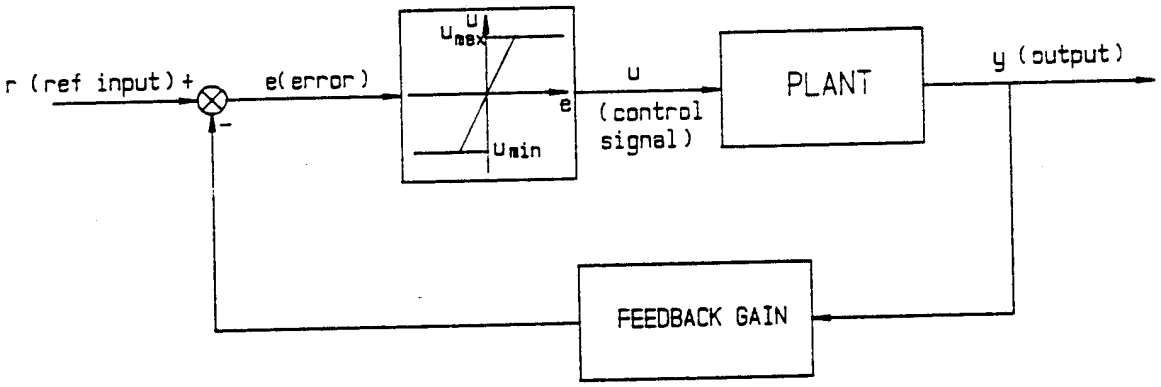

Figure 4.5. Presence of Saturation Non-Linearity in a Control System

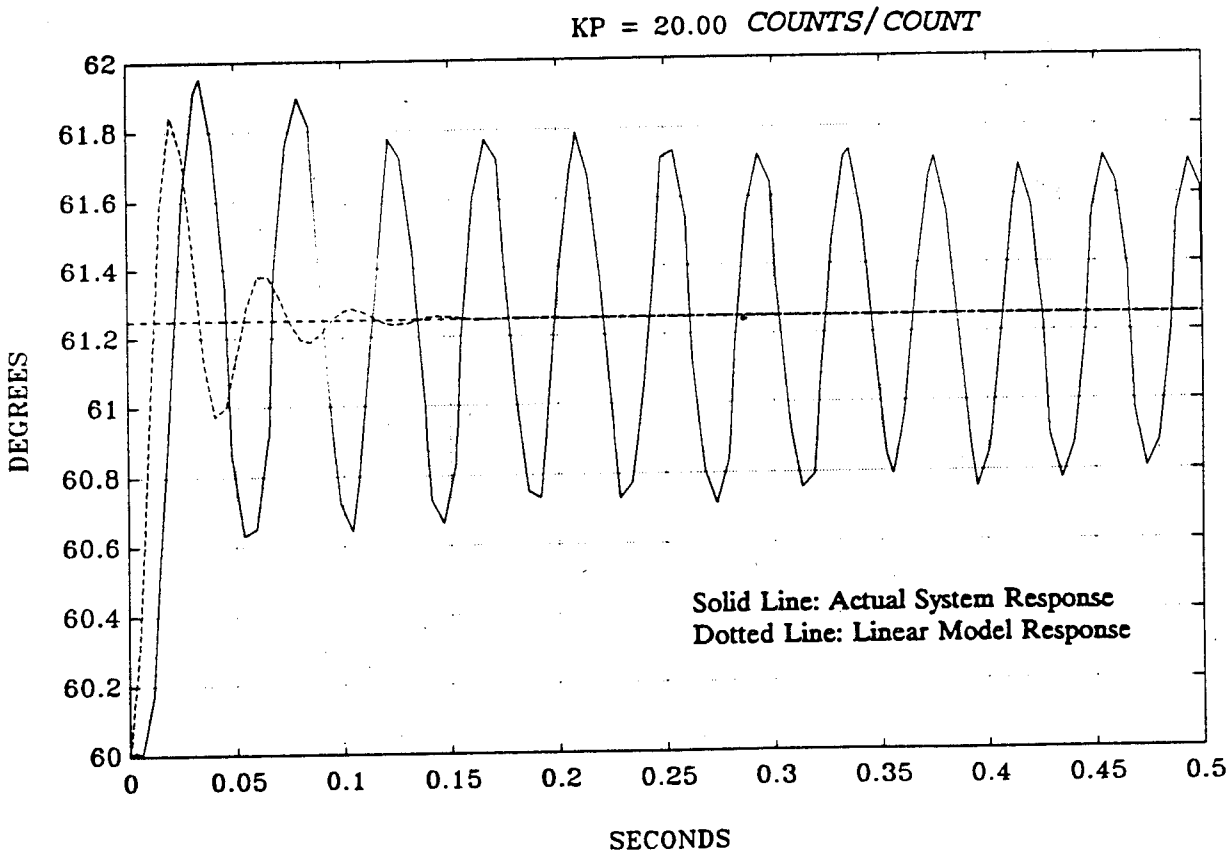

Figure 4.6. Limit Cycle Behavior of End-Effector

2. The system damping constant is less than 0.29. Lauer et al.[19] show that a servo system will undergo sustained oscillations of constant magnitude provided that the damping constant, ζ, is less than 0.29. When K_p is 20.0 counts/count, the damping constant of the end-effector system is equal to 0.23, causing the system to limit cycle in the presence of backlash.

3. Material properties of the gear elements such as elasticity and resilience cause the impacts between gear teeth to self-sustain. Under suitable conditions, impacts of mating gear teeth could set up oscillations in the system that could lead to the system entering into a limit cycle.

Limit cycling causes deterioration of the mechanical components and affects the performance of the end-effector. The non-linearities mentioned above and other unmodelled end-effector dynamics such as belt and torsional compliance, motor and amplifier dynamics, and sampling time of the DCX servo control module, must be considered to understand their influence on system dynamic performance.

Although the end-effector curves show steady state errors of less than 0.005 degrees (1-2 encoder counts), these graphs depict the positioning accuracy of the motor shaft, not the pitch axis. Backlash present in the planetary gearhead is not sensed by the encoder which is mounted directly on the motor shaft. The backlash is of the order of 0.5 degrees which yields an error of 0.1 inches at the gripper jaws.

Lateral Gripper Motion Implementation and Performance

The lateral gripper motion is actuated by a stepper motor in an open loop control system. The only step motor

parameters that need to be adjusted are the pull-in velocity or the velocity with which the motor can start instantaneously without loosing steps, the maximum velocity and maximum acceleration. Based on these parameters, the step motor controller generates pulses at a rate corresponding to a defined trapezoidal velocity profile. Programming velocities and accelerations higher than that achievable by the system will cause the step motor to loose steps, thereby loosing positional information.

Determination of the velocities and accelerations that result in the fastest motion was accomplished experimentally. A linear potentiometer was attached to one of the ball nuts which moves the grippers laterally so that displacement of the gripper could be measured. The output of the potentiometer was read through a 12-bit A/D converter on a Data Translation data acquisition board. The digital data was normalized and plotted against time using MATLAB. The fastest system response with acceptable steady state error of 0.05 inches is shown in Figure 4.7. The gripper jaws translate at a maximum velocity of 3 inches/second. At high velocities, the grippers tend to vibrate due to the presence of clearances in the ball nuts. The amplitude of vibrations can be reduced by providing extra bearing support to the grippers.

Collar Handling Demonstration

The end-effector design concepts were tested by demonstrating the ability of the end-effector to acquire a collar, transport it to the turning machine, and unload it from the

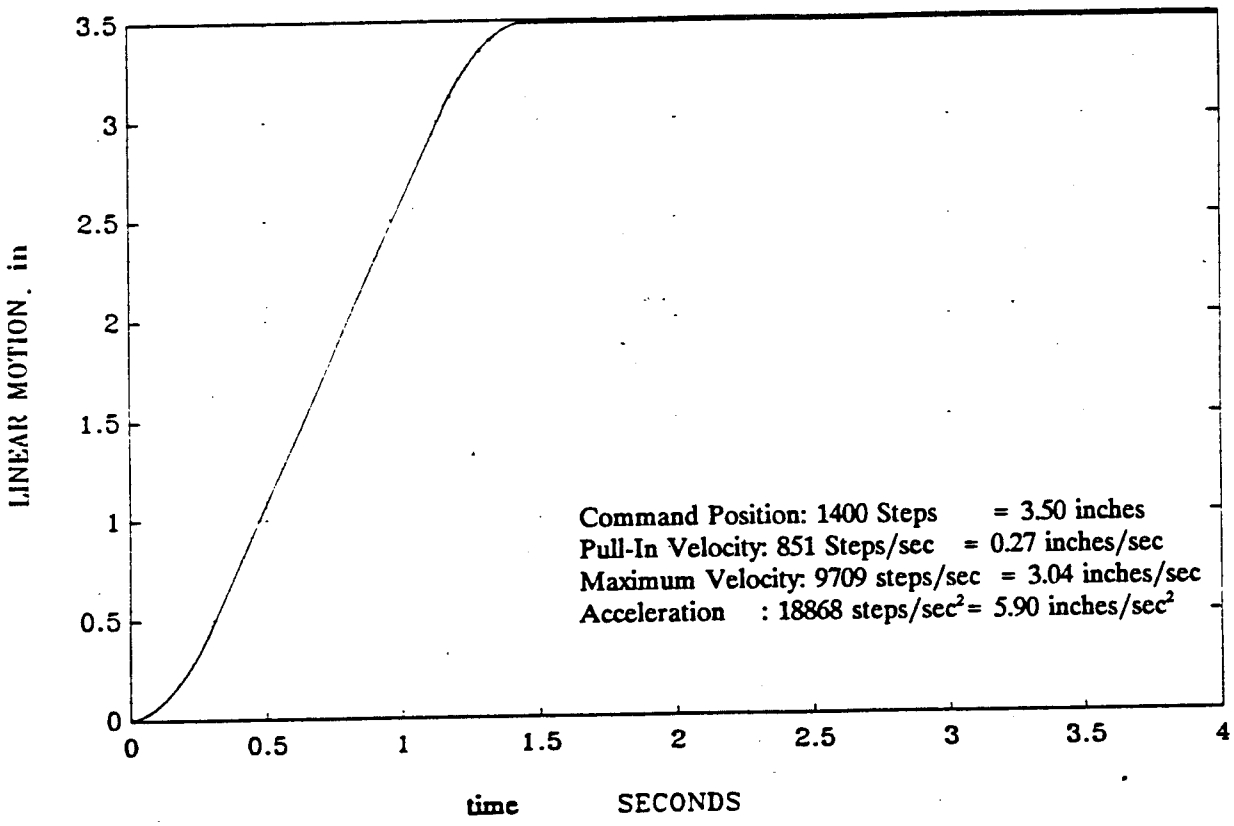

Figure 4.7. Step Motor Response Measured with Linear Potentiometer

turning machine after the collar had been turned. The demonstration provided a qualitative measure of the performance of the end-effector design implementation.

At the beginning of the demonstration, the end-effector performs a motion sequence that initializes the pitch motion. The end-effector does not at present include sensors which indicate when the pitch motion has reached a particular position. The homing sequence is implemented by programming the pitch motor to move slowly in one particular direction until a compliant hard stop is encountered. During this motion the encoder count is continuously monitored. When the end-effector encounters the hard stop, the encoder count will remain the same, indicating that the limit of pitch motion travel is reached. The motor is commanded to move a fixed number of encoder counts from this hard stop until the grippers are horizontal. The pitch angle at this end-effector configuration is defined as the home position. The position of the grippers relative to one another during system power-up is initialized manually because of the absence of sensors to indicate when a particular position has been reached. The procedure adopted to home the pitch motion cannot be employed to initialize the position of the grippers since no position feedback device exists.

The demonstration involved the processing of a military shirt collar. The size of the collar is 15 inches measured along the open pocket. Once the end-effector has been initialized, the two grippers move apart until the grippers are

situated about 12 inches from one another. The collar was manually loaded on the end-effector with the individual plies of the collar separated.

The grippers are actuated to grasp the top ply of the collar. As illustrated in Figure 4.8, the lower ply is separated from the grasped ply due to gravity. The robot transports the collar to the turning machine. The end-effector simultaneously performs a pitch motion to increase the opening between the collar plies. The increased opening between the collar plies enables the collar to be loaded more reliably over the clippers of the turning machine. Figure 4.9 shows the end-effector loading the collar on the turning machine. The turning machine clippers swivel out until the collar points are encountered. When the clippers encounter the collar tips, considerable force is applied to the collar points possibly causing the fabric to slip from the grippers of the end-effector. However, in about 25 runs of the demonstration, the fabric has slipped from the gripping surface only once. This fact confirms the utility of using pinch grippers to grasp the fabric for this application.

The correct loading of the collar on the turning machine validates other end-effector design concepts. The demonstration runs showed that the end-effector was uniformly successful in loading collars in such a way that the two collar plies enclose both turning machine clippers. The concept of using gravitational force to separate the collar plies is valid. However, for apparel processing operations which are

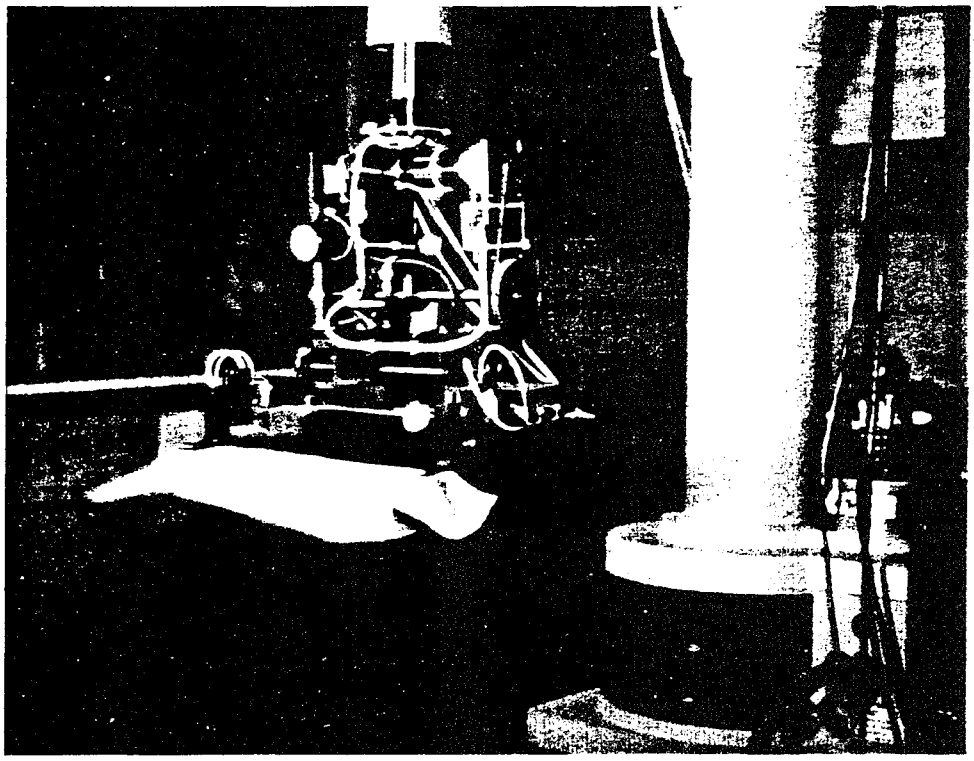

Figure 4.8. End-Effector with Grasped Collar

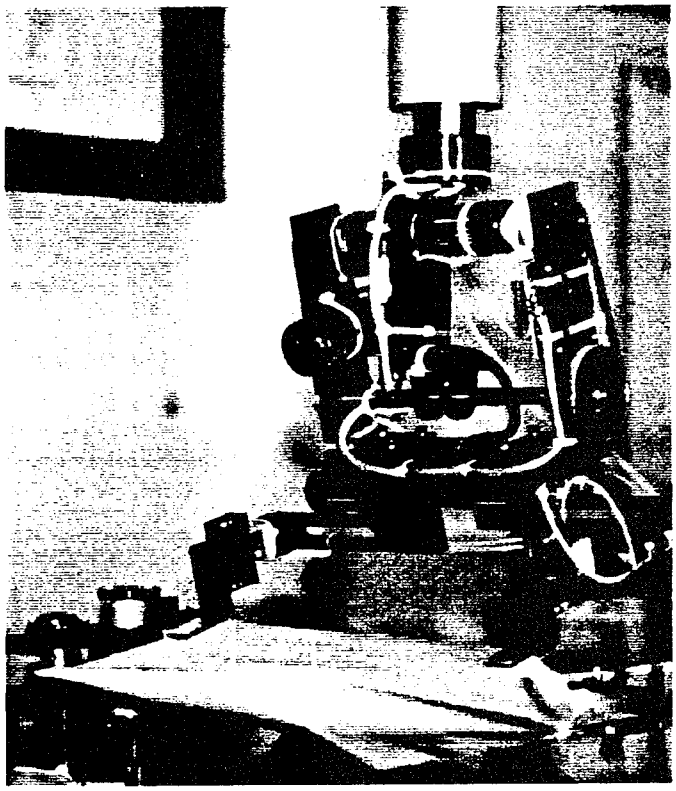

Figure 4.9. End-Effector Loading Collar on Turning Machine

carried out in a vertical plane as opposed to a horizontal one, a method other than gravity will have to be employed. The proper loading of the collar points on the clippers also shows that gripping the collar at two locations is sufficient to ensure that fabric drape is controllable at the collar points.

After the collar has been loaded, the grippers release the collar and the end-effector moves away from the turning machine. Following the turning operation, the collar is supported by the turning machine at its two tips. The end-effector must translate the grippers closer together during the unloading operation to prevent collisions with turning machine components. The grippers are aligned with the top ply of the collar via a pitch motion. The absence of tension on the top ply of the collar as it is supported on the turning machine makes it difficult to predict the position of the ply edge. During the demonstrations, the end-effector frequently would grasp the ply edge at only one location while the other gripper failed to grasp any part of the collar. The problem can be corrected by introducing a mechanism in the turning machine that stretches the top ply of the collar after it has been turned.

The end-effector upon acquiring the turned collar deposits it at a specified location. The current collar processing workstation does not include the pressing device. After the pressing device is integrated into the collar

processing workstation, the end-effector will have to manipulate the collar to load it on the pressing device.

End-effector motion trajectories during the demonstration were controlled by software routines written in the 'C' programming language. All end-effector motions were coordinated with the robot and turning machine motions, showing that the end-effector can be integrated with the hierarchical control scheme for the robot-assisted collar processing workstation. This evaluation procedure has showed that the end-effector is capable of manipulating a multiple-ply apparel component (in this case, a shirt collar) in three dimensional space.

CHAPTER V

CONCLUSIONS AND RECOMMENDATIONS

Conclusions

An end-effector capable of manipulating multiple-ply apparel workpieces in three dimensional space has been developed. The mechanical design concepts for the end-effector were developed after visual observation of manipulation of an apparel shirt collar by a human operator. Implementation of these concepts for the particular task of robot handling of shirt collars yielded a two degree-of-freedom (DOF) end-effector. The end-effector employs two pinch grippers to grasp the unfused collar ply. The collar plies are separated from one another by gravitational force. A translatory motion of the gripper jaws enables the end-effector to tension the grasped ply and to handle different workpiece sizes. A pitch motion on the end-effector orients the grippers during loading and unloading operations on the turning and pressing machines.

The grippers are actuated pneumatically providing a maximum opening of a half inch between the gripper jaws. This opening is sufficient for acquiring the collar from the destacking and turning machines. The motion that varies the distance between the grippers is actuated by a stepper motor. The gripper translation mechanism was designed so that interferences with the robot workspace is minimized. The velocity

and acceleration parameters of the stepper motor were determined by experimentally obtaining the response of the lateral gripper motion. The range of lateral gripper motion is five to fourteen inches at a maximum velocity of six inches/second.

The pitch motion of the end-effector incorporates a novel design to minimize the peak torque and size required by the motor drive. The DC servo motor, which actuates the motion, rotates about the pitch axis to act as a counterbalance to the rest of the end-effector mass. The unique feature of the design is that counterbalancing is achieved with an active end-effector component (the DC servo motor) as opposed to using a passive mass that does not contribute towards the functioning of the end-effector. Wider use of such counterbalancing mechanisms in robots and end-effectors could result in more efficient designs.

The design and evaluation procedure for the pitch motion control system indicated that a proportional controller is adequate for satisfying the performance specifications of zero overshoot and low steady state error (less than 0.1% which corresponds to 1-2 encoder counts for a 1.25 degrees position command step). Deviations from the expected linear behavior of the end-effector for large motion commands and large controller gains were observed, indicating that nonlinearities such as motor drive saturation and gearbox backlash need to be modeled to more accurately predict the dynamic behavior of the end-effector. The pitch motion has a

range of travel of plus and minus 90 degrees from the position when the grippers are horizontal and achieves a maximum velocity of 90 degrees/second.

The performance of the end-effector system was demonstrated by carrying out actual collar manipulation tasks within a robot-assisted collar processing workstation. The end-effector was able to successfully load the collar on the turning machine. However, the task of collar acquisition from the turning machine was not reliable since the ply to be grasped was not under tension. Modifications in the design of the turning machine which tension the collar ply after turning will enable the end-effector to acquire the collar more reliably. The demonstration showed the feasibility of accomplishing three dimensional apparel workpiece manipulation with a robot end-effector.

Recommendations

Analysis of Fabric Behavior

The design of the end-effector has been based on observation of a human operator handling fabric workpieces. Limited research has been conducted to understand and predict fabric behavior. Present research efforts have concentrated on modeling the behavior of single-ply fabric components under limited loads and boundary conditions. As more results become available of multiple-ply fabric component behavior, techniques for their handling by automated devices can be developed analytically. Robot end-effector designs based on these analytical methods will be more reliable and optimum

with respect to the number of degrees-of-freedom and sensors required.

Improvements in Mechanical Design

The following improvements are suggested for the mechanical design of the end-effector:

1. The planetary gearhead which reduces speed between the motor and the pitch axis introduces errors in the position of the grippers due to presence of backlash in the gear system. This backlash is not sensed by the encoder that serves as the position transducer since it is mounted at the motor shaft. Better positional accuracy would result if the encoder were to be mounted at the pitch axis; however, the system would tend to hunt for the desired position due to inclusion of backlash in the feedback loop. A solution to the problem could be to use a dual-loop control system. Encoders could be mounted both at the motor axis and at the pitch axis. During a motion, the motor position is fed back to the controller. Once the motion is completed, the position of the pitch displacement is fed back. The backlash error is determined and the motor is commanded to move to eliminate this error.

2. Although the implementation of the counterbalancing concept has resulted in reduction of peak torque by the actuator, the center of gravity of the end-effector is offset from the pivot axis by approximately 1.5 inches. The design of the end-effector can be optimized so that the center of gravity coincides exactly with the pitch axis. An end-effector design with the center of gravity coinciding with its pitch axis is perfectly balanced. A balanced end-effector does not require the DC servo motor to overcome a static imbalance torque; the motor would have to overcome only the inertia and damping of the system.

3. Clearance in the ball nuts results in vibration of the grippers as they translate. The design of the mechanism can be improved by providing extra linear bearing supports to the carriages which transport the grippers laterally.

4. The normal force exerted by the grippers on the grasped apparel workpiece can be improved by using a gripping surface with a higher coefficient of friction.

Refinement in Pitch Control System Analysis

Analysis of the pitch motion control system revealed presence of non-linearities such as actuator saturation, static friction and backlash in the gearbox. The model of the end-effector developed in this thesis is linear. This model needs to be extended to include the effects of non-linearities for more accurate prediction of the performance of the end-effector to different motion commands and controller structure.

Addition of Sensors

The reliability of fabric handling operations by the end-effector can be improved by providing sensory feedback of the state of the apparel workpiece. Break-beam sensors can be included on the grippers to indicate the presence of the workpiece between the gripper jaws. Sensors must be included which determine the tension on the grasped ply. Their inclusion will determine the amount of lateral gripper motion required to stretch the grasped ply in order to control fabric drape at the workpiece edges.

APPENDICES

Appendix A

Kinematic and Dynamic Analysis

An analysis was conducted to determine the kinematic and dynamic equations of the pitch motion. The derivation of the equations is presented in this Appendix.

The following assumptions are made in the analysis:

1. The dynamics of the robot and the end-effector are decoupled. This is true during most motion trajectories involving simultaneous end-effector and robot motion. The end-effector executes the pitch motion during collar loading or unloading operations on external processing devices, during which times the robot links are either stationary or moving at low velocities.

2. Compliance due to belt extension and torsional deflection of the transmission shaft is assumed negligible.

3. Clearance between the belt and sprocket teeth, and backlash in the gearhead is neglected.

4. Friction in the motor and gearhead is assumed negligible.

5. The mass of the end-effector components that do not rotate about the motor axis is assumed to be concentrated at a single point.

Kinematic Analysis

The kinematic relationship between the angular rotation of the motor shaft relative to the moving axis and the pitch displacement is shown in Figure A.1. The dynamic analysis requires that the determination of the kinematic relationship between the absolute angular rotation of the motor shaft and the pitch displacement be determined. The derivation of the kinematic equations follows an analysis procedure given by Mabie and Ocvirk [20].

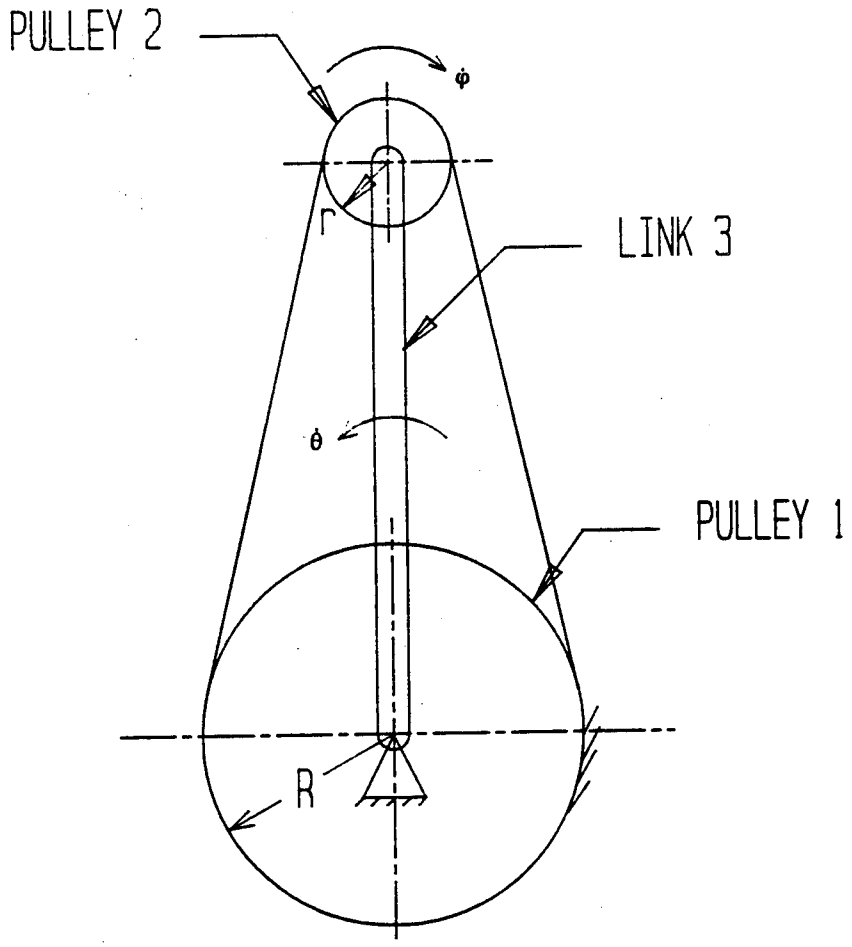

Figure A.1. Conceptualization of End-Effector Kinematics

The pitching mass of the end-effector is approximated as a link 3 that pivots about fixed point O. Pulley 2 is coupled to the motor shaft and Pulley 1 is fixed so that it does not rotate about the pitch axis. Initially, consider that the mechanism is changed in such a way that link 3 is fixed and pulleys 1 and 2 are free to rotate about their respective axes. This results in a normal belt drive, where the kinematic relationship is given by

$$\frac{\omega_{23}}{\omega_{13}} = \frac{R}{r} \quad , \tag{A.1}$$

where, ω_{23} and ω_{13} are the angular velocities of pulleys 2 and 1 with respect to the link 3 respectively. If the mechanism is now inverted back to its original configuration, that is link 3 is free to rotate and pulley 1 is non-rotating about the pitch axis, Equation (A.1) is still valid. However, we are interested in determining the angular velocity, ω_{31} of link 3, which is the angular velocity of the pitch motion, with respect to the stationary pulley 1. Since $\omega_{31} = -\omega_{13}$, then substituting in Equation A.1 gives

$$\frac{\omega_{23}}{\omega_{31}} = -\frac{R}{r} \quad . \tag{A.2}$$

Equation A.2 describes the relationship between the angular velocity of pulley 2 with respect to the rotating link 3 and the absolute angular velocity of link 3. However, for the dynamic analysis, the relationship between the absolute

angular velocities of the pulley 2 and link 3 is of more interest. The absolute angular velocity of pulley 2 is given by

$$\omega_{21} = \omega_{23} + \omega_{31} \quad , \tag{A.3}$$

where ω_{21} is the absolute angular velocity of pulley 2. Dividing Equation A.3 by ω_{31} and substituting Equation A.2 yields

$$\frac{\omega_{21}}{\omega_{31}} = -\left(\frac{R}{r} - 1\right) = 1 - \frac{R}{r} \quad . \tag{A.4}$$

The relationship between the magnitudes of the velocities, $\dot{\phi}(=|\omega_{21}|)$ and $\dot{\theta}(=|\omega_{31}|)$ is given by

$$\frac{\dot{\phi}}{\dot{\theta}} = \left|\frac{\omega_{21}}{\omega_{31}}\right| = \left|1 - \frac{R}{r}\right| \quad . \tag{A.5}$$

Since in this particular end-effector design implementation, $R > r$, that is the radius of the stationary pulley is greater than the radius of the moving pulley,

$$\left|1 - \frac{R}{r}\right| = \frac{R}{r} - 1 \quad . \tag{A.6}$$

Therefore, from Equation (A.5), we get

$$\frac{\dot{\varphi}}{\dot{\theta}} = \frac{R}{r} - 1 \quad . \tag{A.7}$$

Interesting observations can be made by considering three different $\frac{R}{r}$ possibilities.

1. When R > r, as in this case, the moving pulley appears to rotate in a direction opposite to that of the pitch direction.
2. When R < r, the moving pulley appears to be rotating in the same direction as the pitch motion.
3. When R = r, the moving pulley has zero absolute angular velocity and appears to translate about the pivot point.

Dynamic Analysis

The end-effector system considered for the analysis of the pitch motion consists only of the moving elements. All external forces and torques acting on the system are shown in Figure A.2. Derivation of the equation is first accomplished using the principles of classical mechanics. The correctness of this equation is verified by rederiving the equation using Lagrange's equations.

The end-effector dynamic equations are derived by considering the free body diagram of two sub-systems. The first sub-system considered consists of bodies that rotate relative to the motor axis and include the motor rotor, gears present in the planetary gearhead and the rotating pulley. The mass of this sub-system is designated as m_p. The second sub-system consists of bodies that pivot about the stationary shaft except those included in sub-system 1. The mass of sub-

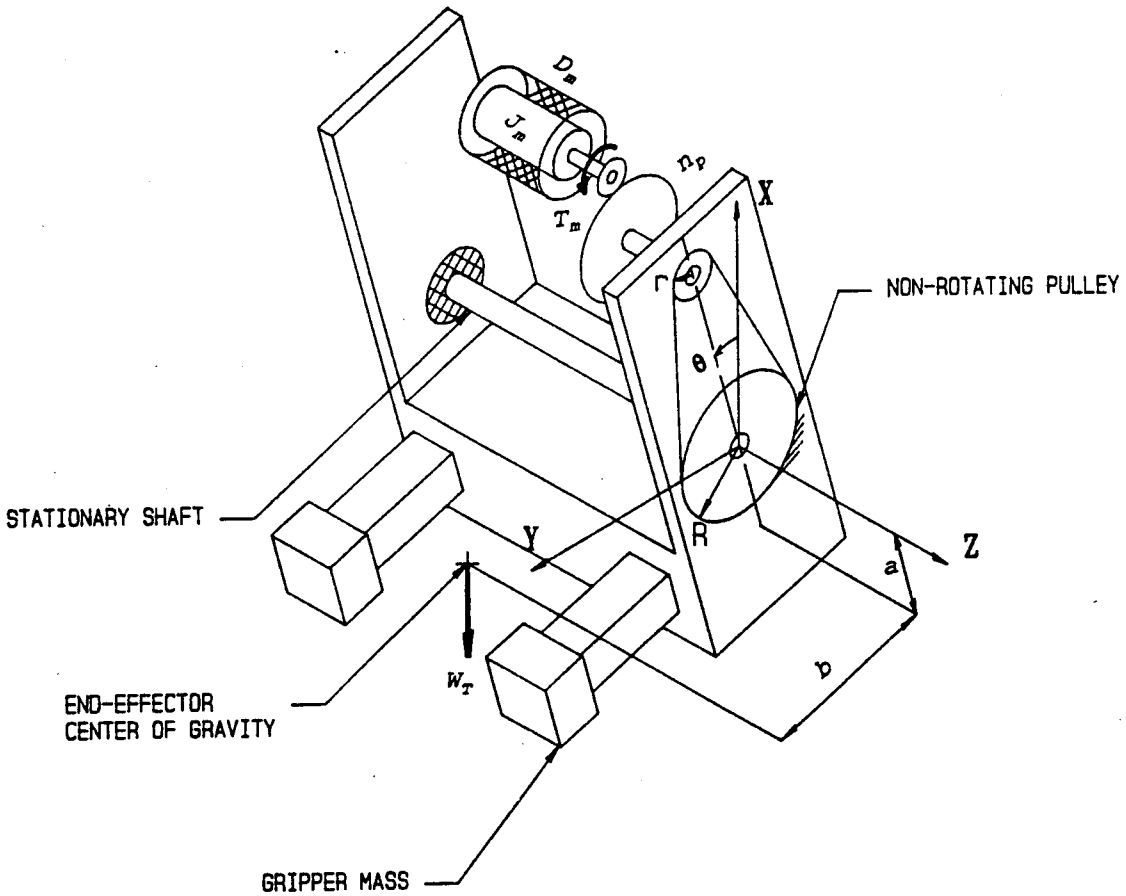

Figure A.2. Conceptualized 3-D Model of End-Effector for Dynamic Analysis

system 2 is designated as m_e. The total mass, m_T of the end-effector is

$$m_T = m_p + m_e \quad . \tag{A.8}$$

Derivation Using Newtonian Mechanics

The free body diagram of the moving pulley is shown in Figure A.3. J_m, the centroidal moment of inertia of the motor rotor is magnified through the planetary gearhead with a transmission ratio of n_p. I_r, the centroidal moment of inertia of the motor rotor reflected at the gearhead shaft is $J_m n_p^2$. Forces acting on the pulley are resolved along the 'n' and 't' directions. Summing forces along the positive 't' direction defined in Figure A.3, and moments about point C produces the following equations:

$$S_\theta + T_1 \sin\alpha - T_2 \sin\alpha + m_p g \sin\theta = m_p a_\theta \quad , \tag{A.9}$$

$$-M_r + (T_1 - T_2) r = -I_r \ddot{\phi} \quad . \tag{A.10}$$

The formulas for $\sin\alpha$ and a_θ are given by

$$\sin\alpha = \frac{R-r}{l} \quad , \tag{A.11}$$

$$a_\theta = l\ddot{\theta} \quad . \tag{A.12}$$

Substituting for $T_1 - T_2$ from Equation A.10, $\sin\alpha$ from Equation A.11 and a_θ from Equation A.12 into Equation A.9

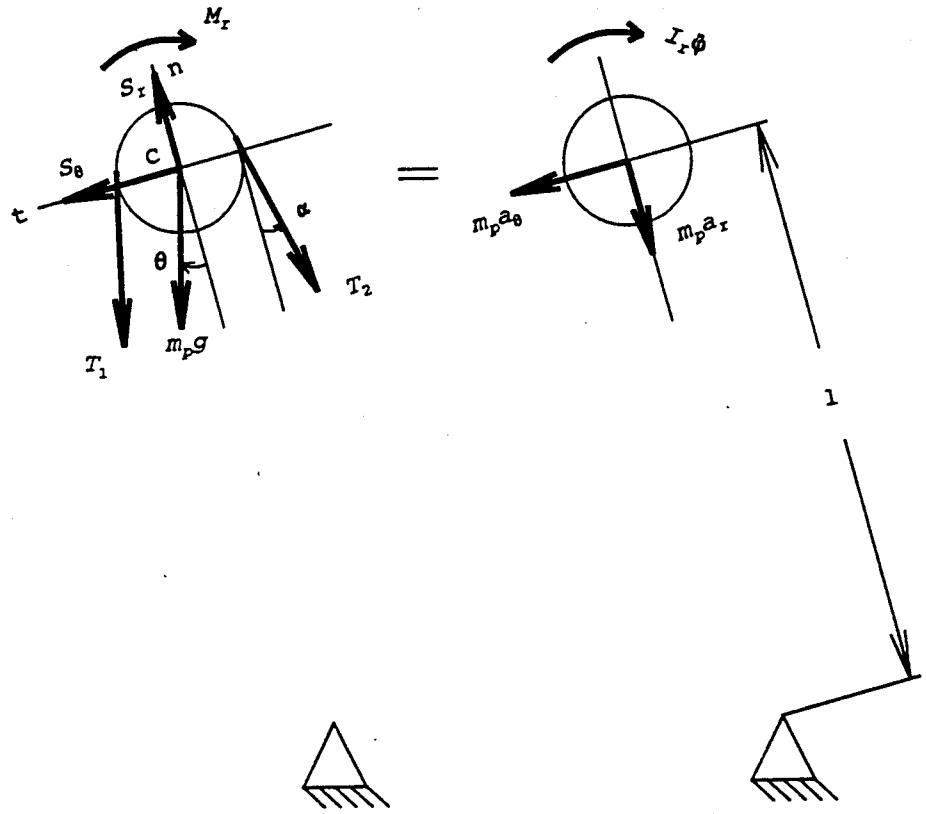

Figure A.3. Free Body Diagram of Moving Pulley

yields the following expression for S_θ:

$$S_\theta = m_p l\ddot{\theta} + \frac{I_r\ddot{\phi}}{l}\left(\frac{R}{r} - l\right) - \frac{M_r}{l}\left(\frac{R}{r} - 1\right) - m_p g\sin\theta \quad . \qquad (A.13)$$

The free body diagram of sub-system 2, i.e. the end-effector mass that does not contain elements rotating about the motor axis, is shown in Figure A.4. Considering counter-clockwise moments to be positive and summing about point O gives the following equation:

$$M_r + m_e g(q\cos\theta - p\sin\theta) - S_\theta l = m_e(p^2+q^2)\ddot{\theta} \quad . \qquad (A.14)$$

Rearranging the terms yields

$$S_\theta l = M_r - m_e(p^2+q^2)\ddot{\theta} + m_e g(q\cos\theta - p\sin\theta) \quad . \qquad (A.15)$$

Multiplying Equation A.13 by l and substituting for $S_\theta l$ into Equation A.15 gives

$$M_r\frac{R}{r} = [I_r(\frac{R}{r}-1)^2 + m_e(p^2+q^2) + m_p l^2]\ddot{\theta} + (m_e gp - m_p gl)\sin\theta - m_e gq\cos\theta \quad . \qquad (A.16)$$

The coordinates of the center of gravity of the two-mass system shown in Figure A.5 can be determined as follows:

$$a = \frac{m_e p + m_p(-l)}{m_p + m_e} \qquad (A.17)$$

and

$$b = \frac{m_e q + m_p(0)}{m_p + m_e} \quad , \qquad (A.18)$$

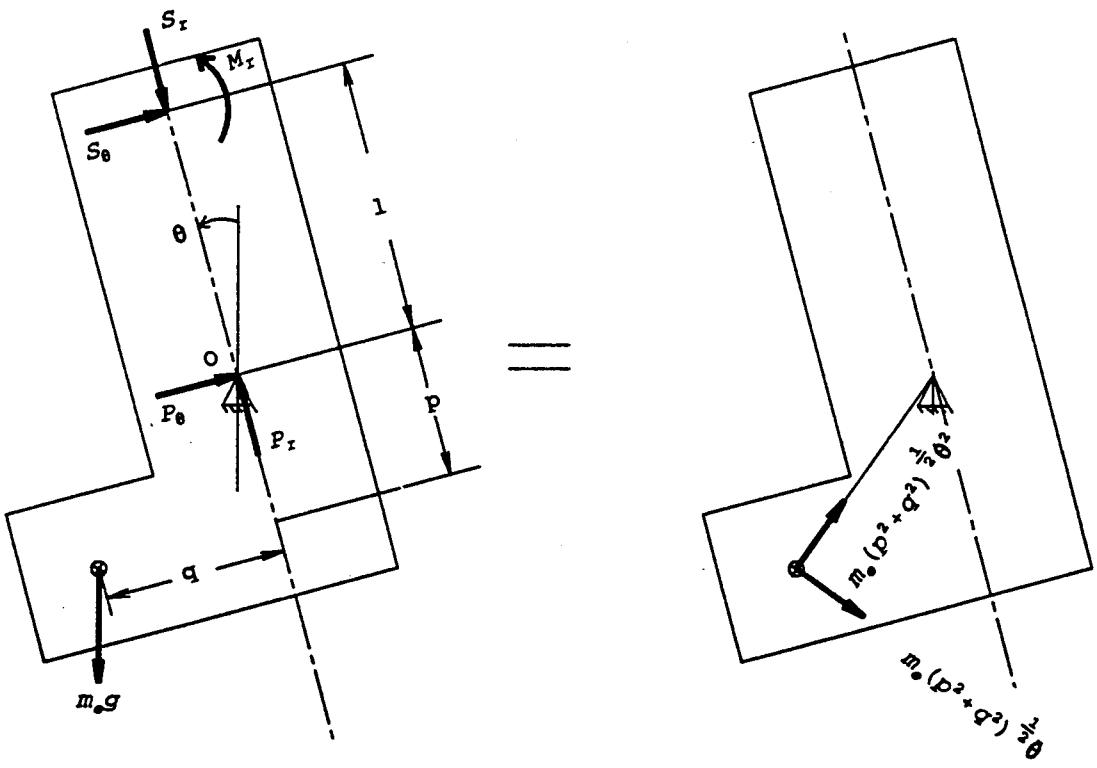

Figure A.4. Free Body Diagram of Sub-System 2

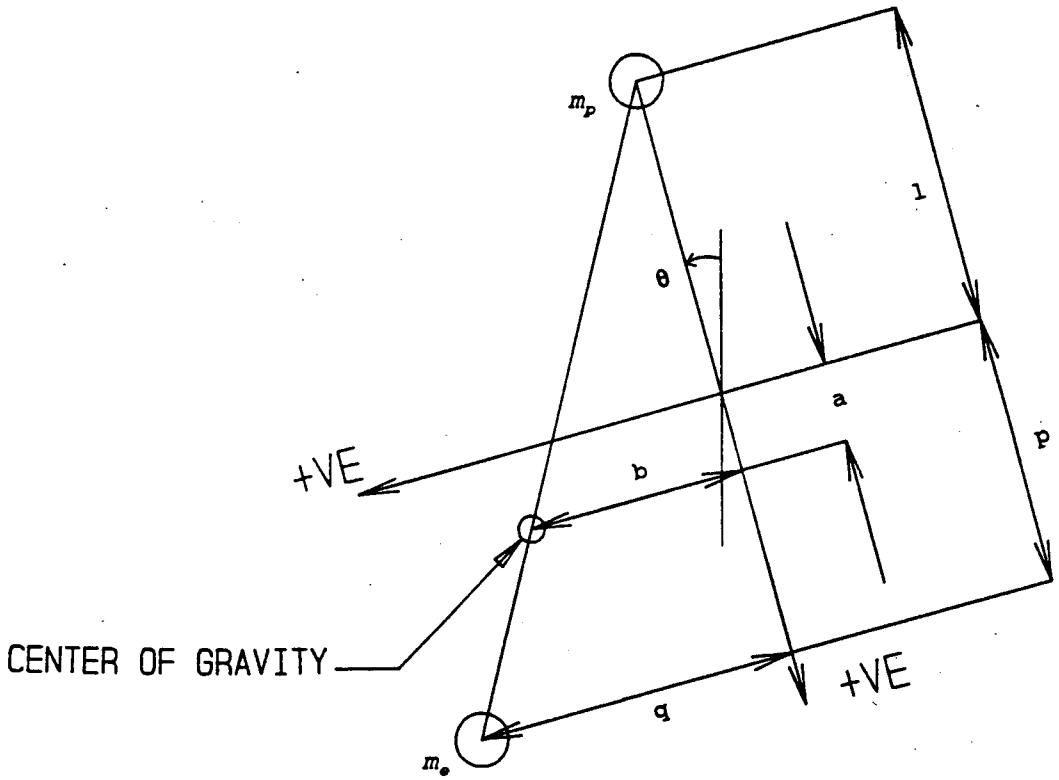

Figure A.5. Center of Gravity of Two Mass System

from which can be obtained

$$m_e p - m_p l = m_T a \tag{A.19}$$

$$m_e q = m_T b \quad . \tag{A.20}$$

The inertia of point masses, m_p and m_e can be substituted by the equivalent inertia of the center of gravity of the end-effector, i.e.,

$$m_e(p^2+q^2) + m_p l^2 = m_T(a^2+b^2) \quad . \tag{A.21}$$

Substituting Equations (A.19), (A.20), (A.21) into Equation (A.16) gives the equation of motion of the system

$$M_r \frac{R}{r} = [I_r(\frac{R}{r}-1)^2 + m_T(a^2+b^2)]\ddot{\theta} + W_T a\sin\theta - W_T b\cos\theta \quad . \tag{A.22}$$

Derivation Using Lagrangian Method

For the end-effector system under consideration, it is convenient to choose θ and φ as the generalized coordinates, whose motions are geometrically constrained according to Equation A.7. Lagrange's equations in this case is

$$\frac{d}{dt}\left(\frac{\partial \mathcal{L}}{\partial \dot{\xi}_j}\right) - \frac{\partial \mathcal{L}}{\partial \xi_j} = \Xi_j + \sum_{l=1}^{m} a_{lj}\lambda_l \quad , \tag{A.23}$$

where j is the number of generalized coordinates and l is the number of constraint equations. $\mathcal{L}$ is the Lagrangian, ξ_j's are the generalized coordinates, Ξ_j's are the generalized forces, λ_l's are the Lagrangian multipliers and a_{lj} are

obtained from the constraint equations. For the end-effector system, j = 2 and l = 1 and the generalized coordinates are given by

$$\begin{aligned} \xi_1 &= \theta, \text{ and} \\ \xi_2 &= \varphi \ . \end{aligned} \tag{A.24}$$

The generalized coordinates are related by constraint equations of the form

$$\sum_{j=1}^{n} a_{lj}\delta\xi_j + a_l = 0 \qquad l = 1,2,\ldots\ldots,m. \tag{A.25}$$

The constraint equation given by Equation A.7 can be rewritten as

$$(R-r)\dot{\theta} - r\dot{\varphi} = 0 \ . \tag{A.26}$$

Comparing Equations A.25 and A.26, and noting that in the present case, l = 1, the following expressions can be obtained:

$$\begin{aligned} a_{1\theta} &= R-r, \\ a_{1\varphi} &= -r, \text{ and} \\ a_1 &= 0 \ . \end{aligned} \tag{A.27}$$

Lagrange's equations for the end-effector system are

$$\frac{d}{dt}\left(\frac{\partial \mathcal{L}}{\partial \dot{\theta}}\right) - \frac{\partial \mathcal{L}}{\partial \theta} = \Xi_\theta + a_{1\theta} \ , \tag{A.28}$$

$$\frac{d}{dt}\left(\frac{\partial \mathcal{L}}{\partial \dot{\phi}}\right) - \frac{\partial \mathcal{L}}{\partial \varphi} = \Xi_{\varphi} + a_{1\varphi} \quad . \tag{A.29}$$

The Lagrangian is given by

$$\mathcal{L} = T^* - V \quad , \tag{A.30}$$

where T^* is the kinetic energy and V is the potential energy of the system and are expressed as

$$T^* = \frac{1}{2} I_r \dot{\phi}^2 + \frac{1}{2} m_T (a^2 + b^2) \dot{\theta}^2 \quad , \tag{A.31}$$

$$V = -m_T g (b\sin\theta + a\cos\theta) \quad . \tag{A.32}$$

Substituting Equations A.31 and A.32 into Equation A.30 yields

$$\mathcal{L} = \frac{1}{2} I_r \dot{\phi}^2 + \frac{1}{2} m_T (a^2 + b^2) \dot{\theta}^2 + m_T g (b\sin\theta + a\cos\theta) \quad . \tag{A.33}$$

The partial derivatives of Equations A.28 and A.29 are evaluated as follows:

$$\frac{\partial \mathcal{L}}{\partial \dot{\theta}} = m_T (a^2 + b^2) \dot{\theta} \quad , \tag{A.34}$$

$$\frac{\partial \mathcal{L}}{\partial \theta} = -m_T g a \sin\theta + m_T g b \cos\theta \quad , \tag{A.35}$$

$$\frac{\partial \mathcal{L}}{\partial \dot{\phi}} = I_r \dot{\phi} \ , \tag{A.36}$$

$$\frac{\partial \mathcal{L}}{\partial \varphi} = 0 \ . \tag{A.37}$$

The generalized forces corresponding to a particular generalized coordinate are determined by evaluating the work done along the direction of the coordinate when all other coordinates are constrained to remain fixed. The generalized forces corresponding to the two generalized coordinates, θ and φ are

$$\Xi_\theta = M_r \ ,$$

$$\Xi_\varphi = M_r \ . \tag{A.39}$$

Substituting Equations A.27, A.34, A.35 and A.38 into Equation A.28 gives

$$m_T(a^2+b^2)\ddot{\theta} + m_T g a \sin\theta - m_T g b \cos\theta = M_r + (R-r)\lambda \ . \tag{A.40}$$

Equations A.27, A.36, A.37 and A.39 are substituted into Equation A.29 to give

$$I_r \ddot{\phi} = M_r - r\lambda \ . \tag{A.41}$$

Substituting for λ from Equation A.41 and for $\ddot{\phi}$ from Equation A.26 into Equation A.40 gives the equation of motion for the system

$$M_r\frac{R}{r} = [I_r(\frac{R}{r}-1)^2+m_T(a^2+b^2)]\ddot{\theta}+W_T a\sin\theta - W_T b\cos\theta \ . \quad (A.42)$$

Equations A.22 and A.42 derived independently by Newtonian mechanics and Lagrange's equations respectively are identical, confirming the correctness of the obtained equation of motion.

M_r, the torque reflected at the output of the planetary gearhead is the resultant of the torque generated by the motor and the opposing velocity dependent torque due to viscous damping present in the motor. M_r is given by the following relationship:

$$M_r = (T_m - D_m\frac{R}{r}n_p\dot{\theta})n_p \ , \quad (A.43)$$

where, T_m is the torque generated by the motor and D_m is the viscous damping of the motor. Substituting the expression for M_r into Equation A.42 gives

$$T_m\frac{R}{r}n_p = [I_r(\frac{R}{r}-1)^2+m_T(a^2+b^2)]\ddot{\theta}+D_m(\frac{R}{r})^2n_p^2\dot{\theta} + W_T a\sin\theta - W_T b\cos\theta \ . \quad (A.44)$$

Equation A.44 may be rewritten as

$$J\ddot{\theta}+D\dot{\theta}+W_T a\sin\theta - W_T b\cos\theta = \tau \ , \quad (A.45)$$

where $J = J_m n_p^2(\frac{R}{r}-1)^2+m_T(a^2+b^2)$ is the equivalent moment of inertia of the end-effector about the pitch axis and $D = D_m n_p^2(\frac{R}{r})^2$

is the effective damping at the pitch axis, and $\tau = T_m n_p \frac{R}{r}$ is the reflected torque at the axis of rotation.

Linearization of the Equation of Motion

The sine and cosine terms present in Equation A.45 render it non-linear. The equation is linearized so as to enable the application of standard linear systems analysis techniques to the end-effector. Linearization is accomplished by solving for the equilibrium position of the end-effector and obtaining the Taylor series expansion about the equilibrium point. Substituting θ_o, the displacement of the end-effector at its equilibrium position for θ in the equation of motion, and noting that at equilibrium, $\ddot{\theta}_o$ and $\dot{\theta}_o$ are both equal to zero, and knowing that the end-effector is in equilibrium when no external torques are applied i.e., τ_o is zero, we obtain the following expression to determine the equilibrium position:

$$W_T a \sin\theta - W_T b \cos\theta = 0 \quad . \qquad \text{(A.46)}$$

The equation of motion is linearized about the end-effector equilibrium position, θ_o. The Taylor series expansion for $\sin\theta$ and $\cos\theta$ are given by

$$\sin\theta = \sin\theta_o + \frac{d}{d\theta}\sin\theta\Big|_{\theta_o} (\theta-\theta_o) + \ldots\ldots$$
$$= \sin\theta_o + (\cos\theta_o)\hat{\theta} \quad , \tag{A.47}$$

$$\cos\theta = \cos\theta_o + \frac{d}{d\theta}\cos\theta\Big|_{\theta_o} (\theta-\theta_o) + \ldots\ldots$$
$$= \cos\theta_o - (\sin\theta_o)\hat{\theta} \quad . \tag{A.48}$$

Equation A.45 can be rewritten as

$$J(\ddot{\theta}_o+\ddot{\hat{\theta}}) + D(\dot{\theta}_s+\dot{\hat{\theta}}) + W_T a[\sin\theta_o + (\cos\theta_o)\hat{\theta}]$$
$$- W_T b[\cos\theta_o - (\sin\theta_o)\hat{\theta}] = \tau_o + \hat{\tau} \quad . \tag{A.49}$$

Noting that $\ddot{\theta}_o$, $\dot{\theta}_c$ and τ_o are equal to zero and substituting Equation A.46 into Equation A.49 we get the linearized equation of motion

$$J\ddot{\hat{\theta}} + D\dot{\hat{\theta}} + (W_T a\cos\theta_o + W_T b\sin\theta_o)\hat{\theta} = \hat{\tau} \quad . \tag{A.50}$$

Appendix B

Determination of Control System Parameters

The dynamic equation of pitch motion given by Equation (A.50) can be rewritten as

$$\hat{T}_m n_p \frac{R}{r} = [J_m(\frac{R}{r}-1)^2 n_p^2 + m_T(a^2+b^2)]\ddot{\hat{\theta}} + [D_m n_p^2(\frac{R}{r})^2]\dot{\hat{\theta}} + [W_T a\cos\theta_o + W_T b\sin\theta_o]\hat{\theta} \quad . \tag{B.1}$$

The transfer function between θ, the pitch displacement and T_m, the torque generated by the DC servo motor is given by

$$\frac{\hat{\theta}(s)}{\hat{T}_m(s)} = \frac{n_p \frac{R}{r}}{[J_m(\frac{R}{r}-1)^2 n_p^2 + m_T(a^2+b^2)]s^2 + [D_m n_p^2(\frac{R}{r})^2]s + [W_T a\cos\theta_o + - W_T b\sin\theta_o]} \quad . \tag{B.2}$$

The motor inertia is obtained from the manufacturers catalog as $J_m = 5.97x10^{-5}$ $lb\text{-}in\text{-}sec^2$. The timing belt transmission ratio, $\frac{R}{r}$ is numerically equal to 3.0. The planetary gearhead ratio is equal to 35.0. W_T is the estimated design weight of the end-effector and was calculated to be 8.0 lbs. The distance of the center of gravity of the end-effector from the pivot was experimentally determined to be 1.5 inches. The equilibrium position of the end-effector, θ_o, was determined to be 60 degrees in the direction shown in Figure

A.2. a and b were calculated to be 0.75 inches and 1.3 inches respectively. The equivalent inertia at the pitch axis, J is given by

$$J = J_m(\frac{R}{r} - 1)^2 n_p^2 + m_T(a^2 + b^2) \\ = 0.664 \ lb\text{-}in\text{-}sec^2 \qquad (B.3)$$

The motor damping constant, D_m, can be approximately determined using the formula

$$D_m = \frac{J_m}{\tau_m} \qquad (B.4)$$

where J_m is the motor inertia and τ_m is the mechanical time constant of the motor. To obtain a more accurate estimate of D_m, an experimental procedure was adopted.

Under steady state conditions, i.e., when the load is not accelerating or decelerating, the motor has to overcome only velocity related opposing torques. Neglecting Coulomb friction and damping at the pitch axis, the motor torque has to overcome the motor damping. The generated motor torque is then given by

$$T_m = D_m \omega_m \ . \qquad (B.5)$$

The motor torque, T_m can be determined by measuring the current, i_m passing through the armature when the motor is rotating at constant velocity. The formula, $T_m = K_T i_m$, where K_T is the motor torque constant, is used to determine the

torque generated by the motor. The speed, ω_m of the motor is measured experimentally. The data points are joined using linear interpolation. The slope of the torque versus speed straight line shown in Figure B.1 gives the motor damping constant.

$$(B.6) \quad D_m = 0.0697 \, oz\text{-}in\text{-}sec = 0.00425 \, lb\text{-}in\text{-}sec \, .$$

The equivalent damping of the end-effector, D is given by

$$D = D_m n_p^2 \left(\frac{R}{r}\right)^2 = 46.836 \, lb\text{-}in\text{-}sec \, . \qquad (B.7)$$

The load torque term is given by

$$W_T a \sin\theta_o + W_T b \cos\theta_o = 12 \ \ in\text{-}lb \, . \qquad (B.8)$$

Substituting the values obtained from Equations (B.3), (B.7) and (B.8) into Equation (B.2), we obtain the transfer function between $\hat{\theta}$ and $\hat{T}_m$ to be

$$\frac{\hat{\theta}(s)}{\hat{T}_m(s)} = \frac{105.0}{0.664s^2+46.836s+12.0} = \frac{158.3}{s^2+70.54s+18.07} \, . \qquad (B.9)$$

In order to control the position of the pitch, the loop is closed as shown in Figure B.2. The motor torque constant is obtained from the manufacturers catalog as

$$K_T = 0.465 \ \ \frac{in\text{-}lb}{ampere} \, . \qquad (B.10)$$

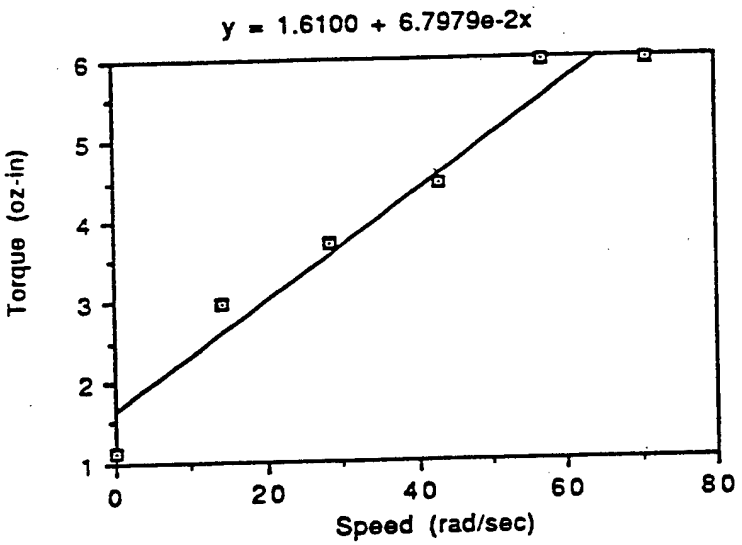

Figure B.1. Measured Torque versus Measured Speed of DC Servo Motor to Determine Damping Constant

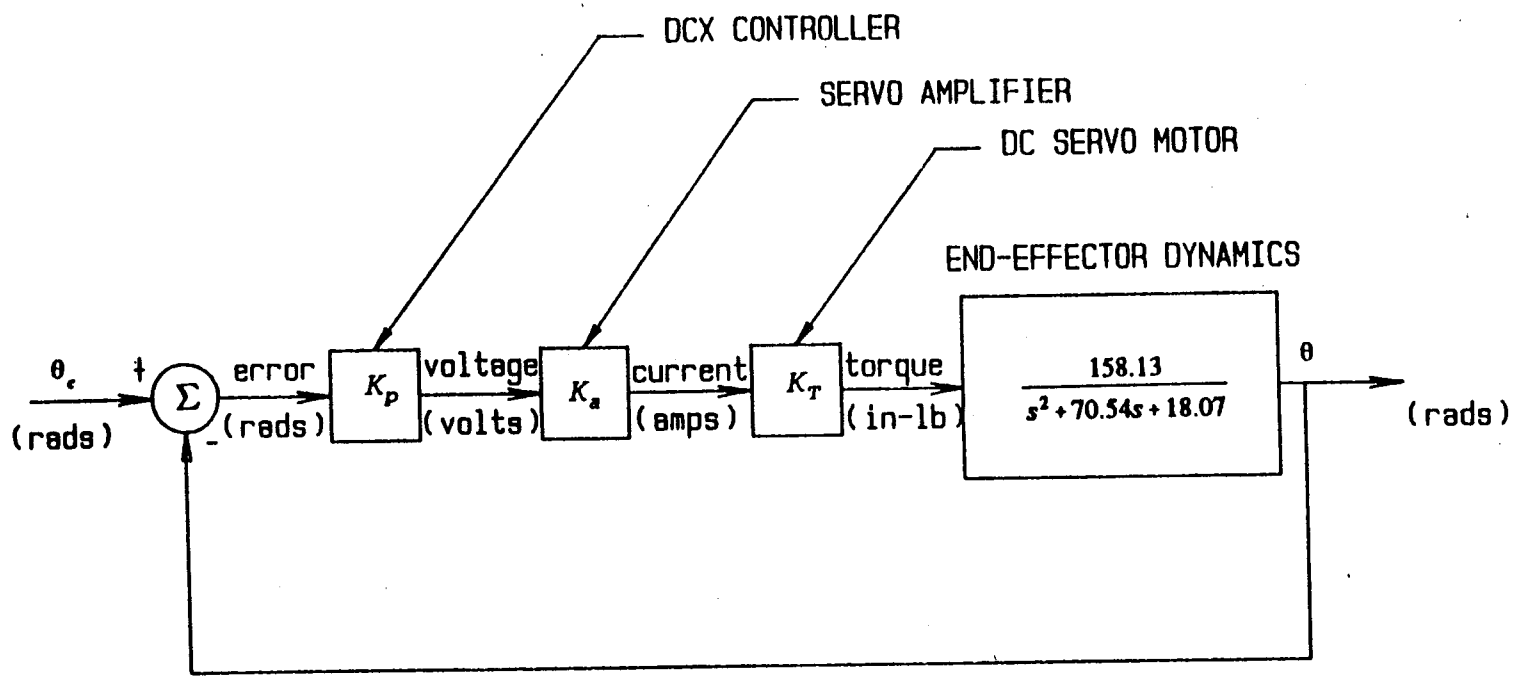

Figure B.2. Pitch Motion Control System Block Diagram

The servo amplifier was set to operate in the torque control mode and its gain adjusted to 0.1 amperes/volt. The transfer function between θ, the actual pitch displacement and θ_c, the commanded pitch displacement is given by

$$\frac{\theta(s)}{\theta_c(s)} = \frac{7.35K_p}{s^2+70.54s+(18.07+7.35K_p)} \quad . \qquad (B.11)$$

The block diagram of the control system that includes the D/A converter and encoder gains is shown in Figure B.3. The D/A converter on the servo controller module of the DCX board converts a 12 bit binary number into a voltage level between +10 volts -10 volts. The gain of the D/A converter is thus given by

$$K_{DA} = \frac{20 \ volts}{2^{12} \ counts} = 0.00488 \ \frac{volts}{count} \quad . \qquad (B.12)$$

The encoder used for position feedback generates 500 pulses for every revolution of the motor shaft. The DCX controller decodes the quadrature output from the encoder to increase the resolution of the encoder by a factor of four. The controller is thus able to read 2000 counts per revolution of the motor shaft. Therefore, the encoder gain is given by

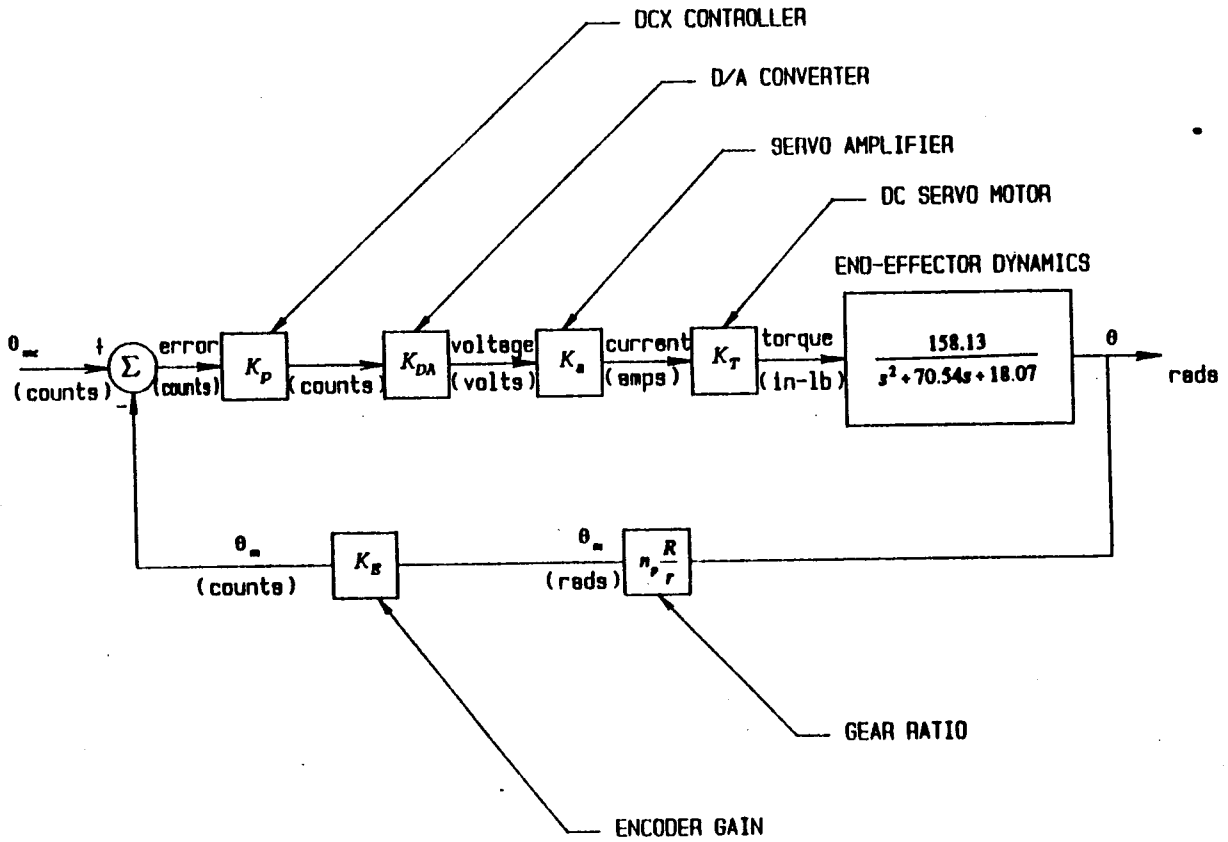

Figure B.3. Actual System Block Diagram

$$K_E = \frac{2000 \ counts}{2\pi \ radians (of \ motor \ shaft)}$$
$$= 318.31 \ \frac{counts}{radian} \ . \qquad \text{(B.13)}$$

The transfer function of the control system between the actual pitch displacement, θ (in radians), and the desired motor displacement, θ_{mc} (in counts) is given by

$$\frac{\theta(s)}{\theta_{mc}(s)} = \frac{0.036K_p}{s^2+70.54s+(18.07+1203.21K_p)} \ . \qquad \text{(B.14)}$$

Appendix C

End-Effector Hardware Specifications

Controller Hardware

Controller Board

Manufacturer: Precision Micro Control Corp.
3555 Aero Court
San Diego, CA 92123
(619) 565 1500

Vendor: Acquired directly from manufacturer

Part Number: DCX

Description: Eight-Axis Motion Controller Board

Analog Signal Output Module

Manufacturer: Precision Micro Control Corp.
3555 Aero Court
San Diego, CA 92123
(619) 565 1500

Vendor: Acquired directly from manufacturer

Part Number: DCX-MC100

Description: Plug-in module for controlling DC servo motor for pitch motion (inserted into axis # 3 on DCX mother board)

Stepper Motor Module

Manufacturer: Precision Micro Control Corp.
3555 Aero Court
San Diego, CA 92123
(619) 565 1500

Vendor: Acquired directly from manufacturer

Part Number: DCX-MC150

Description: Plug-in module used for controlling stepper motor for lateral gripper motion (inserted into axis # 4 on DCX mother board)

Data Acquisition Board

Manufacturer: Data Translation, Inc.
100 Locke Drive
Marlboro, MA 01752-1192
(617) 481 3700

Vendor: Acquired directly from manufacturer

Part Number: DT 2821

Description: 8 channel differential or 16 channel single-ended 12-bit A/D converters, 2 12-bit D/A converters and 16 I/O lines

Electronic Hardware

Stepper Motor and Driver

Manufacturer: Oriental Motor U.S.A., Corp.
Head Office:
2701 Plaza Del Amo, Suite 702
Torrance, CA 90503
(213) 515 2264

Vendor: EMCO, Inc.
P.O. Box 5618
Greenville, S.C. 29606
(803) 232 7616

Part Number: UMD 245-AA

Description: SUPER VEXTA Mini UMD Step Motor/Driver package

Servo Motor System

Manufacturer: Maxon Precision Motors, Inc.
838 Mitten Road, Burlingame, CA 94010
(415) 697 9614

Vendor: Acquired directly from manufacturer

(a) Part Number: RE035-071-34EAB 00 A

Description: 40 W DC Motor

(b) Part Number: 2932.702 - 0035.0 - 000

Description: 35:1 Planetary Gearhead

(c) Part Number: mmc - QR 030 024-02 LD 00A

Description: 50 W Linear Servo Amplifier

Encoder

Manufacturer: Hewlett-Packard, U.S.A.
P.O. Box 10301, Pala Alto
CA 94303-0890

Vendor: Motor, Gearhead and Encoder were acquired from Maxon Precision Motors, Inc. as a single package

Part Number: HP HEDS 5010

Desription: 500 Line Digital Encoder

Pneumatic Valves

Manufacturer: Clippard Instrument Laboratory, Inc.
7390 Colerain Road, Cincinnati, OH 45239
(513) 521 4261

Vendor: Barker Air & Hydraulics, Inc.
211 Eisenhower Drive
Greenville, SC 29606
(803) 271 4910

Part Number: EMC-12-24-40

Description: Electronic Manifold Card with 12 3-way pneumatic valves operating on 24 V

Mechanical Hardware

Grippers

Manufacturer: Compact Air Products, Inc.
P.O. Box 499
Westminster, SC 29693-0499
(803) 647 9521

Vendor: Acquired directly from manufacturer

Part Number: PSG052x1/4 (2 off)

Description: Two jaw parallel gripper

Gripper Jaw Liners

Manufacturer: Stock Drive Products, Inc.
2101 Jericho Turnpike
New Hyde Park, NY 11040
(516) 328 3330

Vendor: Acquired directly from manufacturer

Part Number: D68S87MGU2

Description: Rubber Jaw Liner

Gears

Manufacturer: Winfred M. Berg, Inc.
499 Ocean Avenue
East Rockaway, NY 11518
(516) 599 5010

Vendor: Acquired directly from manufacturer

Part Number: P32A28-36 (2 off)

Desription: 1.125" 36 teeth 20 degrees pressure angle Aluminum gears

Timing Belt System

Manufacturer: Winfred M. Berg, Inc.
499 Ocean Avenue
East Rockaway, NY 11518
(516) 599 5010

Vendor: Acquired directly from manufacturer

(a) Pitch Motion System

Part Number(s): 20TP4-14 (pulley), 20TP4-42 (pulley), 20TB-75 (belt)

(b) Lateral Gripper Motion System

Part Number(s): 20TP4-14 (pulley), 20TP4-28 (pulley), 20TB-95 (belt)

Description: 1/5" Pitch (XL) 0.200" Circular Pitch Belt System

Ball Bearings

Manufacturer: Fafnir Bearing Division of The Torrington Company,

New Britain, CT 06050

Vendor: Dixie Bearings, Inc.
215 McGee Road
Anderson, SC 29621
(803) 225 3791

(a) Pitch Bearings

Part Number: S7PP (2 off)

Description: Extra small radial bearings 5/8" bore

(b) Ball Screw Supports

Part Number: S1PP7 (4 off)

Description: Extra small radial bearings 1/4" bore

Linear Bearings

Manufacturer: Thomson Industries, Inc.
Port Washington, NY 11050
(516) 883 8000

Vendor: Dixie Bearings, Inc.
215 McGee Road
Anderson, SC 29621
(803) 225 3791

Part Number: SUPER-4 (4 off)

Description: Super ball bushing bearings

Part Number: 60 Case Shaft Class 'L' 1/4" Diameter

Description: 2 7.25" (length) linear bearing shafts

Ball Screws

Manufacturer: Saginaw Steering Gear Division
General Motors Corporation

Vendor: Dixie Bearings, Inc.
215 McGee Road
Anderson, SC 29621 (803) 225 3791

Part Number: 0375 - 0125 (B2) 5707502 (2 off)

Description: 0.375" nominal diameter, 0.125" pitch right-hand ball nut

Part Number: 0375 - 0125 5669420 (2 ft.)

Description: 0.375" nominal diameter, 0.125" pitch right-hand ball screw

Appendix D

Electrical Wiring Diagrams

This appendix shows the electrical wiring for the servo motor, stepper motor and pneumatic gripper systems.

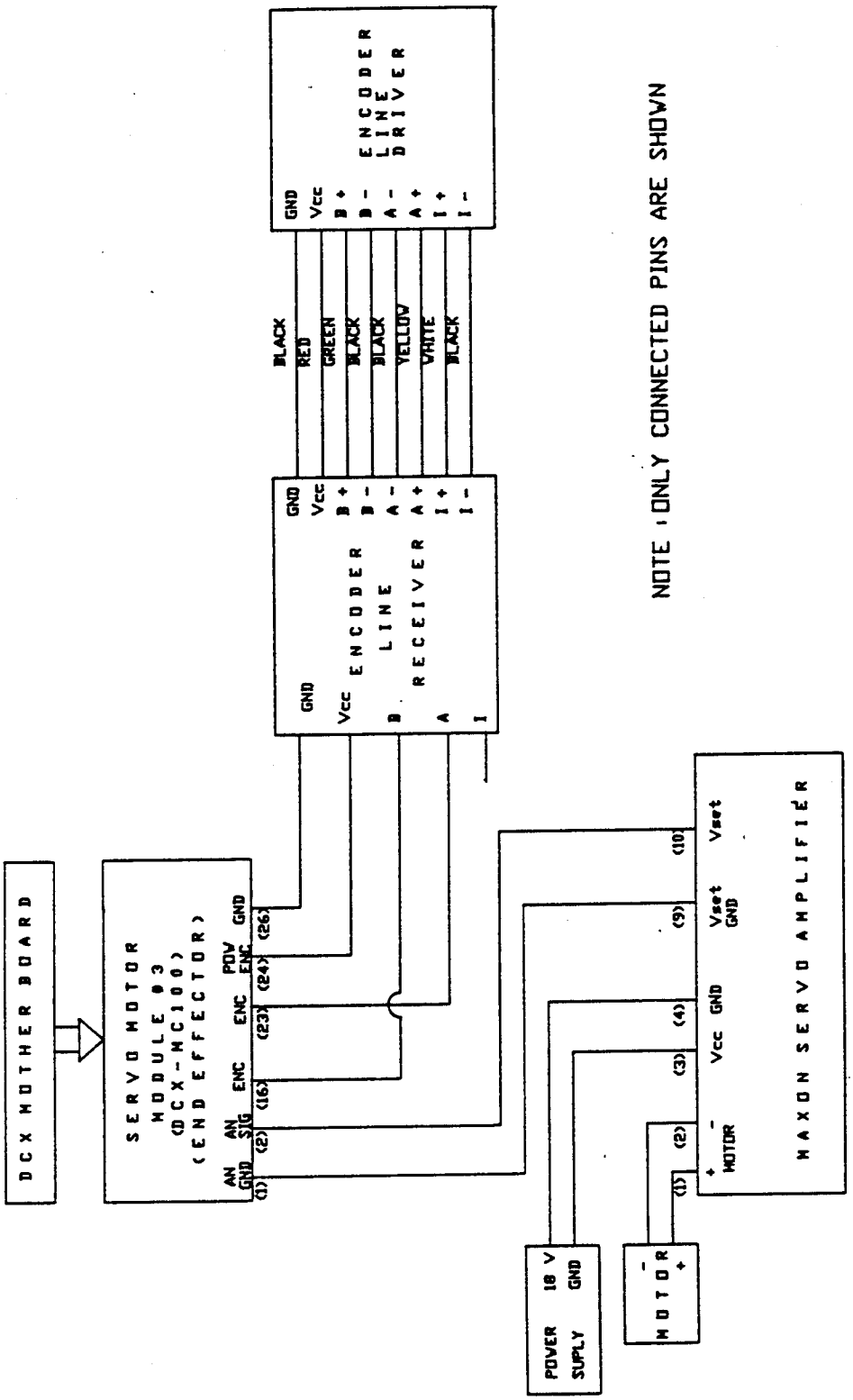

Figure D.1. Servo Motor Drive Circuit

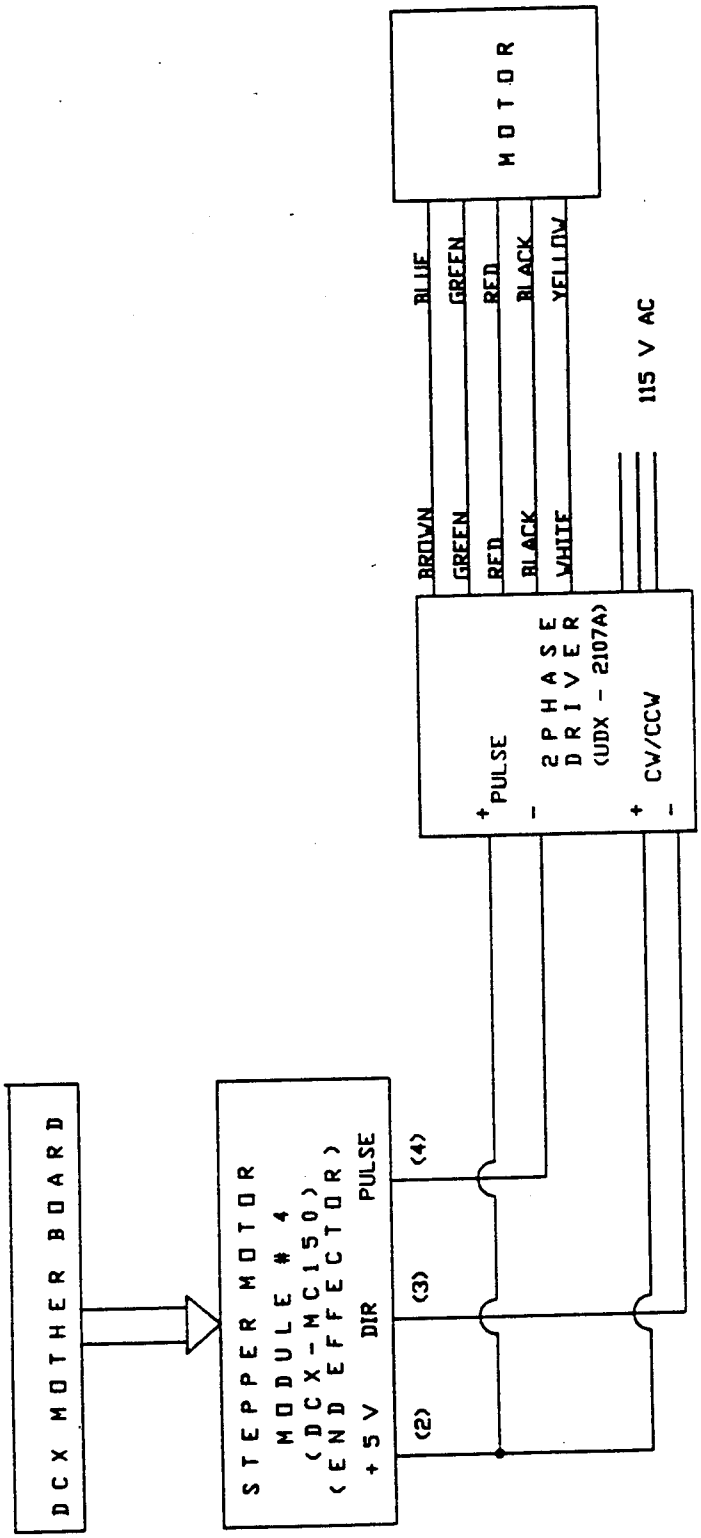

Figure D.2. Stepper Motor Drive Circuit

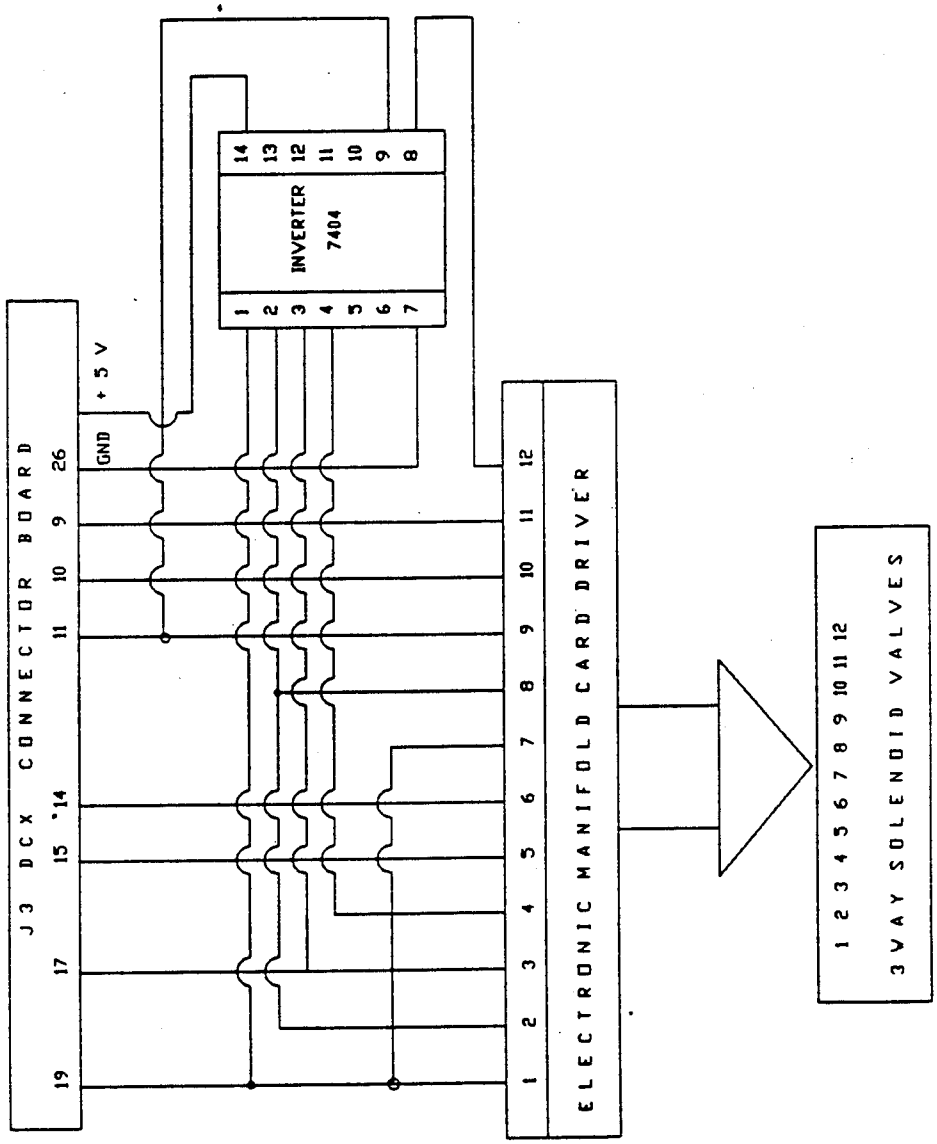

Figure D.3. Pneumatic Valve Drive Circuit

Appendix E

Program Listing

This appendix includes listings of programs RESP.C and ATOD.C which record the experimental performance of the end-effector pitch and lateral gripper motions respectively.

The following sequence of operations need to be carried out to obtain the simulated and experimental response curves of the pitch motion.

1. Manually position the end-effector so that it is at 60 degrees in the direction shown in Figure A.2.
2. Ensure that the power supply to the servo amplifier is set at 15 V.
3. Execute RESP.EXE after compiling and linking RESP.C.
4. Input the desired gain value (in COUNTS/COUNT) and the desired angular pitch displacement in DEGREES. Ensure that the angular displacement does not exceed the physical limits of the motion (+90 degrees to - 60 degrees from the horizontal position).
5. After execution of RESP.EXE, go into the MATLAB environment and execute TIMERESP.
6. To obtain a hard copy of the response curves, use the MATLAB meta file, RESPONSE.MET.

```
/* RESP.C  */
/* A program to compare the simulated and experimental re-
sponses of the end-effector pitch motion */

#include <dos.h>
#include <stdlib.h>
#include <stdio.h>
#include <hand.h>   /* includes routines to issue commands
                       and receive status information from
                       the DCX board  */
#include <math.h>

void init_hand();
long mv, ma, skp, kd, ki, lim;
float kp;
long max_vel, max_acc;

main()
{

    struct rpyfmt32 pos[4];
    FILE *out;
    long y[2000];
    long enc_counts;
    int i, j;
    float degrees, ref[2], tref[2];
    double angle, z, inst[2000];

/* open a file of MATLAB commands */

    out = fopen("timeresp.txt", "w");
    fprintf(out, "clear\n");
    fprintf(out, "!del c:\\tr.out\n");
    fprintf(out, "!del c:\\matlab\\response.met\n");
    fprintf(out, "diary c:\\tr.out\n");
    init_hand();    /* sets velocity, acceleration and gain
                       parameters */

    j = 0;
    inst[0] = 0.0;
    z = 0.0;
    y[0] = 0;
    printf("How many degrees do you want to move?\n");
    printf("A positive number pitches the end-effector such
          that\n");
    printf("the end-effector gripper points towards the
          floor\n");
    scanf("%f", &degrees);
    /*  The desired pitch displacement must be converted from
        DEGREES to COUNTS */
    enc_counts = (long) (583.33333*degrees);
    dcxcmd(0, 1, AXIS3 + MR, enc_counts);  /* moves the end-
                effector by the desired number of counts  */
```

```
    /*  the pitch displacement is continuosly read and writ
        ten into an array */
    for ( i = 1; i < 2000; i++)
        {
           dcxcmd(0, 1, TP, 0L);
           dcxrpy(0, sizeof(pos), (int far *)pos);
           y[i] = pos[2].val;
        }

i = 1;
fprintf(out, "d = [\n");
fprintf(out, "%lf\n", 60.0);
while (z < 500.0)
    {
       if (abs(y[i] - y[i - 1]) == 0)
           {
             z = z + 2.82;
           }
       else
           {
             angle =  60.0 + 0.0017142857*(double)(labs(y[i]
                      - y[0])); /* converts COUNTS to DEGREES
                                   */
             fprintf(out, "%lf\n", angle);
             z = z + 2.82;  /* it takes 2.82 milliseconds
                               to obtain the encoder count
                               from the DCX board */

             j++;
             inst[j] = z/1000.0;
           }
       i++;
    }
fprintf(out, "%lf\n", 60.0 + 0.0017142857*(double)(labs(y[i]
- y[0])));
fprintf(out, "];\n");
fprintf(out, "z = [\n");
for (i = 0; i <= j; i++)
    {
      fprintf(out, "%lf\n", inst[i]);
    }
fprintf(out, "%lf\n", 0.5);
fprintf(out, "];\n");

/* reference input */

    ref[0] = 60.0 + fabs(degrees);
    ref[1] = 60.0 + fabs(degrees);
    tref[0] = 0.0;
    tref[1] = 500.0;

    fprintf(out, "tref = [\n");
    for (i = 0; i < 2; i ++)
        {
          fprintf(out, "%lf\n", ((double)tref[i])/1000.0);
```

```
        }
    fprintf(out, "];\n");
    fprintf(out, "ref = [\n");
    for (i = 0; i < 2; i ++)
        {
          fprintf(out, "%lf\n", (double)ref[i]);
        }
    fprintf(out, "];\n");

    /* SIMULATION TIME RESPONSE */
    /* the theoretical transfer function is computed based on
       the input gain and the desired displacement; the
       simulated step response of the transfer function is
       computed using the STEP command of MATLAB  */

    fprintf(out, "pgain = %f;\n", kp);
    fprintf(out, "degrees = %f;\n", fabs(degrees));
    fprintf(out, "n = 1199.87*pgain*degrees;\n");
    fprintf(out, "num = [n];\n");
    fprintf(out, "wn2 = 18.07 + 1198.701*pgain;\n");
    fprintf(out, "den = [1 70.54 wn2];\n");
    fprintf(out, "s = 0:0.005:0.5;\n");
    fprintf(out, "t = s\';\n");
    fprintf(out, "r = step\(num,den,t\);\n");
    fprintf(out, "u = 60.0 + r;\n");

    /* plot options  */

    fprintf(out, "plot\(z,d,\'-\',t,u,\'--\',tref, ref,\'-.
                                \'\)\n");
    fprintf(out, "title\(\'KP = %2.2f  \')\n", kp);
    fprintf(out, "xlabel\('SECONDS'\)\n");
    fprintf(out, "ylabel\('DEGREES'\)\n");
    fprintf(out, "grid\n");
    fprintf(out, "meta response\n");
    fprintf(out, "diary off\n");
    fclose(out);
}

void init_hand() /* Servo Motor Initialization  - axis # 3 */

{
  /* the velocity and acceleration are set to very high
values to approximate the trapezoidal velocity profile gener-
ated by the DCX board as a step position input */

  max_vel = 20000000;
  max_acc = 2000000;
  dcxcmd(0, 2, AXIS3 + SV, max_vel, AXIS3 + SA, max_acc);
  printf("Enter Kp - Proportional Gain\n");
  scanf("%f", &kp);
  skp = (long)(kp*16.0);
```

```
 /* the desired gain value is multiplied by a factor of 16 to
    compensate for division by 16 by the DCX board prior to
    outputting the count to the D/A converter */

  dcxcmd(0, 1, AXIS3 + SG, skp);
  /* The derivative and integral gains are set to zero */
  kd = 0;
  dcxcmd(0, 1, AXIS3 + SD, kd);
  ki = 0;
  dcxcmd(0, 1, AXIS3 + SI, ki);
  lim = 0;
  dcxcmd(0, 1, AXIS3 + IL, lim);
  dcxcmd(0, 2, AXIS3 + MN, 0l, AXIS3 + DH, 0L);
}

/* End of RESP.C */
```

The following steps must be executed in sequence to obtain the experimental response of the translating motion of the grippers.

1. Connect the moving part of a linear potentiometer to one of the ball nuts that translate the grippers. Ensure that the axis of the potentiometer is parallel to the axis of motion.

2. Connect the electrical contact of the moving part of the potentiometer to the positive terminal of Channel 0 of the Data Translation DT 2821 board.

3. A +/- 10 V supply must be applied to the potentiometer.

4. Compile, link and execute ATOD.C. Select a gain of 1 and ensure that the commanded motion does not exceed the limits of the end-effector.

5. Enter the MATLAB environment and execute ATOD to observe the response.

6. To obtain a hard copy of the response curve, use the MATLAB meta file, POTRESP.MET.

```
/* atod.c */
/* A program to measure the performance of the lateral grip-
per motion of the end-effector */

#include <dos.h>
#include <stdlib.h>
#include <stdio.h>
#include <time.h>
#include <conio.h>   /* Console I/O header file. */
#include <atldefs.h> /* ATLAB function definition file. */
#include <atlerrs.h> /* ATLAB error definition file. */
#include <hand.h>
#include <math.h>
#include <atod.h>

#define TRUE 1
#define FALSE 0

FILE *out;

int channels[16]; /* channel scan list */
int gains[16]; /* gains for channels */
long i, num = 11849;
int pot_read[15000];
double inches, inst [5000], t = 0.0;
double distance;
int j, sine = 0;
long init_vel, final_vel, acc, steps;

struct dostime_t tm1, tm2;
double diff;


AL_CONFIGURATION configuration; /* storage for unit config
data */

double elap_time();

main ()
{
char input[10];
int max_channel;
unsigned value;

/* This portion of the code adapted from Data Translation's
example program */

AL_INITIALIZE ();

/* Select board 1, the first unit. */

AL_SELECT_BOARD ( 1 );

/* Perform a reset on the device. */
```

```
AL_RESET ();

/* Display the current unit configuration. */

/* Get the unit configuration for the number of A/D channels.
*/

AL_GET_CONFIGURATION ( &configuration );

max_channel = configuration.channel_count - 1;

/*
   Request channel and gain.  Note the use of unit configu-
ration data to determine the max channel number and the need
for gain values.
*/

/* Get the channel number, considering how many we have.*/

printf("Enter desired channel [0-%2d]:  ", max_channel );
scanf( "%d%*c", &channels[0] );

/* Get the gain if the unit has programmable gain.*/

if ( configuration.device_id &
( DT2821 | DT2821_F_DI | DT2821_F_SE | DT2821_G_DI |
  DT2821_G_SE | DT2824_PGH ) ) {
printf("Enter desired gain [1,2,4 or 8]:  ");
scanf( "%d%*c", &gains[0] );
}
else if ( configuration.device_id & ( DT2825 | DT2824_PGL ) )
{
printf("Enter desired gain [1,10,100 or 500]:  ");
scanf( "%d%*c", &gains[0] );
}
else
gains[0] = 1;

/* End of Data Translation's Code */


printf("Input Initial Velocity\n");
scanf("%ld", &init_vel);
printf("Input Final Velocity\n");
scanf("%ld", &final_vel);
printf("Input Acceleration\n");
scanf("%ld", &acc);

dcxcmd(0, 3, AXIS4 + SI, init_vel, AXIS4 + SV, final_vel,
AXIS4 + SA, acc);
dcxcmd(0, 1, AXIS4 + MN, 01);

printf("Input distance in inches that you need to move\n");
printf(" CAUTION !!! \n");
```

```
printf(" Input a positive number \(0 to 3.125\) to move the
grippers together \n");
printf(" Input a negative number \(0 to - 3.125\) to move
grippers apart\n");
printf(" Otherwise you may cause damage to the potentiometer
!\n");
scanf("%lf", &distance);
steps = (long)(distance * 8.0 * 400.0); /* inches x no. of
steps per revolution of ball screw / pitch of ball screw */
dcxcmd(0, 1, AXIS4 + MR, steps);

_dos_gettime(&tm1);  /* To determine the abcissa values of
                        the plot */

for ( i = 0; i < num; i++)
        {
           AL_ADC_VALUE ( channels[0], gains[0], &value );
           pot_read[i] = value;
           AL_DAC_VALUE ( 0, &value );
        }

_dos_gettime(&tm2);

diff = elap_time(&tm1, &tm2);

dcxcmd(0, 2, AXIS4 + WS, 1001, AXIS4 + MF, 01);

printf("It took %f seconds to execute %ld A/D conversions\
                    n", diff, num);
printf("At a rate of %f seconds per conversion\n", diff/
                      (double)num);

/* Terminate ATLAB operations.*/

AL_TERMINATE ();

/* open a file of MATLAB commands */

out = fopen("atod.txt", "w");
fprintf(out, "clear\n");
fprintf(out, "!del c:\\pot.out\n");
fprintf(out, "!del c:\\matlab\\potresp.met\n");
fprintf(out, "diary c:\\pot.out\n");

inst[0] = 0.0;
fprintf(out, "y = [\n");
fprintf(out, "%lf\n", 0.00);
for (i = 1; i < num; i++)
    {
       if (abs(pot_read[i] - pot_read[i - 1]) <= 1)
           {
             t = t + 0.000422;
           }
       else
```

```
            {
              sine = abs(pot_read[i] - pot_read[0]);
              inches = (double)sine * 0.001953125;
              fprintf(out, "%lf\n", inches);
              t = t + 0.000422;
              j++;
              inst[j] = t;
            }
    }
fprintf(out, "%lf\n", inches);
fprintf(out, "];\n");
fprintf(out, "t = [\n");
for (i = 0; i <= j; i++)
    {
       fprintf(out, "%lf\n", inst[i]);
    }
fprintf(out, "%lf\n", 4.0);
fprintf(out, "];\n");

/* MATLAB Plot Options  */
fprintf(out, "plot\(t,y,\'-\'\)\n");
fprintf(out,  "title\(\'IV = %ld   FV =   %ld ", init_vel,
final_vel);
fprintf(out, "ACC  =  %ld  REF = %6.3lf\'\)\n", acc, fabs
           (distance));
fprintf(out, "xlabel\('SECONDS'\)\n");
fprintf(out, "ylabel\('LINEAR MOTION  in'\)\n");
fprintf(out, "grid\n");
fprintf(out, "meta potresp\n");
fprintf(out, "diary off\n");
fclose(out);
}

double elap_time(tm1, tm2)  /* Determines the elapsed time
                               between two instants */
struct dostime_t *tm1, *tm2;
{
  double diff, tsec1, tsec2;

  tsec1 = ((double)((*tm1).hour))*3600.0 +
          ((double)((*tm1).minute))*60.0 +
          ((double)((*tm1).second))      +
          ((double)((*tm1).hsecond))/100.0;
  tsec2 = ((double)((*tm2).hour))*3600.0 +
          ((double)((*tm2).minute))*60.0 +
          ((double)((*tm2).second))      +
          ((double)((*tm2).hsecond))/100.0;
  diff = tsec2 - tsec1;
  if(diff < 0.0)
    diff = diff + 86400.0;
}

/*  End of ATOD.C  */
```

REFERENCES

1. Gaetan, M., "Robots: Their Potential in the Apparel Industry", Bobbin, August 1981, pp. 83-92.

2. Parker, J.K., R. Dubey, F.W. Paul, and R.J. Becker, "Robotic Fabric Handling for Automated Garment Manufacturing", Transactions of the ASME, Journal of Engineering for Industry, June 1985, pp. 4-46 - 4-66.

3. Kemp, D.R., G.E. Taylor, P.M. Taylor, and A. Pugh, "A Sensory Gripper for Handling Textiles", Proceedings of the 13th International Symposium on Industrial Robots and Robots 7, Chicago, April 1983, pp. 18-23 - 18-29.

4. Taylor, P.M., G.J. Monkman, and G.E. Taylor, "Electrostatic Grippers for Fabric Handling", Proceedings of the IEEE International Conference on Robotics and Automation, Philadelphia, April 1988, pp. 431-433.

5. Torgerson, E. and F.W. Paul, "Vision Guided Robotic Fabric Manipulation for Apparel Manufacturing", IEEE Control Systems Magazine, Vol. 8, No. 1, February 1988, pp. 14-20.

6. Gershon, D. and I. Porat, "Vision Servo Control of a Robotic Sewing System", Proceedings of the IEEE International Conference on Robotics and Automation, Philadelphia, April 1988, pp. 1830-1835.

7. Dlaboha, I., " Robotics Technology Makes Gains in Apparel Industry", Apparel World, July 1982, pp. 17-20.

8. Nakamura, T., T. Arai, Y. Tanaka, M. Satoh, and Y. Imazu, "Trajectory Generation of Redundant Manipulator for 3-D Sewing System", ASME Proceedings of the USA-Japan Symposium on Flexible Automation, Minneapolis, July 1988, pp. 35-40.

9. Taylor, P.M. and S.G. Koudis, "The Robotic Assembly of Garments with Concealed Seams", Proceedings of the IEEE International Conference on Robotics and Automation, Philadelphia, April 1988, pp. 1836-1838.

10. Bernardon, E. and T.S. Kondoleon, "Real Time Robotic Control for Apparel Manufacturing", Proceedings of Robots 9, Detroit, June 1985, pp. 4-46 - 4-66.

11. Jacobsen, S.C., J.E. Wood, D.F. Knutti, and K.B. Biggers, "The UTAH/M.I.T. Dextrous Hand: Work in Progress", International Journal of Robotics Research, Vol. 3, No. 4, 1984, pp. 21-50.

12. Salisbury, J.K. and J.J. Craig, "Articulated Hands: Force Control and Kinematic Issues", International Journal of Robotics Research, Vol. 1, No. 1, 1982, pp. 4-17.

13. Grupen, R.A., T.C. Henderson, and I.D. McCammon, "A Survey of General Purpose Manipulation", International Journal of Robotics Research, Vol. 8, No. 1, 1989, pp. 38-62.

14. Torgerson, E.J., Robotic Fabric Acquisition and Manipulation with Machine Vision Assistance, M.S. Thesis, Mechanical Engineering Department, Clemson University, Clemson, S.C., December 1986.

15. Gershon, D., The Application of Robotics to the Assembly of Flexible Parts by Sewing, Ph.D. Thesis, Department of Textile Industries, University of Leeds, Leeds, U.K., March 1987.

16. Paul, F.W., E. Torgerson, S. Avigdor, D. Cultice, A. Gopalswamy, and K. Subba-Rao, "A Hierarchical System for Robot-Assisted Shirt Collar Processing", Proceedings of IEEE International Conference on Systems Engineering, August 1990, Pittsburg, pp. 378-382.

17. Chen, F.Y., "Gripping Mechanisms for Industrial Robots: An Overview", Mechanism and Machine Theory, Vol. 17, No. 5, 1982, pp. 299-311.

18. Pu, J. and R.H. Weston, "A New Generation of Pneumatic Servos for Industrial Robots", Robotica, Vol 7, 1989, pp. 17-23.

19. Lauer, H., R.N. Lesnick and L.E. Matson, Servomechanism Fundamentals, McGraw-Hill Book Company, Inc., 1960.

20. Mabie, H.H. and F.W. Ocvirk, Mechanisms and Dynamics of Machinery, John Wiley and Sons, 1978.